The use of fluorescent microspheres to measure organ blood flows in low flow states.

Colin Andrew Eynon

BSc (Hons), MBBS (Hons), MRCP, FFAEM

In submission for the degree of Doctor of Medicine,

University of London

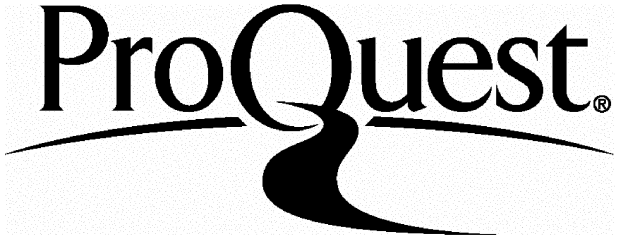

Abstract

Organ perfusion can be measured using microspheres delivered into the blood stream. Blood flow is proportional to the number of microspheres entrapped in the tissue. The commonest method of quantitating the number of microspheres present in a sample is to measure levels of radioactivity from radiolabelled microspheres. The relative expense of radiolabels has led to alternative, non-radioactive, microsphere methods.

The use of fluorescent labelled microspheres for measurement of regional organ perfusion has been validated in comparisons with radiolabelled microspheres in conditions of normal or enhanced flow. In this work, limitations in the fluorescent microspheres technique were established in preliminary experiments. Inter- and intra-animal variability in organ blood flows in conditions of normal flow were studied in a rat model. Fluorescent microspheres were subsequently used to measure organ perfusion in established animal models of low blood flow states. Organ-specific recovery rates for fluorescent microspheres during the extraction process were also studied.

The fluorescent microsphere technique produced high sensitivity with good spectral separation allowing at least four different fluorescent labels to be easily separated. The technique had excellent reproducibility in repeated measurements. Temporal variation in organ blood flows compared favourably with previous studies. Inter-animal variability was <22% for all tissues except the lungs and adrenals. Under conditions of low flow, the fluorescent microsphere technique appeared robust with

organ blood flows following the patterns reported by other groups. Overall recovery of microspheres using KOH digestion and a negative pressure filtration technique was high.

Fluorescent microspheres provide a new method of repeated measurement of regional perfusion over a wide range of organ blood flows. The accuracy of the technique appears superior to other non-radioactive microsphere methods. The principal limitation of the technique is that it is labour intensive. Automation of the process is likely to make the use of fluorescent microspheres more attractive.

Contents

Chapter 1: Introduction to blood flow measurement.

Several methods of measuring cardiac output or organ blood flow in animal models have been described and are in widespread use. These include indicator dilution techniques, electromagnetic or ultrasonic flow transducers, direct collection of venous effluent, and microsphere techniques. Each technique has advantages and disadvantages. The benefits and limitations of each technique need to be assessed for each experiment and the most suitable technique chosen.

Placement of electromagnetic or ultrasonic flow probes allows continuous observations over a period of hours. This is useful if acute physiological and pharmacological influences on the circulation are being studied. The size of the flow probes and the requirement for surgical placement around the supplying blood vessel mean that only single organs or few organs can be studied.

Standard indicator dilution techniques have been modified to measure the fractional distribution of blood flow by injecting a suitable indicator into the circulation and measuring its distribution within various organs during the initial transit. These methods can measure flow per unit weight of the organ but generally require sacrifice of the animal within a few minutes of the injection of the indicator. The technique although accurate, requires extensive surgery and is almost certainly the least physiological.

The indicator dilution technique may be modified by using microspheres as the indicator. Microspheres are trapped in the capillary system on the first circulation

after injection with their distribution being in proportion to the regional blood flow. The primary advantage of the microsphere technique is that blood flows to a number of organs can be studied in a single model. Regional blood flow within an organ can also be measured. The technique is also suitable for use in long-term models. This technique does have certain limitations and requires some assumptions to be met. Measurements cannot be made in real-time as the animal has to be sacrificed to determine microsphere counts. Only a finite number of measurements can be made because of the demands on the instruments that separate the characteristics of the microspheres. Injection and entrapment of microspheres should have no effect on the circulation or on local organ haemodynamics. This is of particular importance if serial measurements are to be made. The results obtained with microsphere techniques have been compared directly with those obtained by other techniques.

a. Electromagnetic flow transducers.

Rudolph and Heymann studied organ blood flow in foetal lambs using cannulating electromagnetic flow transducers and carbonized microspheres (50 μm diameter) (1). Good correlations were obtained between the two methods with the maximum difference being 19%. In one animal, cerebral blood flow was measured using both techniques. Flow calculated from the microsphere injection was 139 ml/min, compared to the measured venous flow from the external jugular veins of 126 ml/min.

Buckberg et al cannulated the right renal artery of dogs and perfused it with an electromagnetic flow transducer in the perfusion line (2). Microspheres (50 μm diameter) were injected into either the left atrium or the left ventricle. Twelve

comparisons of renal blood flow were made in three dogs. Calculated and measured blood flows agreed within 6%.

Measurements of pulmonary artery blood flow and umbilical placental blood flow in foetal lambs have also shown extremely high correlations (3, 4).

b. Direct collection of venous effluent.

Coronary blood flow as measured by the microsphere technique has been compared with direct collection of coronary venous return during right heart bypass. In a study by Domenech et al, 27 measurements were made in seven dogs (5). The calculated flow was within 5% of the measured flow in 12, within 10% in 19, and within 20% in 24 measurements. Two of the three measurements with the largest discrepancies were in one dog with abnormally low coronary blood flow.

Buckberg et al studied coronary blood flow in sheep and dogs (2). In sheep, calculated coronary blood flow after left atrial injection of microspheres averaged 1.4% less than measured flow, with a range of difference from 38% to –26%. Three of 21 calculated flows differed by more than 20% from measured flows. Following left atrial injection of microspheres in dogs, the differences between calculated and measured flows averaged –3.6% with 10 of 50 differences exceeding 20%. After left ventricular injection of microspheres, the mean difference was 4.7% with only 2 of 20 differences being greater than 20%.

Edmunds et al measured left lower lobe pulmonary arterial blood flow using the microsphere technique and compared it with pulmonary venous return from that lung (6). Total pulmonary blood flow was calculated using indocyanine green dye and the proportion of microspheres lodging in the left lower lobe related to the total number in the lung to calculate left lower lobe flow. The average difference between the two techniques was 3%.

c. Other techniques

Regional blood flow calculated using the microsphere technique has also been compared with that obtained using antipyrine steady-state diffusion (7), PAH clearance (8), and radioactive potassium clearance (9). Good correlations have been obtained between the microsphere technique and the other techniques.

Radioactive microspheres have been regarded as the "gold standard" of blood flow determination for nearly four decades. Use of radioactive microspheres in animal experimentation is becoming increasingly problematic due to legislation and the high costs of storage and disposal. The work leading to this thesis was prompted by the need to replace the radioactive microsphere technique with a non-radioactive method in our laboratory. This method should be technically simple, accurate and reliable. Because of the cost of large animals, experiments assessing the technique itself were only possible in a rat model. Following refinement of the methodology, there was opportunity to use the fluorescent microsphere technique in a number of established animal models. The relative error and variability in blood flow measurements with fluorescent microspheres have been studied under conditions of

normal or enhanced flow. In these studies, the variability in organ blood flow in low flow states was assessed.

Chapter 2: The use of microspheres to measure blood flow.

Injection of foreign particles into the intravascular compartment to study the circulation has been performed for many years. In 1909, Pohlman reported his studies of the use of starch particles to trace blood flow in the foetal, porcine heart (3). Prinzmetal et al used glass microspheres to detect vascular anastomoses in human hearts (3). Radioactively labelled microspheres, first described by Rudolph and Heymann in 1967 (1), have become the standard for measurement of tissue blood flow. In their original description, 50 μm diameter microspheres were injected into the circulation and were subsequently trapped in the peripheral vessels. Organs of interest were then removed and their radioactivity was measured. Blood flow to the organ was calculated by measuring the cardiac output and multiplying it by the proportion of microspheres found in the organ compared to the total number of microspheres injected. Makowski et al (7) and Domenech et al (5) subsequently introduced the reference sample method whereby a known quantity of arterial blood (reference sample) is withdrawn at the time of microsphere injection. Organ blood flow is then calculated by comparison of the amount of radioactivity present in the organ to that present in the reference sample.

The use of radioactive microspheres for the measurement of regional blood flow has a number of disadvantages. Storage of microspheres and disposal of radioactive waste are expensive and provide an environmental hazard. Use is restricted to specially licensed laboratories. Radioactive microspheres are also unsuitable for use in long-term experiments because of the short half-lives of the

material (10). Separation of different isotopes because of crossover counting may also be problematic.

In the last ten years a number of techniques using non-radioactive microspheres have been introduced. Currently, three different types of non-radioactive microspheres are available; coloured, heavy metal labelled (X-ray fluorescent), and fluorescent.

Coloured microspheres

Hale et al used coloured microspheres to measure blood flow (11). Blood and tissue samples were digested by a combination of enzymatic and chemical methods. Spheres were isolated by centrifugation and aliquots were then counted in a haemocytometer using a light microscope. Good correlations were reported between coloured microspheres and simultaneously injected radioactive microspheres although, at high blood flows, the coloured microsphere method systematically overestimated blood flow. This report validated the use of only three microsphere colours and the process of counting individual microspheres was extremely time consuming. Microspheres ranged in diameter from 3.3 to 29.2 μm. An alternative to manually counting microspheres was developed by Kowallik et al (12). After isolation of the microspheres, the coloured dye was extracted within a defined volume of solvent and the absorbance spectra measured by spectrophotometry. The separation of composite absorbance spectra was as good as that obtained using radioactive microspheres and a γ-counter. Leaching of dye from the spheres was less than 0.1% over a two month period in vitro and did not occur over eight hours in vivo. In this report, the microsphere diameter was 15 ± 0.1 μm (mean ± SD) with a density

of 1.09 g/ml. Although myocardial blood flow measured using this technique correlated well with radioactive microspheres when coronary inflow was used as a flow reference, the coloured microsphere method underestimated blood flow compared to the arterial reference method. This suggests that either the spheres or the dye are lost from the tissue samples, that colour was overestimated in the reference blood sample, or that other substances interfered with spectrophotometry.

Heavy metal labelled

Morita et al (13) and Mori et al (14) used an x-ray fluorescent system to measure regional blood flow with 15μm diameter microspheres loaded with stable, heavy elements. Following digestion of blood or tissue samples, microspheres were isolated by centrifugation and the pellet, containing the labelled microspheres, was then placed in an x-ray fluorescence spectrometer. Mori et al reported good correlations between regional blood flows measured using heavy metal microspheres and radioactive microspheres (14). The disadvantages of this method are the high cost of the measuring system, the need to read each sample twice, the requirement to use greater numbers of spheres (10 x) compared to radioactive microspheres, and the higher density of the microspheres.

Fluorescent microspheres

Early studies using fluorescent microspheres reported their use for identifying regions of ischaemia or estimating regional blood flow using light microscopy and manual counting techniques (15, 16). In 1993, Glenny et al (17) and Abel et al (18) reported the use of dye extraction techniques similar to those used by Kowallik et al (12). Microspheres were extracted from digested tissue by either vacuum filtration

(17) or centrifugation (18) and the dye was then extracted into an organic solvent. Glenny's group also reported the direct extraction of dye from dried lung samples thus removing the digestion and filtration steps (17). In the study by Abel et al (18), four different colours of fluorescent microspheres were used. The correlation coefficient for radioactive and fluorescent microspheres in individual sections of cardiac tissue was only 0.77. Glenny's group found much better correlations for blood flow to heart ($r=0.96$-0.98) and kidneys ($r=0.99$) (17). Up to ten colours of fluorescent microspheres can be accurately resolved (19). Fluorescent microspheres have the advantage of being relatively inexpensive, have a density of 1.055 g/ml and are far more sensitive compared to coloured microspheres (18). Fluorescent microspheres are also reported to provide reliable blood flow data in long-term experiments (10).

General sources of error with microspheres

Although the microsphere technique has been regarded as the "gold standard" for determining blood flows, there are a number of potential errors. Two classes of error occur, stochastic and methodological. Most of the errors apply to both radioactive and non-radioactive microsphere methods (20). Microsphere entrapment within organs or reference blood samples is not completely predictable, even if spheres are uniformly distributed during injection. Random variation means that entrapment rates form a distribution about a mean value, the shape of the distribution being directly related to the size of the mean. This stochastic variation approximates a Poisson distribution with X being the mean number of spheres reaching the organ and $\sqrt{X}$ the standard deviation. If the number of microspheres per sample exceeds

400, the coefficient of variation is ≤ 5% (20). With 100-400 microspheres per sample the coefficient of variation increases to between 6-9%.

Table 1: *Sources of error in blood flow measurement with microspheres (20)*

Potential error	*Method*				
	RA	CM	CE	FL	XRF
Stochastic errors:	•				
Sphere distribution	•	•	•	•	•
Decay distribution	•				
Gamma counting error	•				
Methodological errors					
Non-uniform mixing	•	•	•	•	•
Aggregation	•	•	•	•	•
Additives	•	•	•	•	•
Reference sample	•	•	•	•	•
Circulatory impairment	•	•	•	•	•
Flow biasing	•	•	•	•	•
Non-entrapment	•	•	•	•	•
Diameter variability	•	•	•	•	•
Loss of spheres from sample	•	•	•	•	•
Stripping errors	•		•	•	•
Detector: geometry	•				
separation	•				
saturation	•				
Signal quenching				•	
Loss of spheres during isolation		•	•	•	•
Low signal: noise ratio			•		
Inaccurate solvent volumes		•	•	•	
Dye stability			•	•	
Background signal			•	•	

RA: radioactive microspheres, CM: counting of microspheres, CE: dye extraction of coloured microspheres, FL: dye extraction of fluorescent microspheres, XRF: x-ray fluorescent microspheres

Immediately following injection, microspheres must be uniformly distributed across the blood stream such that identical concentrations reach all vessel branch

points. Uniform mixing may be facilitated by the use of multi-port catheters to inject the microspheres (20). Microspheres should be injected as distant as possible to the first point of major arterial branching. For measurements of systemic blood flow, either the left atrium or the left ventricle is used as the site of microsphere injection (3). Intra-aortic injection can provide accurate flow measurements if more distal organs such as the kidneys are being studied (21). Microsphere aggregation in the injectate may be reduced by vigorous vortexing prior to injection and either the addition of small amounts of detergent or by suspending the spheres in a solution containing macromolecules (22, 23). The amount of additives should be minimised to prevent effects of these on the circulation (22, 24).

Microspheres must be completely trapped by the vascular beds during the first pass of the circulation and should remain trapped until the tissues are removed. In addition, there should be no effect of the microspheres on systemic or regional haemodynamics. All of these factors are dependent on the size of the microspheres used. Larger diameter microspheres have a tendency to enter regions of higher flow (5, 25), probably due to rheological bias at branch points (25). While this does not significantly affect measurement of overall blood flow to organs, it may affect intra-organ blood flow measurements (3). The difference in density between radioactive and non-radioactive microspheres appears to have minimal effect on their rheological properties (12, 18). Large diameter microspheres (50 μm) have shown no evidence of non-entrapment in a wide range of animal models (3). Non-entrapment of the more commonly used 15 μm diameter microspheres has varied in different models (3) but is generally less than 10%. Conditions that alter the patency of arteriovenous anastomoses in organs, such as anaesthetic agents, pCO_2 and ambient temperature,

may have significant effects on non-entrapment (3, 26). The most commonly used measure of non-entrapment in the peripheral circulation is the amount of microspheres injected systemically that are lodged in the lungs (3). 15μm diameter microspheres fail to pass through the lungs whereas those less than 10μm may pass through in significant amounts (3).

The size and number of microspheres injected may cause acute circulatory changes immediately following injection. Transient hypo- or hypertension, bradycardia and a reduction in cardiac output may occur (3). Injection of large numbers of microspheres may also result in embolisation of a significant fraction of the capillary bed. In a rat model, Tuma et al showed that measured blood flow to organs receiving the highest fraction of cardiac output decreased as increasing numbers of microspheres were injected (21). For organs with high blood flows such as the heart and kidneys, only 10,000 injected microspheres would be required to produce accurate flow measurements. However, the rate of reference sample withdrawal to obtain 400 microspheres in the reference sample would be approximately 2 ml/min. This rate of withdrawal would be likely to cause cardiovascular changes. In tissues with low blood flows such as skeletal muscle, the number of microspheres required to accurately measure organ blood flow would be likely to result in underestimation of heart and kidney blood flows.

Fundamental to the microsphere technique is the assumption that once trapped in a capillary bed, microspheres remain there until the tissue is processed. In severely ischaemic tissue, however, there may be true physical loss of microspheres due to disruption of the normal capillary anatomy. In addition, blood flow may be

underestimated due to oedema of the ischaemic tissue after injection of the microspheres (27, 28).

Spillover of emission spectra from microspheres (stripping errors) may be reduced by the formation of overlap matrices. Alternatively, spillover can be reduced by the use of excitation and emission spectra that are different from the optimal wavelengths for microsphere measurement (20).

Techniques using non-radioactive microspheres suffer from the problem that microspheres may be lost during the processing required to extract the dye from the tissue (20). This loss can be minimised by performing all processing in the same tube. A known amount of microspheres of a colour not used in the experiments may be added to each sample prior to processing. This acts as an internal standard as each sample should have comparable signals for this colour after processing (29).

Both the coloured microsphere method and the fluorescent microsphere method require that the labels be extracted in a given volume of solvent. The colour extraction method requires addition of small volumes of solvent that may introduce a significant amount of noise into the experiment. The sensitivity of detection for fluorescent microspheres is also higher than for coloured microspheres thus reducing the signal to noise ratio (20). The dyes used for both coloured and fluorescent microspheres have been shown to be stable over a wide range of conditions and in different media (12, 17).

Tissue, blood and other chemicals may contain substances that interfere with the accurate determination of blood flows by these methods. Fluorescent porphyrins are generated during ischaemia-reperfusion in gastric tissue in rats (30). The fluorescence emitted by porphyrins did not spill over into the wavelengths measured in the current experiments. Tween-80 is commonly used to prevent microsphere aggregation but emits blue-fluorescence (20). This problem can be overcome by increasing the number of microspheres injected to improve the signal to noise ratio, and assessing background fluorescence for each experiment.

The development of non-radioactive microsphere methods has made significant progress. Good correlations have been found between the three non-radioactive microsphere techniques and radioactive microspheres (4, 11, 17). For most studies, the use of non-radioactive microspheres is cheaper than radioactive microspheres (20). Non-radioactive microspheres also allow blood flow measurements in chronic animal models (10). The high sensitivity of the fluorescent microsphere technique means that the number of microspheres injected can be as low as for radioactive microspheres (20). The good spectral separation that can be obtained with fluorescent microspheres allows up to ten labels to be used (19). The current methodologies for non-radioactive microspheres are, however, relatively primitive. Improvement in these methodologies and automation of the quantification process is likely to increase interest in non-radioactive microsphere techniques.

Chapter 3: Principles of fluorescence

Introduction

Luminescence is the result of a three-stage process that occurs when light is emitted from molecules for a brief period following absorption of light (31). Certain molecules are able to absorb energy at a specific excitation wavelength to create an excited singlet state (Fig 1).

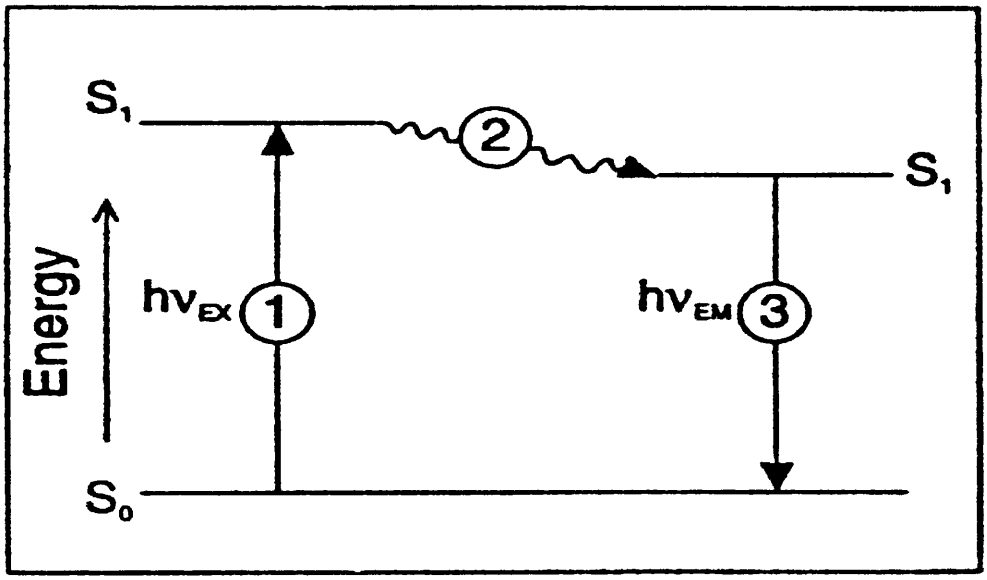

Figure 1: *Jablonski diagram illustrating the processes involved in the creation of an excited electronic singlet state by optical absorption and subsequent emission of fluorescence. Stage 1 is supply of a photon of energy (hv_{EX}) to a fluorophore creating an excited singlet state (S_1). Stage 2 is partial dissipation of the energy to produce a relaxed singlet excited state. Stage 3 is emission of a photon of energy (hv_{EM}), returning the fluorophore to its ground state (S_0).*

This excited state exists for a finite time at the end of which a photon of energy is emitted, returning the molecule to its baseline state. Due to dissipation of energy during the excited state, the photon emitted is of lower energy, and therefore longer wavelength, than the exciting energy. This difference in energy or wavelength is known as the Stokes shift. If the time delay between absorption and emission is 10^{-8} seconds or less, the light emitted is known as fluorescence. If the delay is around 10^{-6} seconds, the term delayed fluorescence is used. Phosphorescence occurs if the delay is greater than 10^{-6} seconds.

The fluorescence emission spectrum of a particular molecule is independent of the excitation wavelength (32). Excitation at different wavelengths produces variation in fluorescence emission intensity but no change in the emission spectrum (Fig 2).

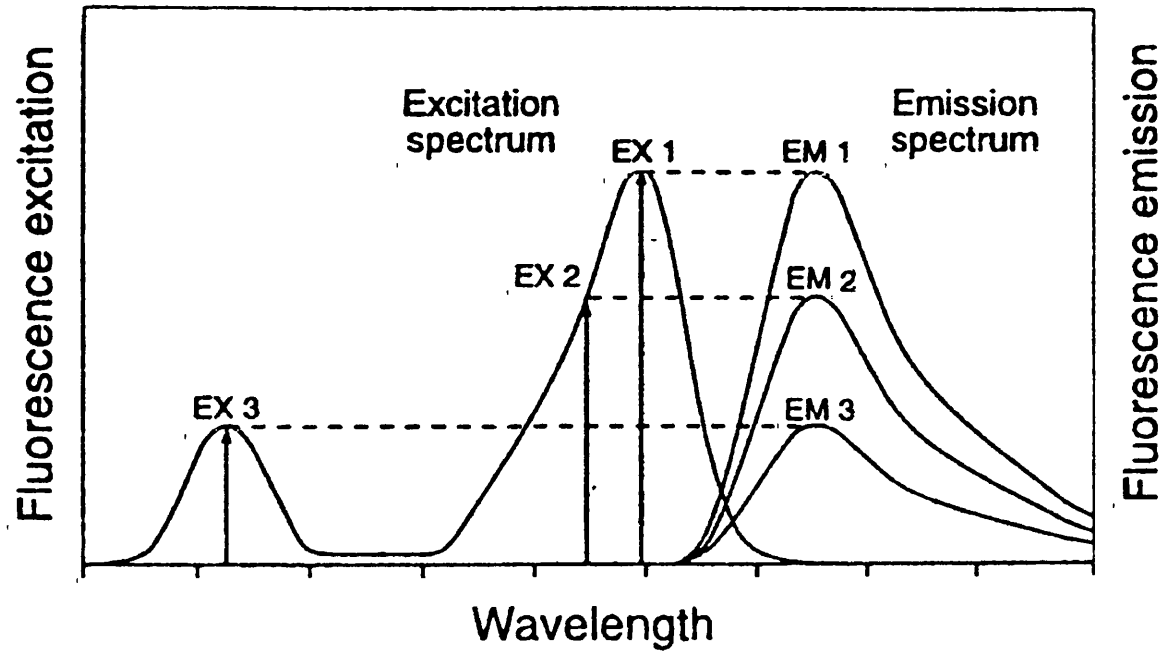

Figure 2: *Excitation of a fluorophore at three different wavelengths (EX1-3) produces variations in fluorescence emission intensity (EM1-3) corresponding to the amplitude of the excitation spectrum. The emission spectral profile is unchanged.*

The intensity of the light emitted is given by the equation:

$$F = \phi Io\ (1\text{-}e^{-\varepsilon bc})$$

where F is the intensity of the emitted light, ϕ the quantum efficiency, Io is the incident radiant power, ε the molar absorbtivity, *b* the path length of the cell and *c* the molar concentration of the fluorescent dye (33).

Quantum efficiency is the percentage of molecules in the excited state that return to the baseline state by fluorescent emission. Incident radiant power is a function of the light source intensity at a specific wavelength. For a constant ϕ, Io, ε, and *b*, the relationship between the fluorescent signal and dye concentration should be linear for dilute dye concentrations (33). At high dye concentrations reactions may occur between two molecules (quenching) that reduce the intensity without altering the emission spectrum (32, Fig 3). This can occur due to collisions that produce

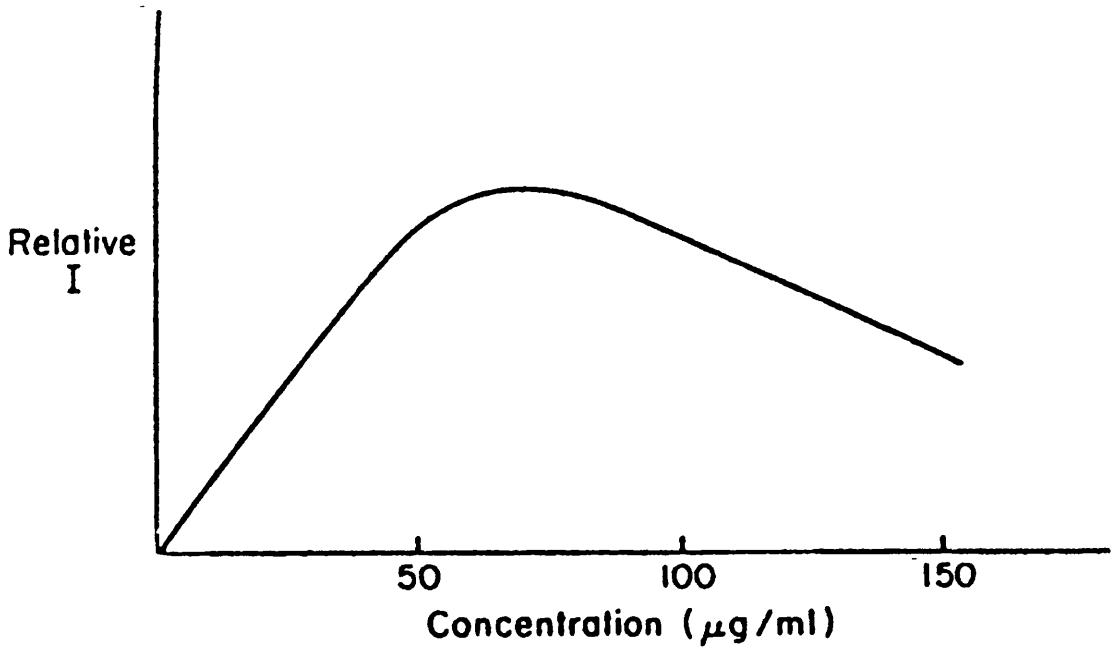

Figure 3: *Effect of fluorophore concentration on relative intensity of fluorescence.*

transient interactions or by formation of non-fluorescent baseline species. Excited molecules may interact to form excimers, excited state dimers that display altered emission spectra. Emitted light from one dye may also be absorbed by a dye with an excitation wavelength close to that emission wavelength. This process (fluorescence resonance energy transfer) is distance dependent.

Fluorescence spectrophotometers contain three basic elements: a light source, a sample holder, and a light detector (Fig 4).

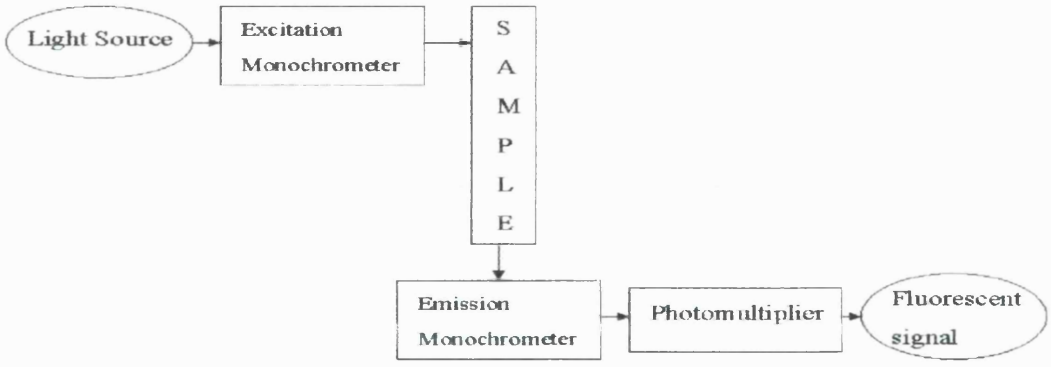

Figure 4: *Schematic representation of a fluorescence spectrophotometer.*

The light source produces photons over a range of wavelengths, typically 200-900 nm. Photons pass through an excitation monochrometer that only transmits light of a specified wavelength (the excitation wavelength). Light exits through adjustable slits that filter radiation outside the range of interest, and passes through the sample cell. The emission monochrometer is positioned at 90° to the light source to reduce the amount of background interference (33). Light again exits via adjustable slits to

enter the photomultiplier tube, where the signal is amplified to produce the fluorescent signal.

Fluorescent techniques have three main advantages over absorption spectroscopy. Firstly, fluorimetry uses two wavelengths rather than the single wavelength used in absorption spectroscopy. Each fluorescent colour has a narrow excitation and emission spectra that permits easy separation. The same sample can be analysed repeatedly with specific excitation and emission filters. Secondly, reading the emitted light at right angles to the exciting light means that there is no background signal from which the fluorescent signal is measured. Thirdly, fluorescent methods have a greater range of linearity. These three factors combined mean that fluorescent techniques have a far higher sensitivity than absorption spectrophotometry.

Practical issues using fluorescence spectrophotometric techniques

1. Quantitation of fluorescence intensity

The fluorescence intensity of a solution is directly proportional to the dye concentration only in dilute samples. If the dye concentration is too great, quenching occurs and the relationship becomes curvilinear. For fluorescent labelled microspheres, standard curves are constructed by analysing serial dilutions of each individual colour in solvent. Standard curves should be constructed for each new batch of microspheres as each microsphere varies in the relative amount of dye attached and in the quantum efficiency of the dye.

2. Background fluorescence

Autofluorescence is the fluorescence emitted by naturally occurring molecules in cells, tissues and biological fluid (31). Most autofluorescence is excited in the near ultraviolet and blue regions of the spectrum (31). The background noise of naturally occurring fluorescence can be minimised by using probes that can be excited at wavelengths above 500 nm (32). Non-specifically bound or unbound probe, and certain solvents can produce reagent background fluorescence.

3. Spectral overlap

For experiments using multiple different fluorescent molecules, maximising the separation of the emission spectra facilitates signal isolation and data analysis. The ideal combination of fluorescent dyes will exhibit strong absorption at a coincident excitation wavelength and well separated emission spectra. In practice, there is little spillover from the emission spectra of one colour into the emission spectra of an adjacent colour. Spillover is a constant percentage of peak emission intensity, does not alter with time, and is dependent on the individual spectrophotometer used. Correction for spectral overlap may be achieved by construction of a spillover matrix for each colour. Spillover can be minimised by the use of narrow excitation and emission slit widths. Alternatively, excitation and emission wavelengths different to those giving the peak readings can be used. Using this method, greater numbers of fluorescent dyes can be accurately resolved (19).

4. Methodological noise

Method noise in fluorescence spectrophotometry consists of variability in the fluorescent spectrophotometer and variability in the operator technique. Cuvette

cleaning, orientation and matching can all affect the background noise of the experiment.

5. Environmental effects

Fluorescence intensity is sensitive to changes in light, pH and temperature (34). Fluorescent dye contained within microspheres is very resistant to light degradation. Once the dye has been extracted in solvent, light stability decreases. Changes in pH alter the fluorescent intensity by changing the ionisable chemical species. For blood flow analysis, a buffering step is used in the processing to reduce the effects of pH variations. Fluorescence intensity decreases as temperature increases due to greater numbers of molecular collisions and quenching. Normal room variations in temperature have minimal effects on commercial fluorescent dyes.

Methods

Fluorescence excitation / emission

Fluorescent labelled polystyrene microspheres of 15 μm diameter (± 3%), in four colours (Table 1), were obtained from Molecular Probes (Eugene, OR, USA). Microspheres had a density of 1.06 g/ml at 20^0C and were suspended in saline with 0.02% Tween-20 and 0.02% thimerosal. Prior to use, microspheres were vortexed vigorously for 15 seconds and then placed in an ultrasonic water bath for 10 minutes.

Table 1: *Excitation and emission wavelengths of fluorescent microspheres in Cellosolve® acetate.*

Colour	Excitation wavelength (nm)	Emission wavelength (nm)
Blue-green	430	457
Green	450	488
Yellow-green	490	506
Orange	530	552

Immediately before experiments, microspheres were removed and again vortexed vigorously. 5 µl of microspheres ($1x10^6$ microspheres per ml) were dissolved in 10ml of Cellosolve® acetate (2-ethoxyethyl acetate, Aldrich Chemical, Milwaukee, WI, USA) to release the fluorescence. Optimum excitation and emission scans for each new batch of fluorescent microspheres were performed using a Perkin-Elmer LS-50B luminescence spectrophotometer (Beaconsfield, Bucks). This has an excitation wavelength of 200-800 nm and emission wavelength of 200-900 nm. A red-sensitive photomultiplier was not available. This machine has a pulsed xenon light that produces a 10 µsec pulse of radiation in 16 msec. A photomultiplier dark current is acquired prior to each lamp pulse and subtracted from that pulse for correction of phototube dark current. Lamp intensity is continuously monitored using a beam splitter to divert part of the emitted light to a sample compartment. The output signal is adjusted to maintain a constant intensity. Excitation and emission slit widths were set at 4 nm for all experiments. Excitation slit width automatically controls the sample photomultiplier tube voltage to provide optimum signal to noise ratio as a function of sample intensity. The spectrophotometer has a wavelength

programme that can perform up to 15 intensity measurements on a single sample at predefined excitation and emission wavelength pairs (wavelength accuracy ± 1 nm). Data were electronically stored (IBM Personal System / 2, Model 55SX). Samples were read in a glass cuvette with a path length of 10mm and a volume of 0.7 ml (Starna Cells, INC., Atascadreo CA, USA). Samples were excited along their entire path length with emitted light read at right angles to the exciting light. Cuvettes were thoroughly washed with methanol between each sample.

Standard curves

Standard curves were constructed for each colour microspheres. The number of microspheres required to yield a fluorescence concentration at the upper limit for the spectrophotometer was calculated. Spheres were dissolved in 10ml Cellusolve® acetate and multiple serial dilutions made. Fluorescence intensities for each dilution were then read and plotted to yield a standard curve. Linearity and concentration ranges for each new batch of microspheres were performed.

Spectral overlap

The spillover of the fluorescent signals into the emission spectra of adjacent colours was measured by studying the fluorescence intensities of pure colours at each pair of excitation and emission spectra used in the experiments. The excitation and emission wavelengths used were those giving maximum fluorescent signals. An overlap matrix for each colour was then constructed.

Machine and operator variability

Control solutions of microspheres were used to ensure minimum machine and operator variability. 10 µl of each colour microspheres were added to 60 ml of Cellusolve® acetate. Samples of this control solution were read in the spectrophotometer immediately prior to, and during each series of experimental samples. The control solution was protected from light when not used. This ensured that the fluorimeter was set up correctly and that the lamp and photomultiplier tube were functioning properly. Machine variability with time was measured by taking multiple readings of the same sample of the control solution without moving the cuvette. Operator variability (adequate cuvette washing and proper orientation within the spectrophotometer) was assessed by examining the measurements for samples of control solution performed during a series of experimental samples.

Solvent blanks

Background fluorescence was measured at the beginning and end of each series of experiments. Samples of pure Cellusolve® acetate were read and the values obtained subtracted from the fluorescence intensities obtained during the experiments.

Results

Emission / excitation scans

Examples of excitation and emission scans for each colour of microspheres are shown in Figs 5-8.

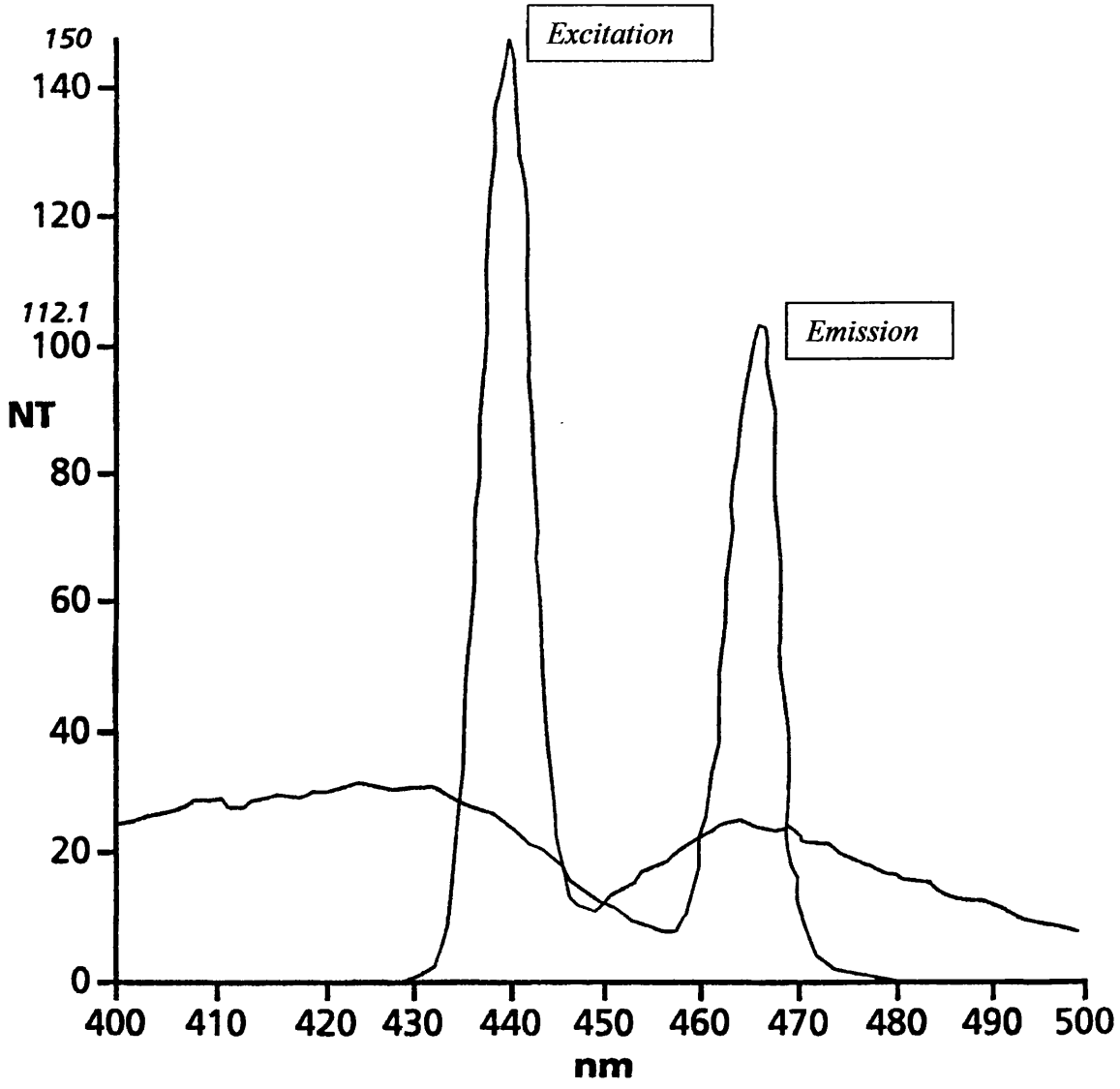

Figure 5: Excitation and emission scans for blue-green microspheres

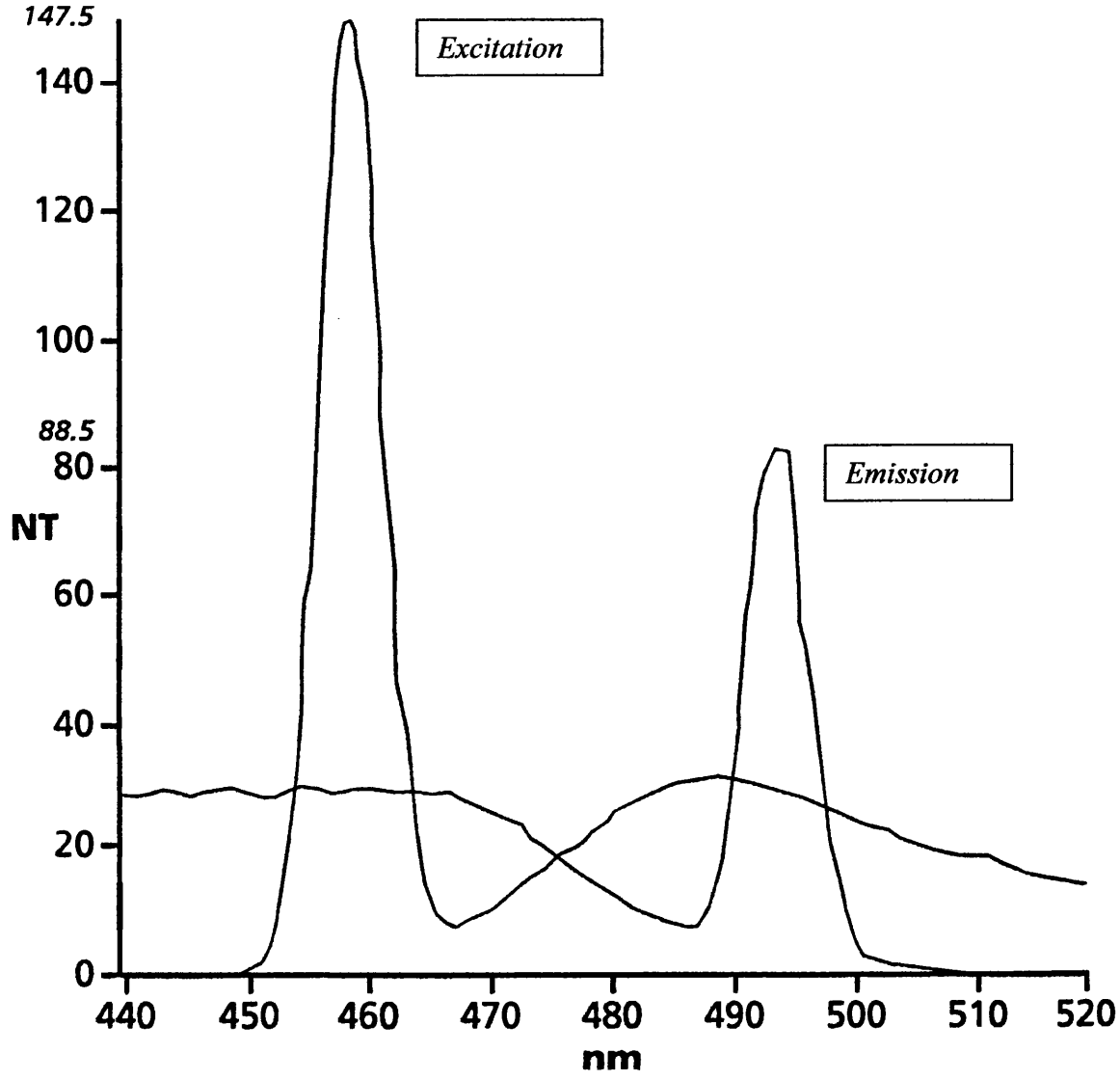

Figure 6: Excitation and emission scans for green microspheres

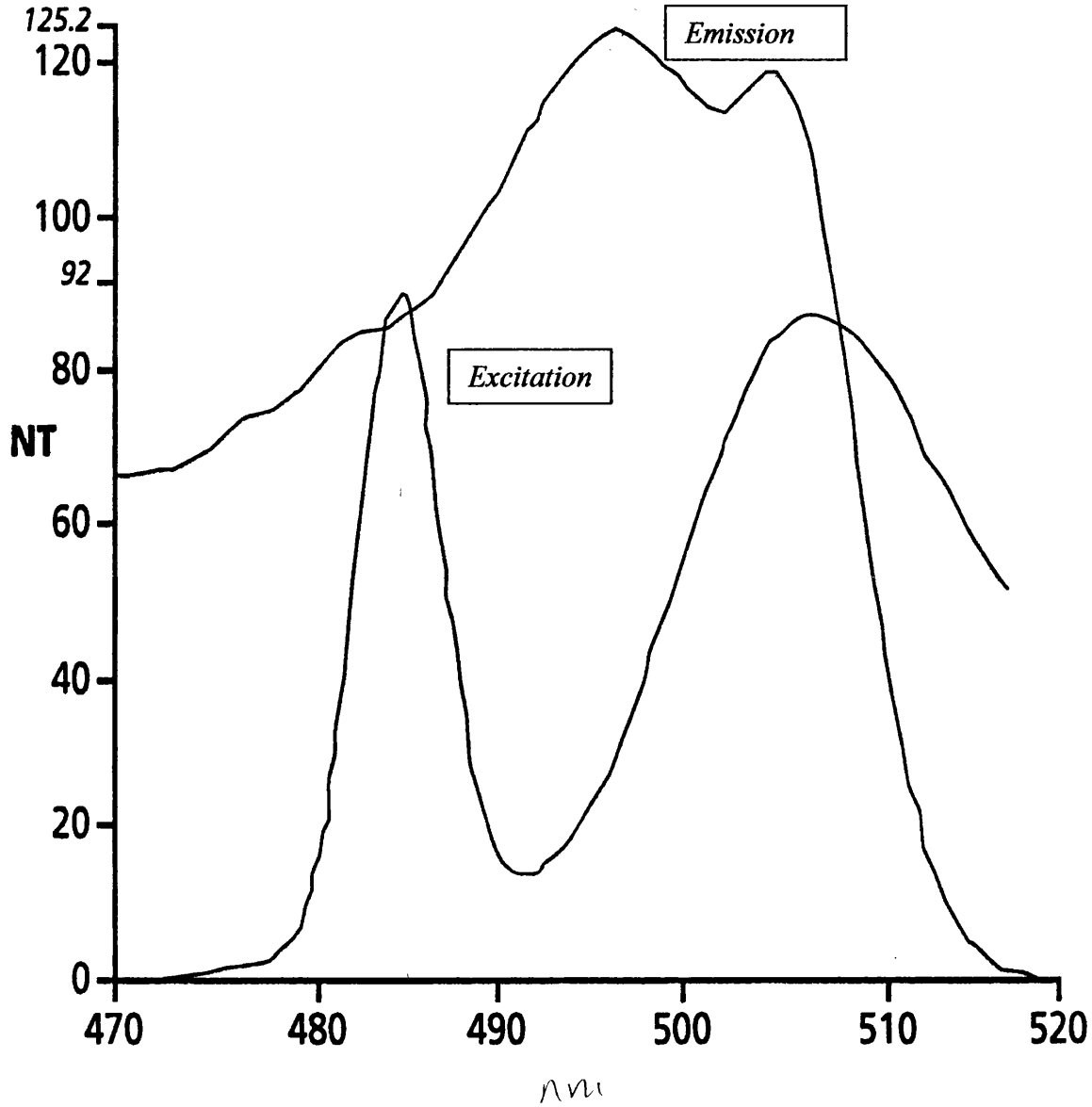

Figure 7: Excitation and emission scans for yellow-green microspheres

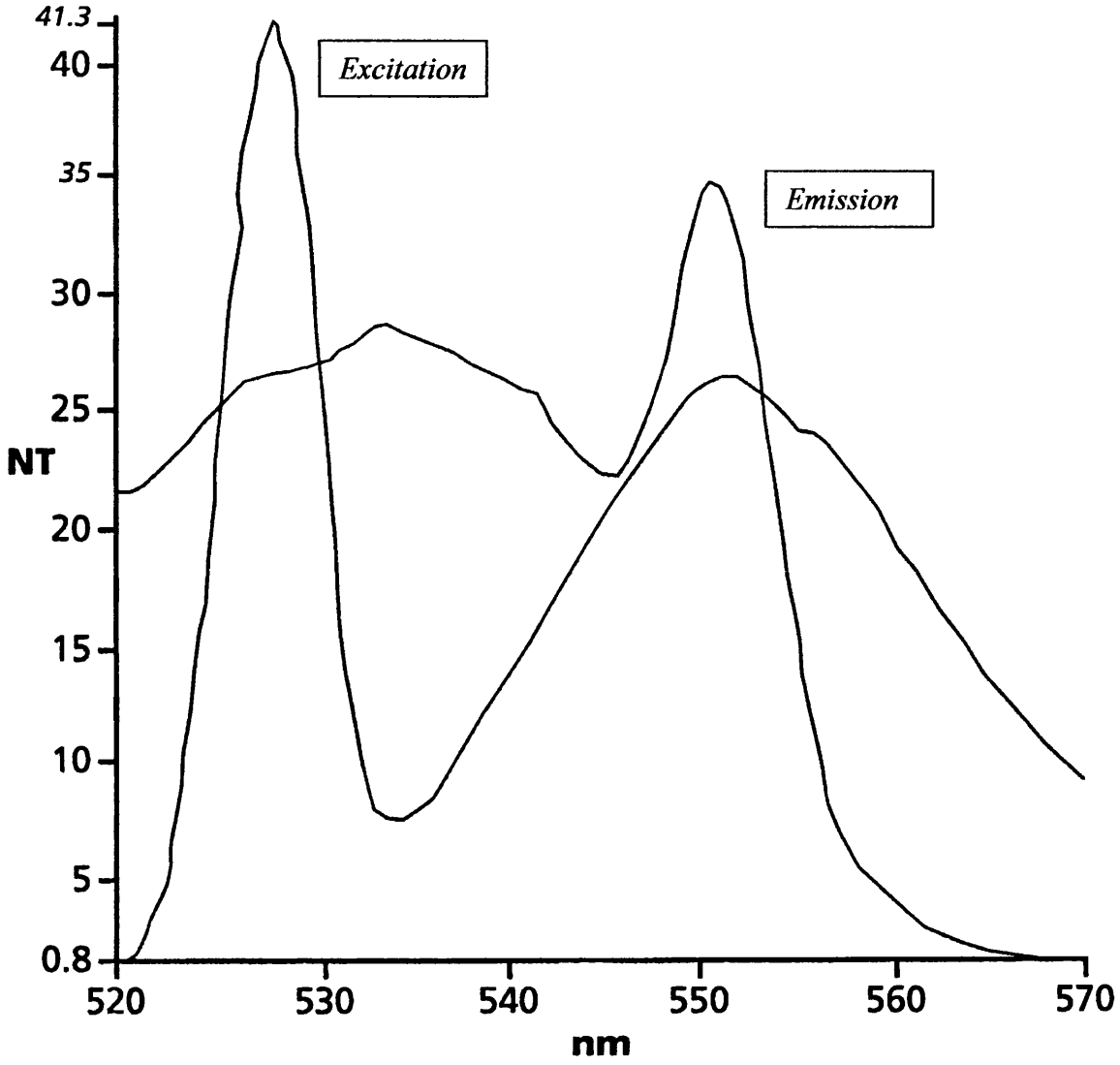

Figure 8: Excitation and emission scans for orange microspheres

Standard curves

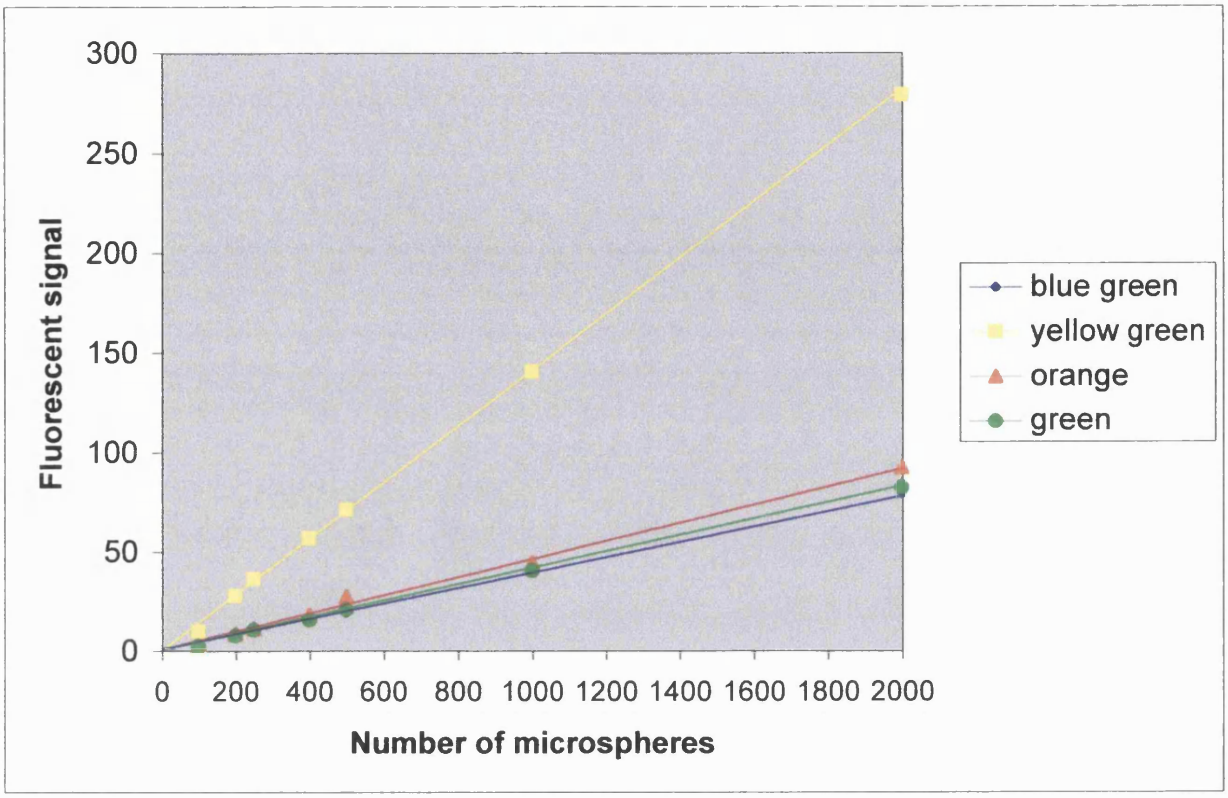

Figure 9: *Fluorescence intensity as a function of the number of microspheres per sample.*

At low concentrations (up to 2000 microspheres per ml of solvent) the fluorescence signal was nearly linear with respect to the number of microspheres in the sample (Fig. 9). At higher concentrations, the relationship became curvilinear, as expected. The linear correlation coefficients (r) were >0.99 for all colours, at the ranges of microsphere numbers used in experiments. The standard error of the estimate (SEE) was determined for each regression analysis to provide a measure of random error. The SEE was 0.43 for blue-green, 2.03 for yellow green, 2.09 for

orange and 0.85 for green. The fluorescence intensity per microsphere was greatest for yellow green and lowest for blue-green and green.

Spectral overlap

Colour	Blue-green	Green	Yellow-green	Orange
Excitation (nm)	430	461	497	534
Emission (nm)	465	493	505	551

	Blue-green % overlap	Green % overlap	Yellow-green % overlap	Orange % overlap
Blue-green	100%	3.6%	0.5%	0%
Green	6.6%	100%	3.3%	0%
Yellow-green	0.3%	5.9%	100%	0.1%
Orange	0.8%	0.3%	0.6%	100%

Table 2: *Spillover matrix of fluorescent colours at optimal excitation and emission spectra.*

The spillover between colours varied from 0-6.6%. The worst cases involved overlap between green and the adjacent colours of blue-green and yellow-green. Overlap into colours beyond those immediately adjacent was <1.0% in all cases.

Machine variability

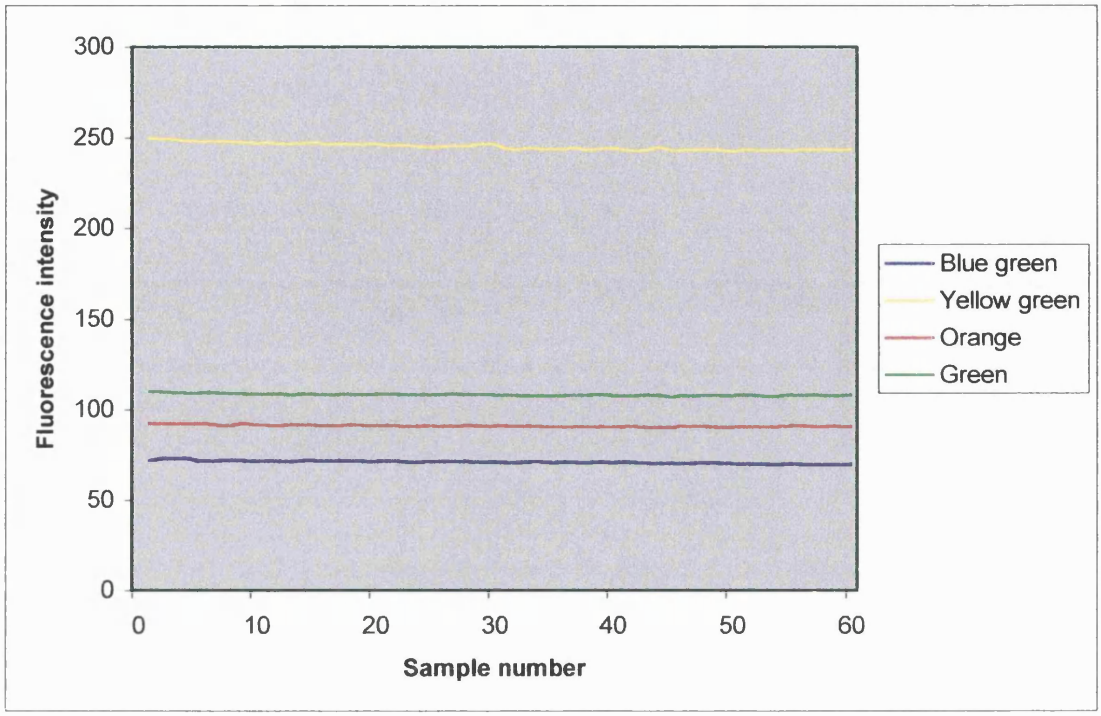

Figure 10: *Example of machine variability from multiple reading of the control solution without moving the cuvette.*

The precision of the fluorescent signal, as assessed by the coefficient of variation (100x std.dev / mean) for repeated measurements of the same sample, ranged from 0.54 to 1.21% when measured on the same day (Table3).

Colour	Mean fluorescent intensity	Std dev	Coefficient of variation
Blue green	70.8	0.86	1.21%
Green	108.2	0.59	0.54%
Yellow green	245.1	1.93	0.78%
Orange	91.1	0.59	1.09%

Table 3: *Machine variability from multiple reading of the control solution*

Operator variability

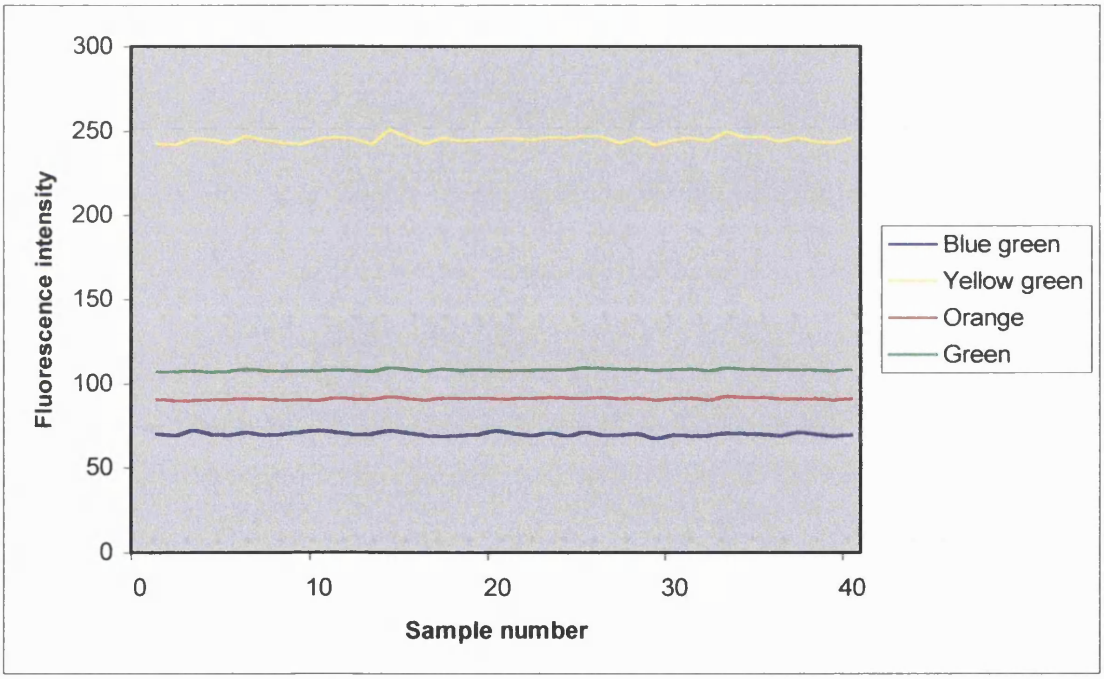

Figure 11: *Example of operator variability with multiple readings of a control solution performed during a series of experimental samples.*

Methodological noise resulting from operator variability had a coefficient of variation of less than 1.0% for all colours with the exception of blue-green which varied up to approximately 2.0% (Table 4).

Colour	Mean	Std dev	Coefficient of variation
Blue green	69.7	1.2	1.72%
Green	107.9	0.71	0.65%
Yellow green	244.9	2.0	0.82%
Orange	91.0	0.67	0.74%

Table 4: *Operator variability from multiple readings of a control solution.*

Solvent blanks

Cellusolve® acetate produced no significant fluorescent signal in the spectra measured.

Discussion

Dye excitation and emission spectra were in accordance with the approximate values supplied by the manufacturers. The linear correlation between amount of fluorescence and number of microspheres per ml indicates that a wide range of blood flows can be accurately measured (19). When very high numbers of microspheres are read (outside the numbers used in these experiments), the relationship between intensity and microsphere numbers is better characterised by a quadratic function

(19). We noted that the greatest variability in fluorescence signal was for the blue-green signal. Glenny et al found that the coefficient of variation for fluorescence intensity per microsphere was also highest for the blue-green microspheres (19).

The minimal spectral overlap between fluorescent dyes is a significant advantage over radioactive or coloured microspheres (35,12). The Fluorescent Microsphere Resource Center recommends particular combinations of colours to minimise spillover and prevent the need for correction (34). van Oosterhout et al showed that up to five fluorescent dyes could be used in the same experiment without the need for spectral spillover correction (36). Absence of a red sensitive photomultiplier meant that, for our experiments, dyes with an emission wavelength longer than orange could not be used. With the colours available, spillover was greatest between green and blue-green (6.6%). Glenny et al reported a spillover from green into blue-green of 8%, and from green into yellow-green of 8.8% (19). In subsequent experiments in this series, mathematical correction was performed in all instances where overlap was greater than 1%.

Measurement of fluorescence intensity is very precise, as demonstrated by the very small coefficient of variation when a single sample is read multiple times. A coefficient of variation ranging from 0.2-1.7% for each colour and dilution was reported by Glenny et al (19). Variation increases if samples are read over a number of days but remains small (19,34). In all subsequent studies, the fluorescence of tissue and arterial reference samples were performed on the same day. Methodological noise may be checked using a commercially available software program that compares current control intensities to past control intensities, notifying

the operator if they differ by greater than 5% (37). We achieved very satisfactory operator technique, with a coefficient of variation of <2%, without the use of this program. This compares favourably with that previously reported (37).

Significant background fluorescence in the blue wavelength range resulting from either Cellusolve acetate® or Tween 80 have previously been noted (19,37). We found no signal from Cellosolve acetate® in the wavelengths used.

Spectrophotometry provides a precise method of measuring fluorescence. With the numbers of fluorescent microspheres used for blood flow experiments, the technique provided a linear measure with respect to the number of microspheres per sample. Measurement of fluorescence intensity is very accurate as demonstrated by the low machine variability. In addition, we were able to obtain excellent operator variability. Multiple colours could be easily separated, allowing up to three measurements of perfusion in a single experiment, with a fourth colour being used as an internal standard.

Chapter 4: Inter- and intra-animal variability in baseline organ blood flows in rats.

Introduction

Use of microspheres to measure regional blood flow assumes that the microspheres are uniformly distributed following injection into the circulation and that their distribution to tissues is in proportion to the blood flow to that tissue (2). Microspheres should be totally extracted in their first transit through the capillary bed and should not alter systemic or regional haemodynamics (2).

The uniformity of mixing of microspheres and their evenness of distribution may be assessed by comparing the concentrations of microspheres in arterial blood samples collected simultaneously from several different arteries. Such studies have been performed in a number of different animal models (3). Evenness of distribution may also be studied by comparing the number of microspheres per gram of tissue for paired organs. Comparisons of the right and left cerebral hemisphere, or the right and left kidney, provide a simple internal assessment for individual studies (3).

Acute haemodynamic disturbances are uncommon following microsphere injection. The incidence of changes depends on the size of the animal and the number and size of the microspheres injected (3). In rats, significant reductions in heart and kidney blood flows occur when large numbers of microspheres are injected (21). The use of either dextran or Tween 80 as suspension agents for microspheres has also been associated with significant haemodynamic effects (22, 24).

Temporal perfusion heterogeneity is the change in regional blood flow occurring over a period of time. Variation in flow has been seen in the myocardium and is believed to be a component of autoregulation (38). In assessing the use of fluorescent microspheres for measurement of regional blood flow it is important to know the amount of variation in baseline blood flow that might be expected due to temporal heterogeneity.

The primary purposes of this study were to examine the inter-animal variation in baseline blood flow and the temporal variation in organ blood flows. We also sought to examine the uniformity of mixing of microspheres by comparison of paired organ blood flows, and the effects of injection of fluorescent microspheres on central haemodynamic variables and regional blood flow distribution.

Methods

The protocol for this study was approved by the Animal Care Committee of Albert Einstein Medical Center, Philadelphia. All work was conducted in accordance with the 'Guide for the Care and Use of Laboratory Animals' prepared by the National Research Council of the NIH (NIH publication 86-32, revised 1985).

Animal preparation

Adult, male Sprague-Dawley rats (mean weight 465 g, SD ± 31 g) maintained on food and water ad libitum were used for this study. Animals were anaesthetised with ketamine (150 mg/kg intra-peritoneally [ip]). Preliminary studies had shown that this maintained anaesthesia for the duration of the experiment. A tracheostomy was

performed and the trachea was intubated with PE-200 tubing to facilitate spontaneous breathing. Animals were maintained on room air. The right femoral artery and the right carotid artery were cannulated with PE-50 tubing and on-line pressure recording continuously monitored and recorded (BioWindow®, Modular Instruments, Malvern, PA, USA). The femoral arterial catheter was used for the measurement of arterial blood pressure and withdrawal of the reference blood sample. The right carotid arterial catheter was advanced into the left ventricle for the injection of microspheres. Position was confirmed by characteristic waveform analysis. A lead II electrocardiogram was also continuously recorded (BioWindow®, Modular Instruments, Malvern, PA, USA). Rectal temperature was monitored (Synergy® Temperature Monitor, American Pharmaseal Company, Valencia, CA, USA) and temperature maintained at 36.5-37.5^{0}C by the use of heating lamps. Animals were allowed to stabilise for 15 minutes following surgery and then baseline haemodynamic data were collected for 10 minutes.

Preparation of microspheres

Fluorescent microspheres (Molecular Probes, Eugene OR, USA) of 15 μm diameter were vortexed thoroughly for 30 seconds and then placed in an ultrasonic bath for ten minutes. The vial was then vortexed for a second time immediately prior to injection.

Inter-animal variation in baseline blood flow

Following collection of baseline haemodynamic data, 0.2 ml of blue-green fluorescent microspheres (1.0 x 10^6 microspheres per ml) were injected into the left ventricle over a period of three seconds. This was followed by a 0.3 ml saline flush.

Reference blood samples were withdrawn from the right femoral artery commencing five seconds prior to the injection of fluorescent microspheres and continuing for thirty seconds after the flush of microspheres into the animal. Blood was withdrawn at the rate of 0.5 ml/min using a Harvard pump (Harvard Apparatus, South Natick, MA, USA) into a heparinised syringe. Animals were killed after ten minutes by means of an overdose of ketamine. Organs were removed and weighed (Metler H54AR, Metler Instrument Corp., Hightstown, NJ, USA, accuracy ± 0.001 g).

Temporal intra-animal variation in baseline blood flow

Three colours of fluorescent microspheres (blue-green, yellow-green, and orange) were injected into the left ventricle at intervals of ten minutes. Each injection was of 0.2 ml (1.0×10^6 microspheres per ml) and was followed by a 0.3 ml saline flush. Reference blood sampling was performed as described above. Animals were euthanised and organ retrieval performed in the manner described above.

Recovery of microspheres and fluorescent dye extraction

These were performed according to the methods recommended by the Fluorescent Microsphere Resource Center (39). Reference blood samples were transferred into labelled vials for further processing. The femoral arterial catheter and the withdrawal syringe were rinsed thoroughly with 2% Tween-80® (Fisher Scientific Co., Pittsburgh, PA, USA) and the rinse added to the blood sample. Prior to digestion, 100 µl of a standard solution of green microspheres (1×10^3 microspheres) was added to each sample vial using a Pipetman pipette (Rainin Instrument Company, Woburn, MA, USA). This colour acted as the internal standard to ensure that there was no loss of microspheres during recovery (29).

Blood samples were digested by adding 10 ml of 16N KOH to each 30 ml of diluted blood. Organ samples were digested by adding 5-10 ml of 4N KOH per 1-2 g of solid tissue. Samples were kept in the dark for 24 hours to allow complete digestion. Following digestion, the blood and tissue pieces were individually filtered through 10 μm pore polycarbonate filters (Poretics, Livermore, CA, USA) using negative pressure. The digestion vials and the burette were then washed with 2.0% Tween 80® and the washings filtered through the same filter to recover any residual material. The filter was then removed carefully using forceps and placed into an individual polypropylene test-tube. 1.25 ml of Cellusolve acetate® were then added to each tube using a calibrated pipette (Eppendorf Repeater Pipet, Brinkmann Instruments Ltd., Mississauga, ON, USA, precision <0.05-0.1%). After 4-8 hours, the tubes were vortexed vigorously and a sample of the solution was pipetted into a glass cuvette (0.7 ml volume, 10 mm path length, Starna Cells, INC., Atascadreo CA, USA). Sample fluorescence was measured using a Perkin-Elmer LS-50B luminescence spectrophotometer (Beaconsfield, Bucks) with excitation and emission slit widths of 4 nm. Sample loss during extraction was corrected by comparing the value of the fourth colour in the sample to the true value for the internal standard.

Tissue blood flows were calculated using the following formula:

$$\text{Blood flow (ml/min/g)} = \frac{\text{Fluorescence signal of sample} \times \text{Reference flow rate (ml/min)}}{\text{Fluorescence signal of reference} \times \text{Weight of sample (g)}}$$

Systemic haemodynamics

Systolic blood pressure, heart rate and left ventricular contractility (dP/dt / P - the ratio of dP/dt to arterial pressure) were recorded at five second intervals throughout the experiment. Mean values for consecutive one-minute intervals were calculated. Values for the five minutes immediately prior to the first injection of microspheres were combined to give a baseline value. The percentage variation from baseline for each subsequent minute interval was then calculated.

Statistics

Statistical analyses were performed using Excel software (Microsoft Corporation, Roselle, IL, USA) and SPSS statistical software (version 9.0, Chicago, IL, USA). Organ blood flows and microsphere recovery rates are expressed as mean ± 95% CI for inter- and intra-animal variability. Paired organ samples were compared using the 95% confidence intervals of the differences between the samples (expressed as the percentage differences). Comparison of systemic haemodynamics before and after microsphere injection was assessed by the percentage variation (mean and 95% CI) from baseline at minute intervals.

Temporal variation was assessed using analysis of covariance. Analysis of variance (ANOVA) results were adjusted for the linear relationships between the dependent variable (blood flow) and the covariates (blood pressure, heart rate, dP/dt / P). The mean and 95% CI for the differences between mean adjusted blood flows at each time point are given.

Results

Inter-animal variability.

The inter-animal variation in baseline organ blood flows is shown in Table 1. The highest variability between animals was seen in the lungs (R 37%, L 41%) and the adrenal glands (R 24%, L 29%). For the remaining organs the 95% CI of variation ranged from 10-22%. The mean percentage difference between the right and left kidneys was 1% ± 5% (mean and 95% CI). Microsphere recovery rates were high and showed no significant differences between organs studied.

Table 1: *Inter-animal variation in baseline organ blood flow (mean ± 95% CI) and recovery of microspheres (mean ± 95% CI), (n=33).*

Organ (n=33)	Blood flow ml/min/g	% recovery	Organ	Blood flow ml/min/g	% recovery
Heart	301 ± 49	89 ± 4	Spleen	130 ± 14	91 ± 4
R lung	71 ± 26	88 ± 6	Liver	23 ± 3	92 ± 8
L lung	58 ± 24	91 ± 6	Duodenum	310 ± 37	90 ± 4
R kidney	556 ± 56	88 ± 6	Jejunum	219 ± 49	89 ± 4
L kidney	554 ± 58	93 ± 5	Ileum	121 ± 20	89 ± 4
R adrenal	534 ± 126	92 ± 5	Colon	63 ± 13	93 ± 7
L adrenal	401 ± 118	90 ± 4	Diaphragm	49 ± 7	99 ± 4
Cortex	92 ± 14	89 ± 4	Skel. muscle	10 ± 2	90 ± 4
Hindbrain	67 ± 7	89 ± 4			

Temporal variation in organ blood flow

Temporal variations in absolute organ blood flows are shown in Table 2. The percentage variations in organ blood flows (mean and 95% CI) between each time point are shown in Table 3. For kidney samples the percentage differences between right and left kidney at each time point were (mean and 95% CI) –4% ± 6% at baseline, 0% ± 16% at 10 minutes and 1% ± 11% at 20 minutes.

Organ (n=9)	0 mins ml/min/100g	10 mins ml/min/100g	20 mins ml/min/100g	% recovery
Heart	353 ± 110	464 ± 131	439 ± 100	91 ± 8
R lung	72 ± 36	73 ± 31	62 ± 26	96 ± 13
L lung	51 ± 19	57 ± 24	45 ± 18	97 ± 10
R kidney	484 ± 109	577 ± 176	460 ± 105	93 ± 14
L kidney	470 ± 119	565 ± 182	465 ± 118	94 ± 19
R adrenal	437 ± 105	649 ± 251	401 ± 129	96 ± 6
L adrenal	341 ± 166	484 ± 192	374 ± 145	97 ± 5
Forebrain	109 ± 28	156 ± 27	140 ± 34	97 ± 48
Hindbrain	77 ± 19	103 ± 21	92 ± 28	97 ± 8
Spleen	107 ± 24	126 ± 21	103 ± 24	98 ± 10
Liver	13 ± 2	19 ± 4	17 ± 4	99 ± 8
Duodenum	261 ± 47	319 ± 85	289 ± 54	93 ± 6
Jejunum	159 ± 29	158 ± 43	192 ± 30	96 ± 4
Ileum	110 ± 32	126 ± 44	114 ± 30	94 ± 10
Colon	47 ± 23	88 ± 61	46 ± 19	94 ± 7
Diaphragm	50 ± 14	53 ± 13	52 ± 13	96 ± 11
Skel. muscle	14 ± 8	16 ± 10	16 ± 10	109 ± 19

Table 2: *Temporal variation in organ blood flow (mean ± 95% CI) and % recovery of microspheres (mean ± 95% CI) (n=9)*

Organ (n=9)	0 to 10 mins % variation	0 to 20 mins % variation	10 to 20 mins % variation
Heart	42 ± 40 ($p<0.05$)	33 ± 27 ($p<0.05$)	-2 ± 13
R lung	10 ± 28	-8 ± 22	-14 ± 16
L lung	15 ± 33	-10 ± 33	-21 ± 21
R kidney	19 ± 24	-3 ± 19	-16 ± 17
L kidney	19 ± 20	1 ± 16	-14 ± 12 ($p<0.05$)
R adrenal	57 ± 34 ($p<0.05$)	-5 ± 16	-35 ± 12 ($p<0.05$)
L adrenal	31 ± 43	3 ± 31	-18 ± 12
Forebrain	56 ± 44 ($p<0.05$)	36 ± 33 ($p<0.05$)	-10 ± 17
Hindbrain	39 ± 24 ($p<0.05$)	20 ± 24	-11 ± 17
Spleen	23 ± 25	-2 ± 18	-18 ± 19
Liver	41 ± 40 ($p<0.05$)	28 ± 29	-5 ± 19
Duodenum	26 ± 39	15 ± 28	-5 ± 15
Jejunum	0 ± 16	25 ± 20 ($p<0.05$)	28 ± 22 ($p<0.05$)
Ileum	21 ± 48	11 ± 36	-1 ± 22
Colon	87 ± 70 ($p<0.05$)	12 ± 35	-30 ± 21 ($p<0.05$)
Diaphragm	16 ± 40	10 ± 25	2 ± 21
Skel. muscle	50 ± 95	-3 ± 42	-28 ± 22

Table 3: *Percentage variation in organ blood flows between each time point (mean and 95% CI).*

Systemic haemodynamics

1. Systolic blood pressure

Table 4 shows the percentage variation (mean and 95% CI) from baseline values (-5 to 0 mins) for each minute. Fluorescent microspheres were injected at 0, 10 and 20 mins.

Time (min)	% variation	Time (min)	% variation
1	0.7 ± 4.9	13	4.6 ± 11.1
2	-1.4 ± 5.6	14	3.9 ± 10.7
3	0.7 ± 5.7	15	3.9 ± 11.5
4	1.9 ± 5.5	16	2.9 ± 12.1
5	2.3 ± 6.1	17	3.4 ± 12.7
6	2.8 ± 6.3	18	4.2 ± 13.1
7	2.9 ± 6.4	19	4.8 ± 13.0
8	3.2 ± 6.2	20	5.3 ± 13.1
9	4.3 ± 6.7	21	4.2 ± 12.5
10	4.6 ± 6.8	22	5.1 ± 11.7
11	4.8 ± 7.4	23	3.4 ± 13.0
12	4.7 ± 10.9	24	7.3 ± 14.5

Table 4: *Percentage variation in systolic blood pressure compared to baseline over time (mean and 95% CI, n=9)*

Figure 1 shows the absolute values for systolic blood pressure (mean and 95% CI) at each minute interval. No significant changes were observed following injection of microspheres. There was a trend toward a higher systolic blood pressure with time but this was not significant.

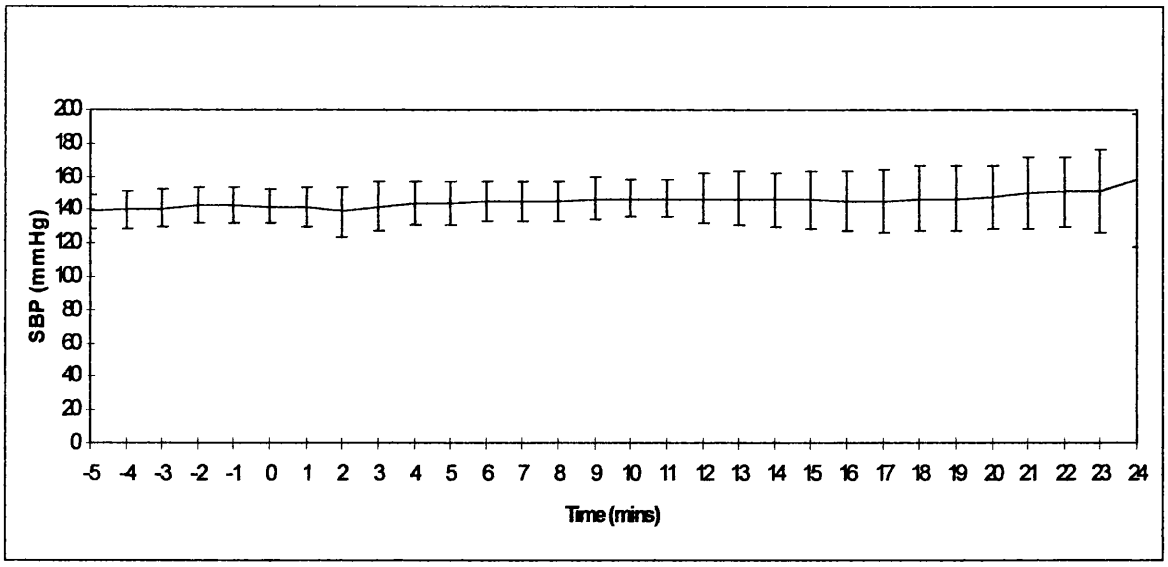

Figure 1: *Systolic blood pressure over time (mean ± 95% CI, n=9). Fluorescent microspheres were injected at time 0, 10 and 20 mins.*

2. Heart rate

Table 5 shows the percentage variation (mean and 95% CI) from baseline values for each minute. Figure 2 shows the absolute values (mean and 95% CI) at minute intervals. No significant differences in heart rate were observed during the experiment although there was a non-significant trend towards an increase with time.

Time (min)	% variation	Time (min)	% variation
1	1.9 ± 2.3	13	7.5 ± 10.3
2	1.7 ± 3.6	14	6.4 ± 10.7
3	1.3 ± 5.8	15	6.5 ± 11.4
4	3.0 ± 5.7	16	5.6 ± 12.0
5	3.2 ± 6.5	17	6.3 ± 12.0
6	3.5 ± 7.2	18	6.9 ± 12.4
7	4.8 ± 7.8	19	7.1 ± 12.8
8	5.5 ± 8.5	20	8.3 ± 13.1
9	6.3 ± 9.7	21	10.9 ± 15.3
10	7.0 ± 9.7	22	11.1 ± 16.2
11	7.1 ± 9.0	23	7.4 ± 21.0
12	8.1 ± 9.6	24	7.3 ± 33.5

Table 5: *Percentage variation in heart rate (mean and 95% CI, n=9) at minute intervals. Fluorescent microspheres were injected at time 0, 10 and 20 mins.*

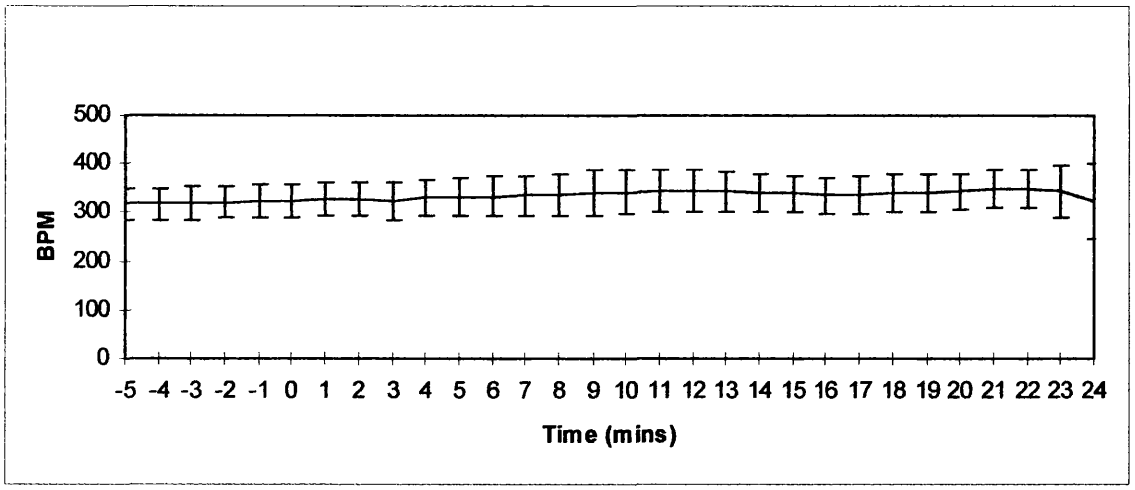

Figure 2: *Heart rate over time (mean and 95% CI, n=9).*

3. Left ventricular dP/dt / P

No significant changes were noted in LV dP/dt / P over time. Table 6 shows the percentage variation from baseline (mean and 95% CI, n = 9) for each minute interval. Figure 3 shows the absolute value at each minute (mean and 95% CI, n = 9).

Time (min)	% variation	Time (min)	% variation
1	11 ± 12	13	15 ± 16
2	13 ± 13	14	15 ± 15
3	14 ± 13	15	15 ± 15
4	13 ± 12	16	15 ± 16
5	15 ± 14	17	16 ± 16
6	16 ± 14	18	17 ± 18
7	17 ± 14	19	15 ± 17
8	18 ± 15	20	16 ± 18
9	17 ± 15	21	14 ± 19
10	17 ± 15	22	15 ± 18
11	16 ± 15	23	10 ± 15
12	16 ± 15	24	11 ± 20

Table 6: *Percentage change in left ventricular dP/dt / P at minute intervals compared to baseline period (mean and 95% CI, n=9).*

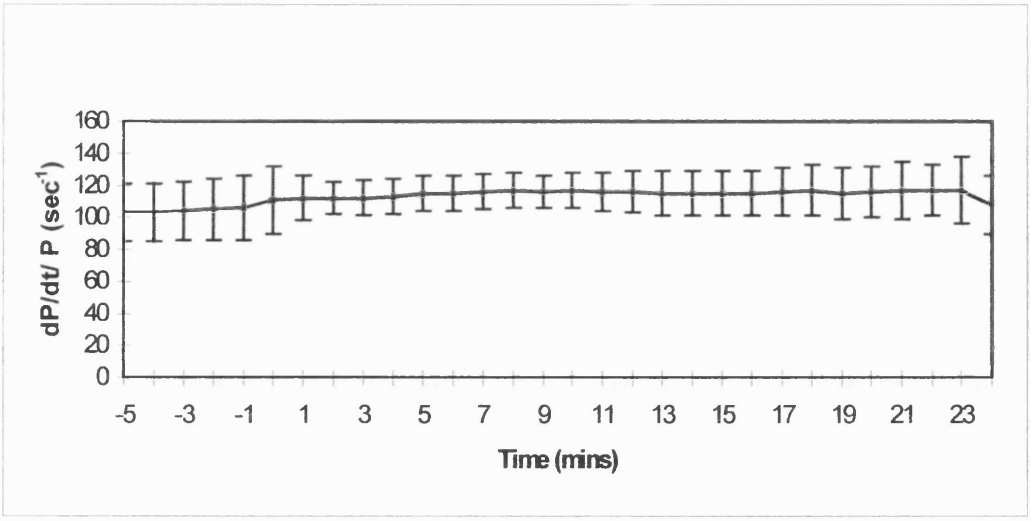

Figure 3: *Left ventricular dP/dt/ P over time (mean and 95% CI, n=9). Fluorescent microspheres were injected at 0, 10 and 20 mins.*

Analysis of covariance

Using blood flow as the dependent variable and blood pressure, heart rate and dP/dt / P as the covariants, significant relationships were found between blood flow and one or all covariant for heart (significance of F=0.008), right kidney (0.003) and left kidney (0.005). No significant differences between the group mean blood flow at any timepoint were found for either heart, right kidney or left kidney after the regression factors were excluded.

what regression factors?

Relationship correlations between blood flow to each organ and the covariants are shown in Table 7. Adjusted mean organ blood flows (after removal of the effects of the covariants) for each organ are given in Table 8.

explain ff in detail

Dependent variable	BP	dP/dt / P	Heart rate
Heart blood flow	0.878	0.356	0.647
R kidney blood flow	0.775	0.797	0.271
L kidney blood flow	0.772	0.795	0.212

Table 7: *Relationship correlations between organ blood flow and the covariants (BP, dP/dt / P and heart rate)*

Timepoint	Heart Obs mean	Heart Adj mean	R kidney Obs mean	R kidney Adj mean	L kidney Obs mean	L kidney Adj mean
Baseline	3.53	3.66	4.84	5.13	4.70	4.98
10 mins	4.64	4.61	5.77	5.63	5.65	5.52
20 mins	4.39	4.29	4.60	4.45	4.65	4.51

Table 8: *Observed and adjusted mean blood flows for heart and kidneys (ml/min/g)*

adjusted how?

The temporal variation in adjusted mean blood flow for each organ is shown in Table 9. There were no significant differences between the adjusted mean blood flows for any time point for all organs studied.

1. Heart

	Adj mean BF	% diff from baseline	% diff from 10 mins
Baseline	3.66		
10 mins	4.61	26 ± 34	
20 mins	4.29	17 ± 33	7 ± 26

2. R kidney

	Adj mean BF	% diff from baseline	% diff from 10 mins
Baseline	5.13		
10 mins	5.63	10 ± 27	
20 mins	4.45	13 ± 27	21 ± 24

3. L kidney

	Adj mean BF	% diff from baseline	% diff from 10 mins
Baseline	4.98		
10 mins	5.51	11 ± 30	
20 mins	4.51	9 ± 30	18 ± 27

Table 9: *Temporal variation in adjusted mean blood flow (% differences, mean and 95% CI)*

Discussion

Microspheres are widely used for the measurement of regional blood flows and cardiac output. A number of methodological factors must be considered in assessing the accuracy of calculated values of regional blood flow as determined by the microsphere technique. The number of microspheres injected, the volumes of fluid introduced during sphere injection and withdrawn to obtain the reference sample, and the site of injection may all influence the measured blood flows (21, 40, 41).

The number of microspheres required to produce accurate blood flow measurements without disturbing systemic haemodynamics to any significant degree is unclear. Tsuchiya et al reported that, in rats, injections of greater than 100,000 microspheres produced significant changes in oxygen consumption, cardiac output, mean arterial pressure, heart rate, total peripheral resistance and AV blood oxygen content difference (41). Tuma et al found that calculated blood flows to the heart and kidneys were significantly lower when 375,000 microspheres were injected compared to either 60,000 or 100,000 (21). No differences were found in flows to other organs. In contrast, Hoffman et al demonstrated that over 300,000 microspheres could be injected into the rat with no significant changes in global haemodynamics or organ blood flows (42). Flaim et al found that injections of up to 850,000 microspheres suspended in isotonic saline plus Tween, could be given without significant effect on heart rate or mean arterial pressure (24). 10% dextran plus Tween, the microsphere suspending solution used by Tsuchiya et al, caused significant haemodynamic effects when injected into animals suggesting that it may be the suspending solution itself

rather than the microspheres that affects haemodynamics (41). Similar findings have been reported in dogs (22).

In the first part of this study we used a single injection of 200,000 microspheres suspended in 0.15 M sodium chloride solution with 0.02% Tween-20 and 0.02% thimerosal. Preliminary experiments had shown that this number was required to obtain accurate measurements of fluorescence in the tissues of interest. In the second series of experiments, three injections of 200,000 microspheres were used. No significant changes in systemic blood pressure, heart rate or left ventricular dP/dt / P were seen during the experiments compared to baseline values. These findings support the work of Flaim et al (24) suggesting that the limit of 100,000 set by Tsuchiya et al (10) is an underestimate. Volume loss due to reference sample withdrawal has been shown to affect cardiac output, gastric and pancreatic blood flows in dogs (43). Close attention should be made to matching volume withdrawal with volume replacement (21). In the current experiments, volume was replaced with isotonic saline. It should be noted that in both of the current studies only gross measurements of haemodynamic status were made. More detailed analysis of regional haemodynamics or measurements of organ metabolic functions may have revealed differences.

Microspheres may be injected into the left atrium, the left ventricle or the ascending aorta (21, 40). Wicker and Tarazi found that variability in coronary blood flow was greater if the microspheres were injected into the left ventricle compared to left atrial injection (40). No significant differences between the two injection sites were found in cardiac output measurements or more distal organ blood flows. Intra-

aortic injection of microspheres was found to underestimate brain blood flow due to incomplete mixing of microspheres before the origin of the left carotid artery (21). Measured blood flows to more distant organs showed no differences whether microspheres were injected into the aorta or the left ventricle. Evenness of mixing of the microspheres in these experiments can be assessed by comparison of the blood flows to the right and left kidneys (3, 42). The mean percentage difference between paired kidney samples in these experiments was small, suggesting that, at least at the level of the renal arteries, microspheres were well mixed and evenly distributed throughout the blood stream.

Inter-animal variability in baseline organ blood flow in these experiments was low. The greatest variability was seen in samples from the lungs (95% CI for dispersion; 39%) and the adrenals (95% CI for dispersion; 27%). For the remaining tissues the 95% confidence intervals for dispersion ranged from 10% to 22%. Lung blood flow in this protocol refers to the microspheres delivered through both the bronchial circulation and the pulmonary artery, the latter after shunting through arteriovenous anastomoses. Non-entrapment of 15 μm microspheres in the systemic circulation is generally small but may be altered by elevation of $PaCO_2$ or acidosis (2,26). Measurements of arterial blood gases were not made during these experiments. Lung variability may also result from variations in the amount of lung water. Since this method of organ blood flow measurement is based on fluorescence per gram of tissue, it is possible that variability may be improved by air drying of lung tissue. In experiments using samples of lung tissues rather than whole organ samples, samples should be taken from similar areas of tissue as considerable heterogeneity of pulmonary perfusion exists within isogravitational planes (44). Adrenal samples in

these experiments are likely to be at the limit of accurate weighing and this may account for the increased variability.

Temporal variation in organ blood flow may result from changes in systemic haemodynamics during the experiments, alteration in regional perfusion due to injection of the microspheres, or from inherent variation in blood flow in the animal. In these experiments temporal variation was highest between the first and second microsphere injection for the heart, and between the second and third injections for kidney tissue. Sasaki et al found that distribution of cardiac output as measured by two injections of 2-3 x 10^3 microspheres (50 μm diameter) was similar for all organs except the kidneys (45). The percentage of cardiac output to the kidneys was always higher with the second injection. They postulated that the first injection of microspheres produced small infarcts leading to a compensatory increase in renal blood flow at the time of the second injection. von Ritter et al performed multiple consecutive blood flow measurements in dogs (43). They injected 1x10^6 microspheres at times 0, 30, 90 and 120 minutes. Significant decreases in cardiac output and gastric mucosal blood flows were noted at 120 minutes. Non-significant increases were seen in cardiac and pancreatic blood flows at 30, 90 and 120 minutes and in renal blood flows at 90 minutes. Marcus et al reported an average range of perfusion in left ventricular samples of 26 ± 2.7% (mean ± SEM) for sequentially injection of microspheres in dogs (46). It should be noted, however, that they excluded 11% of their data because values deviated from their respective intra-animal mean perfusions by greater than 25%. Sestier et al obtained a coefficient of variation of 11.1 ± 1.0% between microsphere injections in their study of perfusion heterogeneity of canine myocardium (38). They suggested that there are regional

variations in flow to the myocardium, both spatially and temporally, and that temporal variation was affected by autoregulation.

We found that high numbers of microspheres were required to obtain adequate signals from tissues receiving relatively low blood flow such as muscle. This may have contributed to the temporal variability that we observed in our experiments. Increasing the amount of fluorescence per microsphere will reduce the number of microspheres required. Tissue and blood samples should, however, receive a minimum of 400 microspheres per sample. It may be impossible to measure blood flow to organs such as resting skeletal muscle without altering blood flow to organs such as the heart and kidneys (21).

In summary, these studies have demonstrated the heterogeneity of organ perfusion that exists in anaesthetised rats studied under basal conditions. Whatever the mechanism of temporal heterogeneity, it needs to be considered whenever organ blood flow is being evaluated in response to interventions; changes may result from temporal heterogeneity, to the intervention being studied, or to both.

Chapter 5: Changes in organ blood flow during haemorrhagic shock in rats.

Introduction

A stress response may be initiated by acute blood loss, trauma, hypoxia, acidosis or hypothermia. The response involves an initial phase characterized by hypovolaemia, low blood flow, and early compensatory changes to shock. Following resuscitation and reperfusion, there is a hyperdynamic response lasting for days to weeks. Finally, there is an anabolic phase characterised by normalisation of haemodynamics, diuresis and restoration of body protein and lipid stores (47-49). Loss of circulating blood volume leads to an immediate neuroendocrine response and sympathetically mediated vasoconstriction (50). Arterial vasoconstriction is not uniform as perfusion to the heart and brain is maintained at the expense of perfusion to other organs (51). This response depends on both the volume of blood lost and the rate at which blood loss occurs (52, 53). With persistent shock, vasodilatation occurs and there is progressive decompensation (48, 54). Even massive volume resuscitation may fail to restore organ perfusion.

Animal models of haemorrhagic shock can be divided into three major categories (55). In constant pressure models (Wiggers models) the animal is bled to a predetermined blood pressure and maintained at that level for a certain period. This model is characterised by profound reductions in cardiac output and impairment of the normal homeostatic responses to haemorrhage. In constant volume models a fixed percentage of the animal's blood volume is removed over a specified period. Blood pressure is therefore variable, in contrast to the Wiggers model. Finally, there are

uncontrolled haemorrhage models where bleeding continues through the experiment (56).

We used a constant pressure model to study the redistribution of cardiac output during severe haemorrhagic shock. The use of fluorescent microspheres allowed sequential estimations of blood flow to a wide range of organs.

Methods

The protocol for this study was approved by the Animal Care Committee of Albert Einstein Medical Center, Philadelphia. All work was conducted in accordance with the 'Guide for the Care and Use of Laboratory Animals' prepared by the National Research Council of the NIH (NIH publication 86-32, revised 1985).

Animal preparation

Male Sprague Dawley rats (n = 10, 420-520g) were fed a standard laboratory diet and provided water ad libitum until the day of the experiment. Animals were anaesthetised with ketamine (150 mg/kg, intraperitoneally (IP)). Preliminary studies had shown that this maintained adequate anaesthesia for the duration of the experiment. A tracheostomy was performed and the trachea was intubated with PE-200 tubing to facilitate ventilation. The right carotid artery and both femoral arteries were exposed and cannulated with PE-50 tubing. The right carotid artery cannula was advanced until it was in the left ventricle. The catheter position was confirmed by analysis of the pressure wave.

Continuous on-line monitoring of systemic haemodynamic variables was performed via the left femoral artery cannula and a lead II electrocardiogram was recorded (BioWindow®, Modular Instruments, Malvern, PA, USA). Rectal temperature was monitored (Synergy® Temperature monitor, American Pharmaseal Company, Valencia, CA, USA) and temperature maintained at 36.5-37.5^0 C by the use of heating lamps. Heparin (100 IU, IP) was given.

Preparation of microspheres

Fluorescent microspheres (Molecular Probes, Eugene, OR, USA) of 15 μm diameter were vortexed thoroughly for 30 seconds and then placed in an ultrasonic bath for ten minutes. The vial was then vortexed for a second time immediately prior to injection.

Experimental protocol

Animals were allowed to stabilise for a period of 15 minutes following surgery and then normal resting data were collected for 10 minutes. At the end of this period, baseline organ blood flow was measured as described below. Blood was then removed from the right femoral artery at a constant rate of 2 ml/min. Animals were bled to a mean arterial pressure of 30-35 mm Hg, which was maintained for 60 minutes by further withdrawal or return of blood. Organ blood flow was measured at 5 minutes after reaching the desired blood pressure and again at 60 minutes. At the end of the experiment, animals were euthanised by injection of an overdose of ketamine. Organs were then harvested and weighed (Metler H54AR, Metler Instrument Corp., Hightstown, NJ, USA, accuracy ± 0.001g).

Microsphere technique

0.2 ml of microspheres were injected at each timepoint followed by an 0.3 ml normal saline flush. Reference blood samples were withdrawn from the left femoral artery catheter into a heparinised syringe using a Harvard pump (Harvard Apparatus, South Natick, MA, USA). A rate of 0.5 ml/min was used for the first and second timepoints and 0.25 ml/min for the third timepoint. Withdrawal was commenced immediately prior to injection of microspheres and continued for two minutes after the flush for the first and second timepoints. Withdrawal was continued for four minutes after the flush for the third timepoint. The withdrawal rate and time were adjusted for the third timepoint because in preliminary experiments it was found that a rate in excess of 0.25 ml/min resulted in breaks in the column of blood presumably due to collapse of the blood vessel.

Recovery of microspheres and fluorescent dye extraction

These were performed according to the methods recommended by the Fluorescent Microsphere Resource Center (39). Reference blood samples were transferred into labelled vials for further processing. The femoral arterial catheter and the withdrawal syringe were rinsed thoroughly with 2% Tween-80® (Fisher Scientific Co., Pittsburgh, PA, USA) and the rinse added to the blood sample. Prior to digestion, 100 µl of a standard solution of green microspheres ($1x10^3$ microspheres) was added to each sample vial using a Pipetman pipette (Rainin Instrument Company, Woburn, MA, USA). This colour acted as the internal standard to ensure that there was no loss of microspheres during recovery. Blood samples were digested by adding 10 ml of 16N KOH to each 30 ml of diluted blood. Organ samples were digested by adding 5-10 ml of 4N KOH per 1-2 g of solid tissue. Samples were kept in the dark

for 24 hours to allow complete digestion. Following digestion, the blood and tissue pieces were individually filtered through 10 μm pore polycarbonate filters (Poretics, Livermore, CA, USA) using negative pressure. The digestion vials and the burette were then washed with 2.0% Tween 80® and the washings filtered through the same filter to recover any residual material. The filter was then removed carefully using forceps and placed into an individual polypropylene test-tube. 1.25 ml of Cellusolve acetate were then added to each tube using a calibrated pipette (Eppendorf Repeater Pipet, Brinkmann Instruments Ltd., Mississauga, ON, USA, precision <0.05-0.1%). After 4-8 hours, the tubes were vortexed vigorously and a sample of the solution was pipetted into a glass cuvette (0.7 ml volume, 10 mm path length, Starna Cells, INC., Atascadreo CA, USA). Sample fluorescence was measured using a Perkin-Elmer LS-50B luminescence spectrophotometer (Beaconsfield, Bucks) with excitation and emission slit widths of 4nm.

Tissue blood flows were calculated using the following formula:

$$\text{Blood flow (ml/min/g)} = \frac{\text{Fluorescence signal of sample x Reference flow rate (ml/min)}}{\text{Fluorescence signal of reference x Weight of sample (g)}}$$

Microsphere recovery rates were assessed for each organ. Sample loss during extraction was corrected by comparing the value of the fourth colour in the sample to the true value for the internal standard.

Microsphere distribution

Paired kidney samples for both control and treated animals were compared to ensure homogeneous mixing of microspheres in blood and the absence of sedimentation.

Statistics

Statistical analyses were performed using Excel software (Microsoft Corporation, Roselle, Il, USA) and SPSS statistical software (version 9.0, Chicago, IL, USA). Organ blood flow values are expressed as mean and standard deviation. The mean percentage change from baseline values are also are shown. Paired organ samples were compared using the 95% confidence intervals of the differences between the samples (expressed as the percentage differences). The accumulated blood volumes shed at each time point are expressed as mean and 95 % confidence intervals.

Results

The volume of blood removed to maintain the mean arterial blood pressure between 30-35 mm Hg is shown in Figure 1. The overall blood volume shed increased through the experimental period although some animals required reinfusion of blood towards the end of the experiment to maintain blood pressure. Three animals died at or near the sixty minute period thus blood flow data at 60 minutes are for the surviving seven animals. Absolute blood flows to each organ at baseline and during the period of shock are shown in Table1. The percentage changes (mean and 95% CI) in organ blood flow at 5 and 60 minutes of shock are shown in Figures 2 and 3.

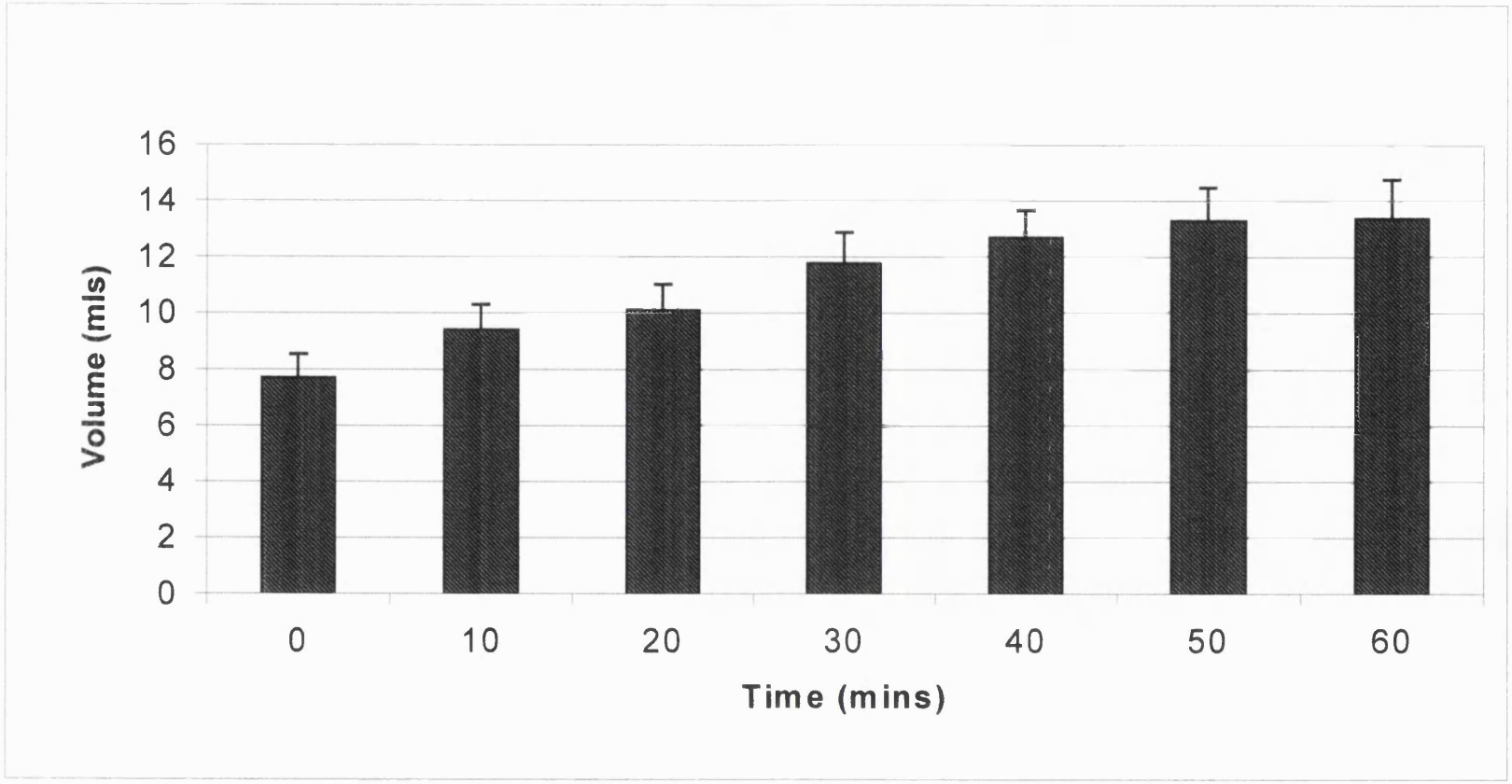

Figure 1: *Volume of blood removed to maintain mean arterial BP of 30-35 mm Hg (mean and 95% CI)*

Organ	Baseline ml/min/g	5 mins of shock ml/min/g	60 mins of shock ml/min/g
Heart	3.83 ± 1.28	3.22 ± 1.96	2.02 ± 0.57
Lungs	0.59 ± 0.52	0.13 ± 0.18	0.03 ± 0.03
Kidneys	5.60 ± 1.42	1.71 ± 0.61	0.46 ± 0.14
Adrenals	5.10 ± 1.37	2.96 ± 1.22	0.65 ± 0.33
Forebrain	0.94 ± 0.34	0.76 ± 0.36	0.24 ± 0.05
Hindbrain	0.62 ± 0.14	0.95 ± 0.40	0.36 ± 0.06
Spleen	1.20 ± 0.38	0.23 ± 0.10	0.05 ± 0.02
Liver	0.27 ± 0.14	0.10 ± 0.03	0.04 ± 002
Duodenum	3.13 ± 1.19	2.06 ± 0.90	0.84 ± 0.14
Jejunum	2.18 ± 0.83	1.20 ± 0.89	0.52 ± 0.26
Ileum	1.08 ± 0.43	0.43 ± 0.22	0.21 ± 0.08
Colon	0.51 ± 0.48	0.31 ± 0.25	0.16 ± 0.09
Diaphragm	0.56 ± 0.22	0.38 ± 0.20	0.18 ± 0.05

Table 1: *Organ blood flows at baseline and during shock (mean and SD)*

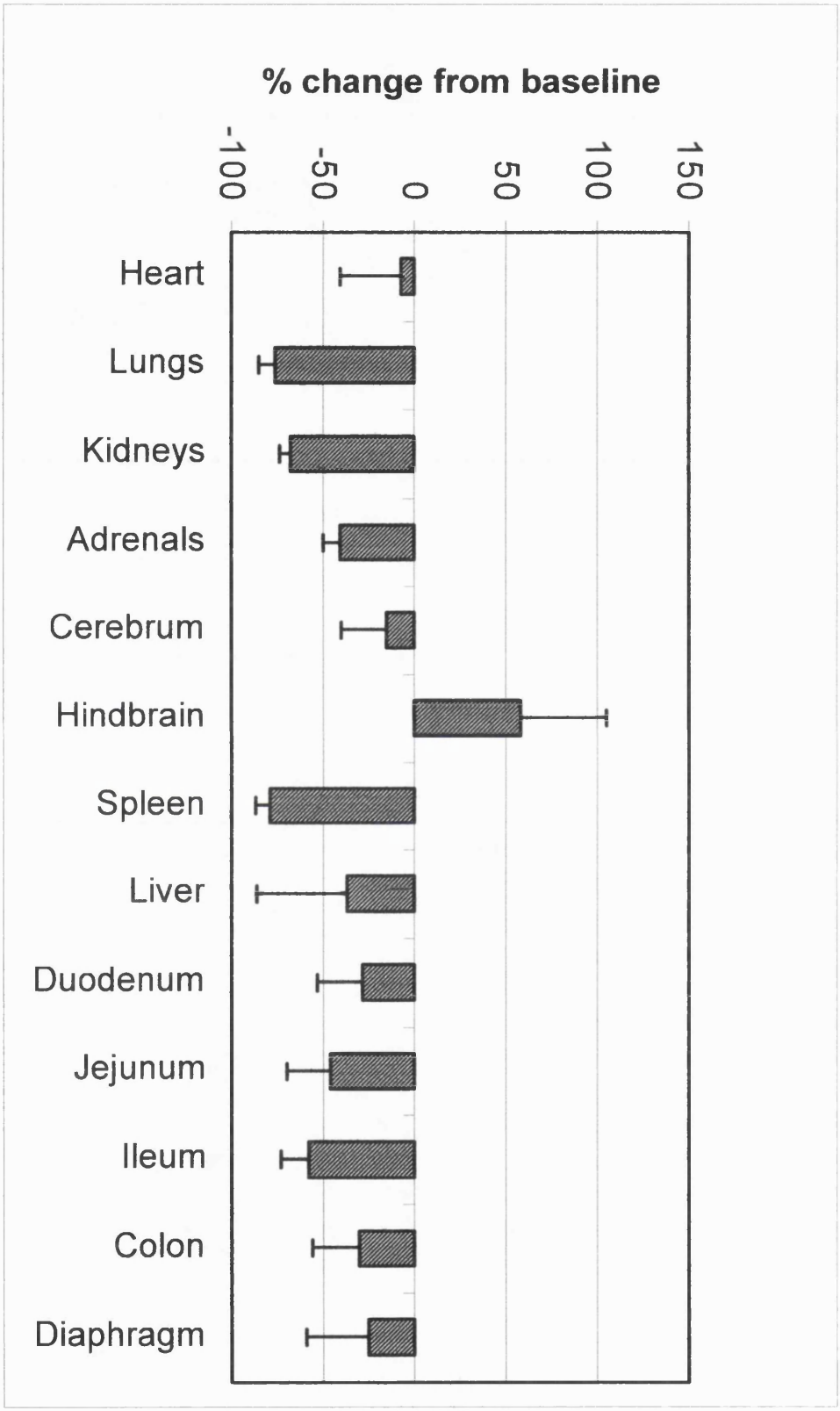

Figure 2: Percentage change from baseline in organ blood flow after 5 minutes of shock (mean and 95% CI)

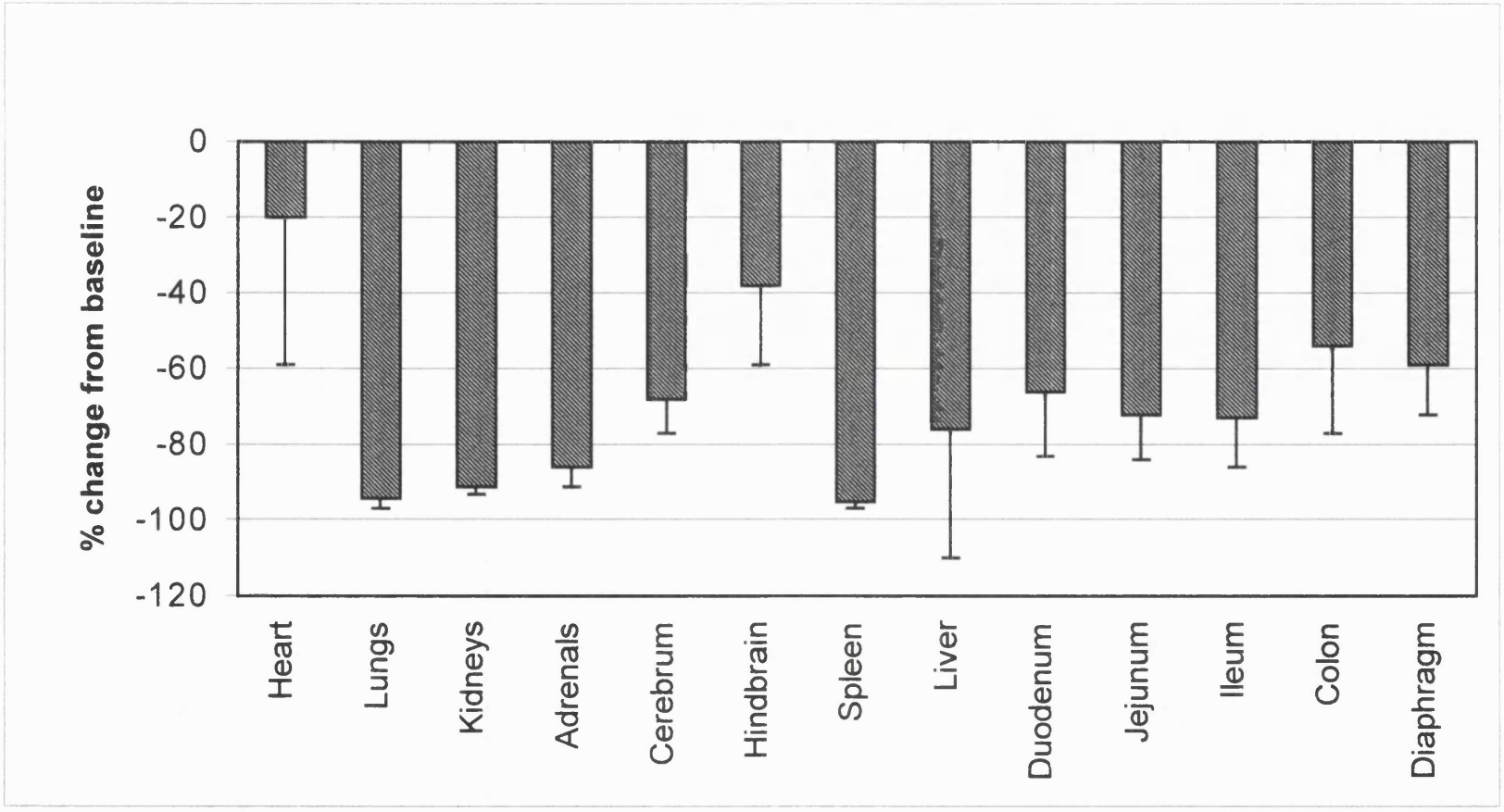

Figure 3: Percentage change from baseline in organ blood flow after 60 minutes of shock (mean and 95% CI).

For paired kidney samples, the percentage differences between right and left kidneys at baseline was –4% ± 10% (mean and 95% CI). During shock the percentage differences were –5% ± 23% (mean and 95% CI) after 5 minutes and 3% ± 31% (mean and 95% CI) after 60 minutes. Microsphere recovery rates for each organ are shown in figure 4 (mean and 95% CI).

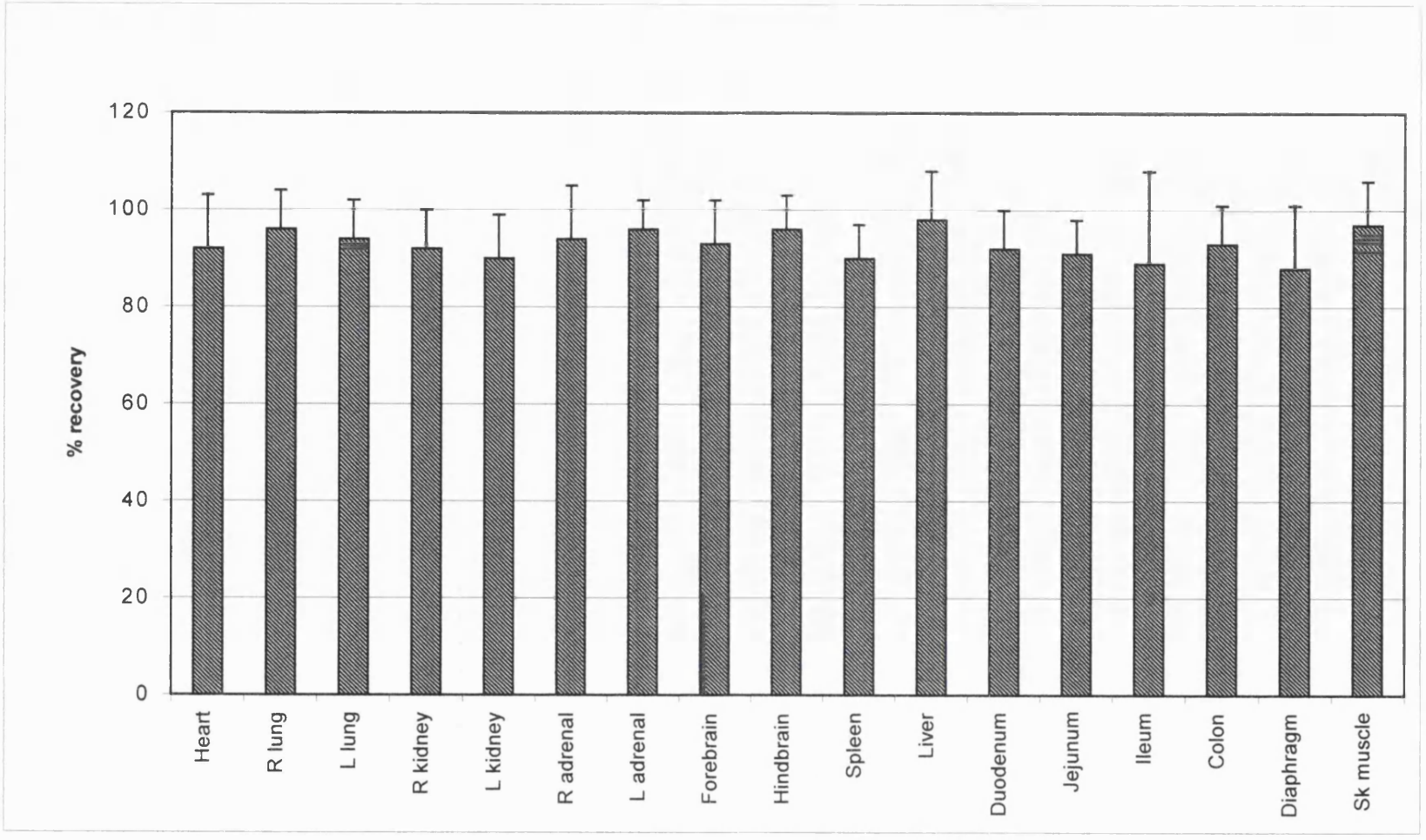

Figure 4: Percentage microsphere recovery for each organ (mean and 95% CI).

Discussion

Shock is a clinical syndrome resulting from organ perfusion that is unable to meet the metabolic demands of the tissues (57). Different stages of haemorrhagic shock have been recognised depending on the amount of blood lost (58). We consider our model to represent a severe physiological insult as evidenced by the need to replace circulating volume in some animals to maintain the desired arterial pressure, and the 30% mortality rate at 60 minutes.

After 5 minutes of shock in this model, the autoregulatory processes affecting coronary and cerebral perfusion appear to be intact with myocardial and brain blood flow little changed from baseline values. Autoregulation of cerebral blood flow maintains vital CNS function (59, 60). However, areas of injury may be seen on histological examination suggesting that regional differences in cerebral blood flow do occur (61). Chen et al found that the fraction of cardiac output supplying the diencephalon and brain stem increased during moderate haemorrhage, whereas flow to other areas remained constant (60). Our findings were in agreement; in the early stages of shock, blood flow to the hindbrain increased compared to baseline values, while that to the cortex remained constant.

The reduction in cardiac output resulting from haemorrhage is initially compensated for by an increase in heart rate, cardiac contractility and vasoconstriction (48, 50). The fraction of cardiac output going to the heart itself is increased during shock. This leads to myocardial blood flows that are near normal (51). Hepatic and diaphragmatic blood flows were also relatively preserved. In moderate haemorrhage,

an increase in arterial blood flow to the liver can maintain hepatic perfusion despite the reduction in portal vein flow resulting from splanchnic vasoconstriction (51, 62, 63). The increased work of respiration is the likely reason for the maintenance of diaphragmatic blood flow (62).

Blood flow to the remaining organs was greatly reduced even in the early stages of shock. This is in agreement with other studies (51, 59, 61). The reduction of blood flow to the kidneys and adrenals leads to increased production of renin, angiotensin and aldosterone in an attempt to restore circulating volume (50). Splanchnic vasoconstriction is seen early in haemorrhagic shock (51, 62). In this studies there was a gradient in blood flow, with the proximal parts of the intestine having a greater blood flow than the distal parts. This gradient was present at baseline and persisted throughout the period of haemorrhage. Similar findings have been reported in both haemorrhagic shock and thermal injury (64).

Skeletal muscle blood flow is profoundly affected by the response to haemorrhagic shock and is one of the major targets for compensatory vascular adjustments. Initial intense vasoconstriction is followed by intermittent tissue perfusion (65). Some capillaries are constantly perfused, with flow rates exceeding baseline values whilst others remain constantly underperfused. Endothelial cell swelling and leukocyte trapping are thought to contribute to capillary occlusion and the maldistribution of blood flow (66, 67).

Following 60 minutes of shock, animals appeared to be entering the period of decompensation. This is characterised by a fall in peripheral resistance. Some

animals required reinfusion of shed blood to maintain a blood pressure of 30-35 mm Hg. Decompensation is thought to result from a variety of factors including alteration in cardiac output distribution, dilatation of small vessels, and increased levels of vasoactive mediators such as cytokines, nitric oxide and adenosine (50, 68). Organ dysfunction may be so severe at this point that even massive volume support fails to maintain blood pressure at a given point and shock becomes irreversible (54). By 60 minutes, organ blood flow had fallen in all organs with apparent failure of the autoregulatory capacity of the brain. Myocardial blood flow remained relatively well preserved.

Although our results follow the pattern reported by other groups, a number of factors may have affected the absolute values obtained for blood flows. Anaesthetic agents and the depth of anaesthesia have effects on bleeding and arterial pressure (69, 70). In order to get comparable mortality rates, blood pressure must be reduced to a much lower value in anaesthetised rats compared to awake animals (71). Longnecker et al found that survival following haemorrhagic shock was greatest in animals anaesthetised with ketamine compared to other anaesthetic agents, despite the maximum shed blood volume being significantly higher (69). The effect of ketamine on regional organ blood flows during low flow states has not been examined. Depth of anaesthesia may also influence the rate and depth of breathing and thus arterial pCO_2. Tracheostomy was performed to facilitate spontaneous breathing but arterial blood gas analysis was not performed. Longnecker et al also found that ketamine anaesthesia did not alter blood gases or acid-base balance during haemorrhage compared to awake animals (70).

Adult male rats were used in these experiments. Other groups have shown gender-specific differences in response to haemorrhage (72) and tolerance to ischaemia (73, 74). Whether there are gender differences in organ blood flow during haemorrhage and reperfusion is not known.

Matsui et al found that under conditions of ischaemia-reperfusion, autofluorescence was generated by the gastric mucosa (30). Protoporphyrin IX and mesoporphyrin IX were produced from porphyrin-iron breakdown under acidic conditions. Fluorescence was observed five minutes after transfusion of shed blood with emission maxima of above 600nm in wavelength. Although we did not test for the presence of autofluorescence in tissue samples, the fluorescence from porphyrins should not spill over into the wavelengths used in the current experiments.

Conclusions

The use of fluorescent microspheres to measure the changes in cardiac output distribution during haemorrhagic shock produced similar patterns of organ blood flows to those reported by other groups. Absolute values are likely to differ because of differences in the models used.

Chapter 6: Organ blood flows following resuscitation from haemorrhagic shock in rats: effects of the adenosine A-1 antagonist NPC 205.

Introduction

Treatment of haemorrhagic shock involves early control of the haemorrhage and adequate volume resuscitation. Even after apparently adequate volume replacement and haemostasis, a state of cardiovascular decompensation may occur with cardiac dysfunction and hypotension unresponsive to further volume support or catecholamine infusion (54). The mechanisms that lead to decompensation and irreversibility include a loss of arteriolar sensitivity as seen by progressive vasodilatation and reduced responsiveness to alpha-agonists, and cellular injury with activation of neutrophils and endothelial cells (50).

Plasma adenosine levels have been shown to increase dramatically during uncompensated haemorrhagic shock (68, 75). High levels of adenosine may adversely depress cardiac mechanical and electrical function and cause vasodilatation (76). Non-specific adenosine receptor blockade can modify the blood pressure response to haemorrhage (77). Selective adenosine A1 receptor antagonism has been shown to enhance myocardial contractility following defibrillation (75) and to improve survival following splanchnic occlusion shock (78). It has previously been shown that the adenosine A-1 receptor antagonist NPC 205 (1,3-dipropyl-8-(4-hydroxyphenyl)xanthine) can improve haemodynamic function and survival following haemorrhagic shock and resuscitation in rats (79, 80). We hypothesized that the survival benefit seen with NPC 205 following resuscitation from

haemorrhagic shock may result from improvement in blood flows to the brain, heart and / or kidneys. Blood flows to other organs are presented for descriptive purposes.

Methods

The protocol for this study was approved by the Animal Care Committee of Albert Einstein Medical Center, Philadelphia. All work was conducted in accordance with the 'Guide for the Care and Use of Laboratory Animals' prepared by the National Research Council of the NIH (NIH publication 86-32, revised 1985).

Animal preparation

Adult, male Sprague Dawley rats (weight 497g ± 44g, mean ± SD) were fed a standard laboratory diet and provided water ad libitum until the day of the experiment. Animals were anaesthetised (ketamine 150 mg/kg, intraperitoneal (ip), booster doses prn) and the trachea was intubated with PE 200 tubing to facilitate ventilation. The right carotid artery, both femoral arteries and one femoral vein were surgically exposed and cannulated with PE 50 tubing. The right carotid artery cannula was advanced into the left ventricle and its position confirmed by waveform analysis. Continuous monitoring of systemic haemodynamic variables was performed via the left femoral artery catheter (BioWindow®, Modular Instruments, Malvern, PA, USA). Rectal temperature was monitored (Synergy® Temperature monitor, American Pharmaseal Company, Valencia, CA, USA) and temperature maintained at 36.5-37.5^0 C by the use of heating lamps. Heparin (100 IU, IP) was given.

Experimental protocol

Animals were allowed to stabilise for a period of 15 minutes following surgery after which normal resting data were collected for 10 minutes. At the end of this period, baseline organ blood flows were measured as described below. Blood was then removed from the right femoral artery at a constant rate of 2 ml / min. Animals were bled to a mean arterial pressure of 30-35 mm Hg, which was maintained for 60 minutes by further withdrawal or return of blood. Shed blood was then reinfused at a rate of 4 ml / min, simultaneously with administration of either 1 mg / kg NPC 205 (n=7) or drug vehicle (10% NaOH) (n=11) intravenously. Organ blood flows were measured at 5 min and 60 min following reinfusion of shed blood. At the end of the experiment, animals were euthanised by injection of an overdose of ketamine. Organs were then harvested and weighed (Metler H54AR, Metler Instrument Corp., Hightstown, NJ, USA, accuracy ± 0.001g).

Microsphere technique

Fluorescent microspheres (Molecular Probes, Eugene OR, USA) of 15 μm were vortexed thoroughly for 30 seconds and then placed in an ultrasonic bath for ten minutes. The vial was then vortexed for a second time immediately prior to injection.

2×10^5 15 μm diameter microspheres were injected via the left ventricular catheter at each timepoint followed by a 0.3 ml flush of normal saline. Reference blood samples were withdrawn from the left femoral artery catheter at a rate of 0.5 ml / min. Blood was withdrawn into a heparinised syringe using a Harvard withdrawal pump (Harvard Apparatus, South Natick, MA, USA). Withdrawal was commenced

immediately prior to injection of microspheres and continued for two minutes after the flush.

Recovery of microspheres and fluorescent dye extraction

These were performed according to the methods recommended by the Fluorescent Microsphere Resource Center (39).

Reference blood samples were transferred into labelled vials for further processing. The femoral arterial catheter and the withdrawal syringe were rinsed thoroughly with 2% Tween-80® (Fisher Scientific Co., Pittsburgh, PA, USA) and the rinse added to the blood sample. Prior to digestion, 100 µl of a standard solution of green microspheres ($1x10^3$ microspheres) was added to each sample vial using a Pipetman pipette (Rainin Instrument Company, Woburn, MA, USA). This colour acted as the internal standard to ensure that there was no loss of microspheres during recovery. Blood samples were digested by adding 10 ml of 16N KOH to each 30 ml of diluted blood. Organ samples were digested by adding 5-10 ml of 4N KOH per 1-2 g of solid tissue. Samples were kept in the dark for 24 hours to allow complete digestion. Following digestion, the blood and tissue pieces were individually filtered through 10 µm pore polycarbonate filters (Poretics, Livermore, CA, USA) under negative pressure. The digestion vials and the burette were then washed with 2% Tween 80® and the washings filtered through the same filter to recover any residual material. The filter was then removed carefully using forceps and placed into an individual polypropylene test-tube. 1.25 ml of Cellusolve® acetate were then added to each tube using a calibrated pipette (Eppendorf Repeater Pipet, Brinkmann Instruments Ltd., Mississauga, ON, USA, precision <0.05-0.1%). After 4-8 hours, the

tubes were vortexed vigorously and a sample of the solution was pipetted into a glass cuvette (0.7 ml volume, 10 mm path length, Starna Cells, INC., Atascadreo, CA, USA). Sample fluorescence was measured using a Perkin-Elmer LS-50B luminescence spectrophotometer (Beaconsfield, Bucks) with excitation and emission slit widths of 4 nm.

Tissue blood flows were calculated using the following formula:

$$\text{Blood flow (ml/min/g)} = \frac{\text{Fluorescence signal of sample x Reference flow rate (ml/min)}}{\text{Fluorescence signal of reference x Weight of sample (g)}}$$

Evenness of distribution of microspheres was assessed by analysis of paired organ samples. Comparison of right and left kidney samples provides a simple internal standard for individual studies. Microsphere recovery rates were assessed for each organ. Sample loss during extraction was corrected by comparing the value of the fourth colour in the sample to the true value for the internal standard.

Statistics

Statistical analyses were performed using Excel software (Microsoft Corporation, Roselle, Il, USA) and SPSS statistical software (version 9.0, Chicago, IL, USA). Baseline values for the two groups are expressed as mean ± standard deviation. Paired organ samples were compared using the 95% confidence intervals of the differences between samples (expressed as the percentage differences). Haemodynamic and blood flow data following reinfusion of shed blood are expressed as the mean percentage change from baseline and standard error of the mean.

Between groups comparisons were performed using repeated measures analysis of variance (RM-ANOVA).

For haemodynamic data, baseline values were used as covariates and all time points from T=0 to T=55 were analysed. For organ blood flows, no covariates were used. Organ blood flows for the heart, kidneys, cortex and hindbrain were compared.

Results

1. Baseline

The weight of the animals was similar for both control (500 g ± 26 g, mean ± SD) and treated animals (493 g ± 59 g, mean ± SD). One animal in each group died during or shortly after reinfusion of shed blood. Data from these animals were excluded from analysis.

Haemodynamics and blood flows

Baseline variables for control and study animals are shown in tables 1 and 2.

Table 1: *Baseline haemodynamic variables for control and treated animals (mean ± SD).*

	Control	Treated
Heart rate (bpm)	364 ± 40	332 ± 53
LV dP/dt / P (sec^{-1})	127 ± 25	124 ± 28
Mean arterial pressure (mm Hg)	117 ± 24	118 ± 17
Systolic BP (mm Hg)	141 ± 25	138 ± 23
Diastolic BP (mm Hg)	95 ± 23	99 ± 15

Table 2: *Baseline organ blood flows (ml/min/g) (mean ± SD)*

Organ	Control	Treated
Heart	4.1 ± 1.6	4.1 ± 1.0
Lungs	9.3 ± 12.2	4.1 ± 8.4
Kidneys	5.2 ± 1.1	4.3 ± 0.6
Adrenals	6.3 ± 3.1	6.1 ± 4.6
Forebrain	1.7 ± 0.7	1.5 ± 1.0
Hindbrain	1.0 ± 0.3	0.9 ± 0.4
Spleen	1.3 ± 0.4	1.5 ± 0.8
Liver	0.3 ± 0.1	0.2 ± 0.1
Duodenum	3.6 ± 1.2	2.9 ± 1.1
Jejunum	2.1 ± 0.8	1.9 ± 0.6
Ileum	1.4 ± 0.6	1.2 ± 0.4
Colon	0.5 ± 0.2	0.6 ± 0.2
Diaphragm	0.6 ± 0.2	1.4 ± 1.9

No significant differences were seen between control and treated animals. The volume of blood withdrawn after 60 minutes of shock for each group was; NPC 205 treated group 13.5 ± 1.9 ml, vehicle 12.9 ± 2.6 ml (mean ± SD).

2. Following reinfusion of shed blood

The dose of ketamine given for anaesthesia following reinfusion for each group was; NPC 205 treated group 0.23 mg ± 0.09 mg, vehicle 0.26 mg ± 0.15 mg (mean ± SD).

Haemodynamics

Heart rate rapidly returned to baseline values following reinfusion of shed blood in both treated and untreated animals (Fig 1). No effect was seen overall between groups for either time ($p=0.87$) or treatment ($p=0.31$). However, a significant time-treatment interaction was present ($p=0.031$). This indicates that treatment had an effect but only at certain timepoints. Left ventricular dP/dt / P increased in both groups following reinfusion of shed blood and then fell back to baseline values (Fig 2). No significant effects of time, treatment or time-treatment interaction were seen between groups. Mean, systolic and diastolic blood pressures are shown in Figs 3-5. Although values trended higher in treated animals following reinfusion, no significant effects of time, treatment or time-treatment interaction were demonstrated. In both groups of animals, systolic blood pressure showed a non-significant decline from baseline over the 60 minutes following reinfusion. Diastolic blood pressures were initially higher than baseline in both groups of animals and then also showed a gradual decline with increasing time post reinfusion.

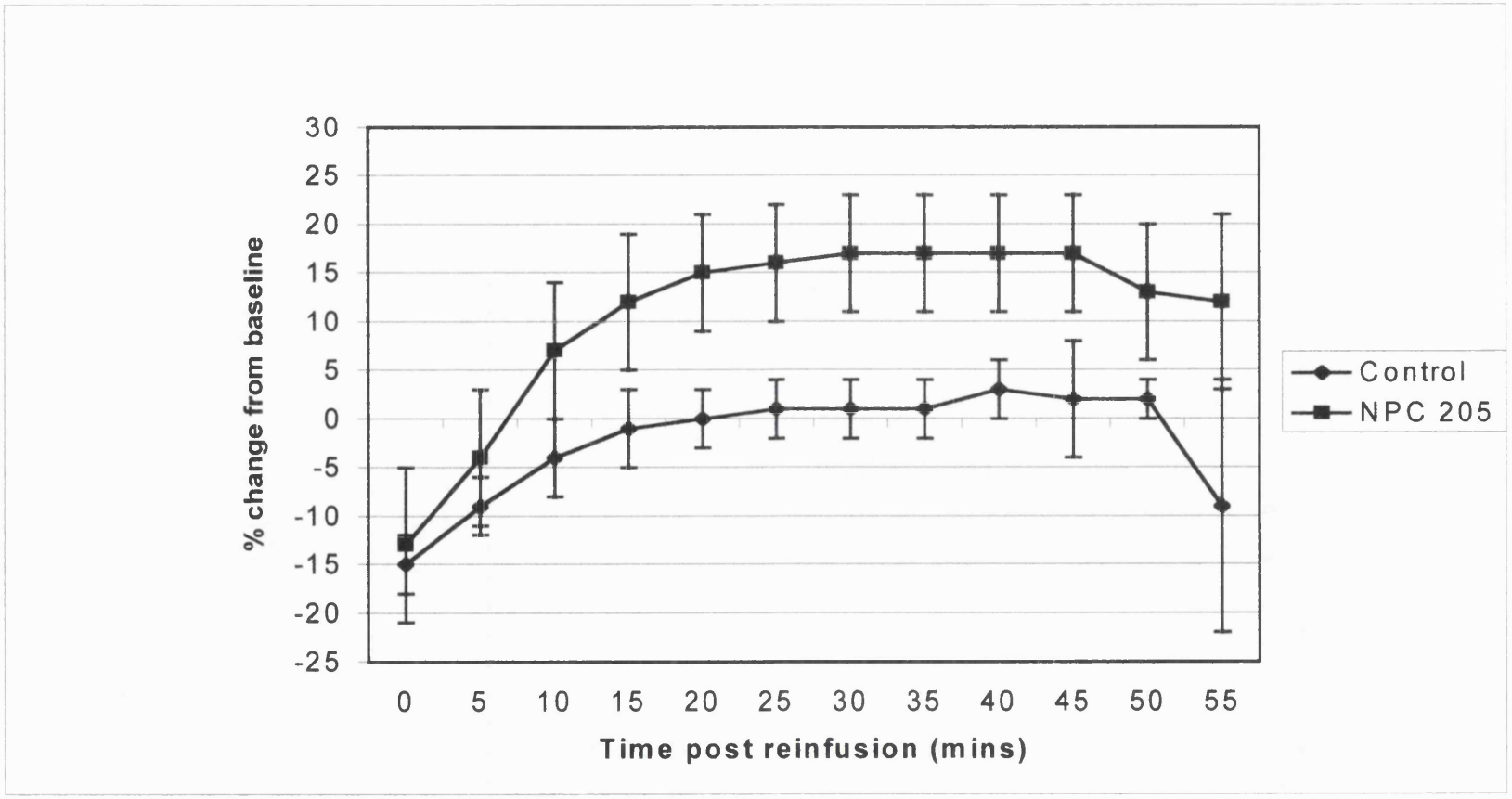

Figure 1: *Heart rate following reinfusion of shed blood (mean and SEM).*

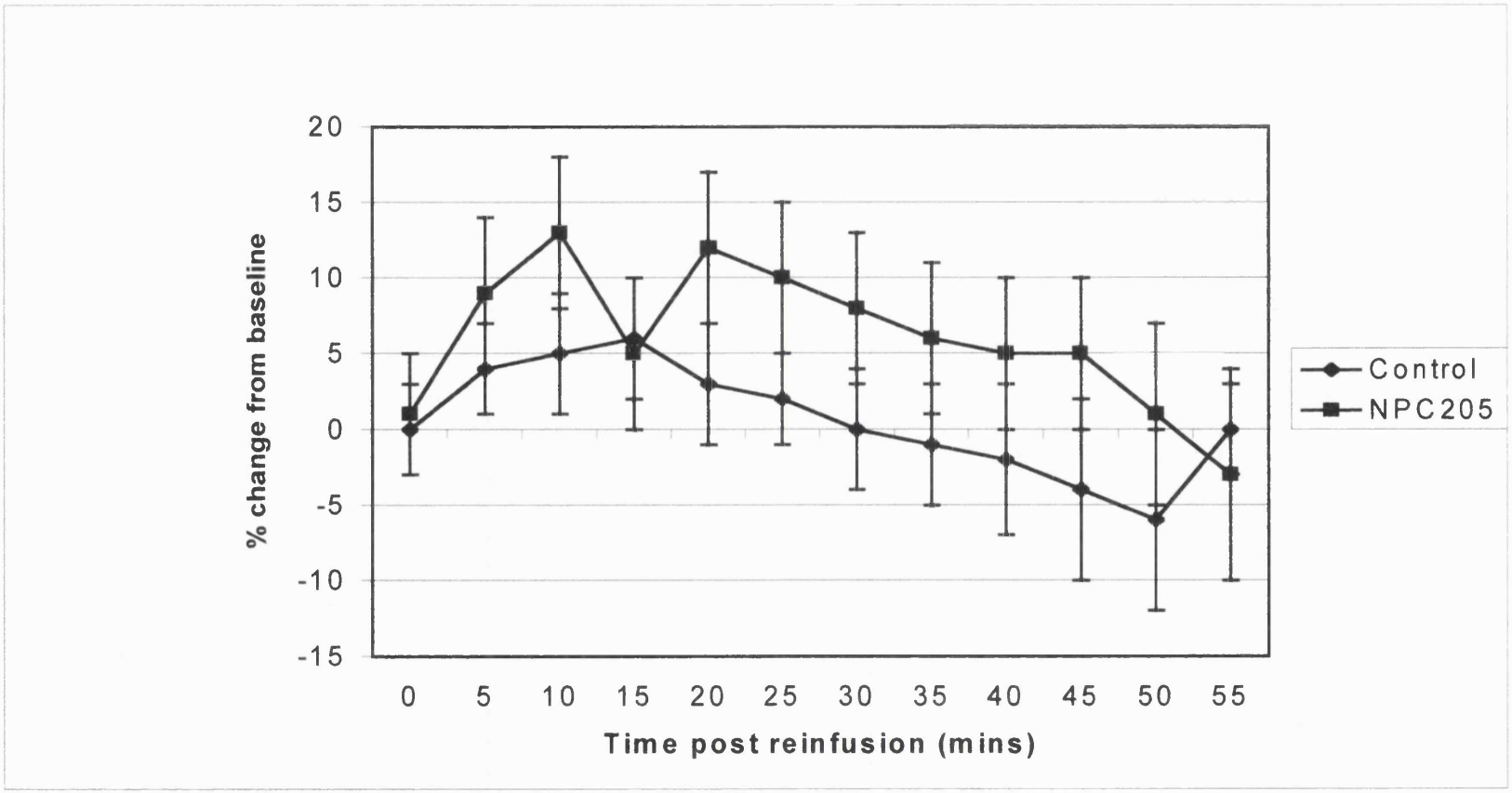

Figure 2: *Left ventricular dP/dt / P following reinfusion of shed blood (mean and SEM).*

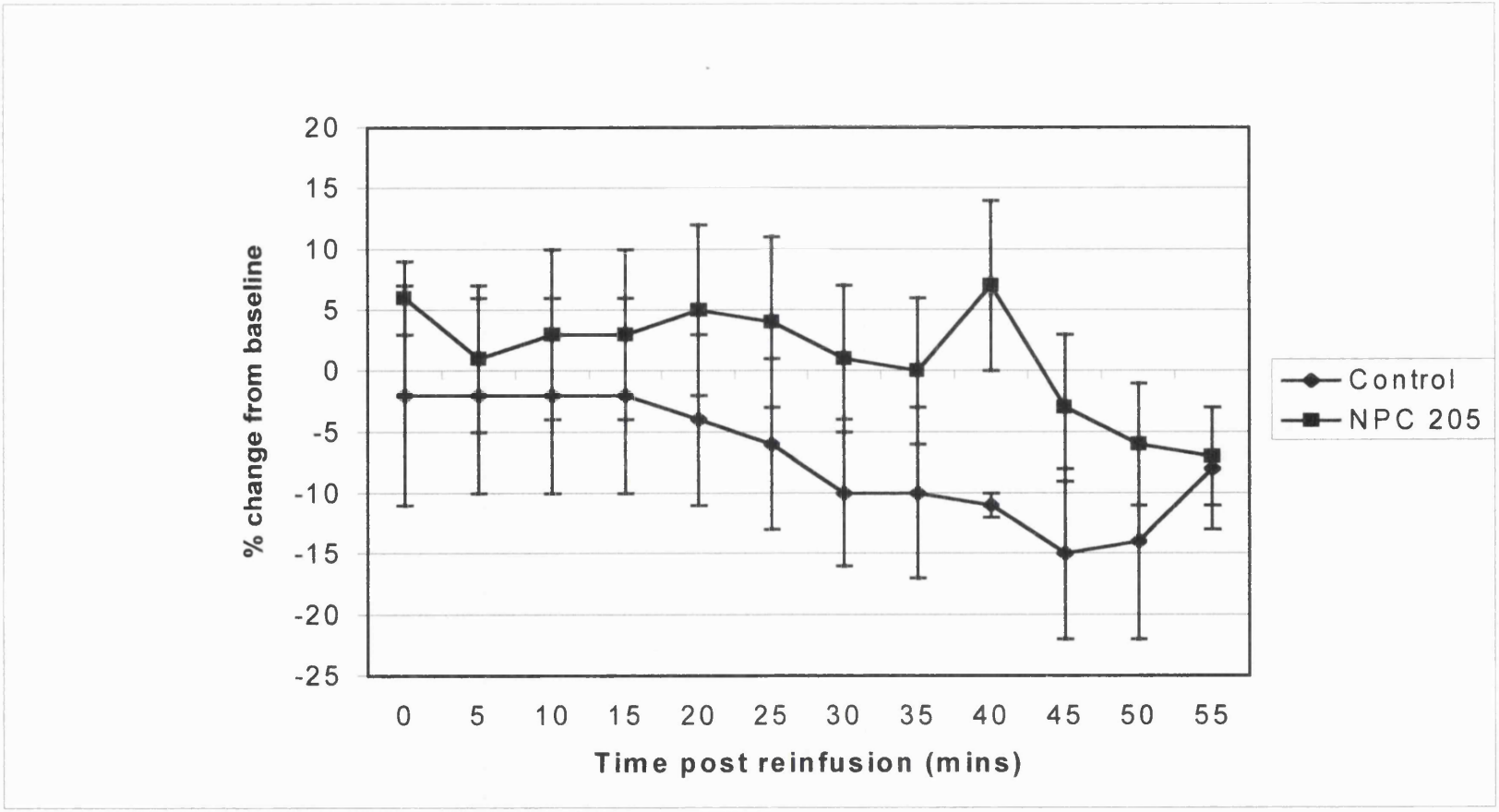

Figure 3: *Mean arterial blood pressure following reinfusion of shed blood (mean and SEM).*

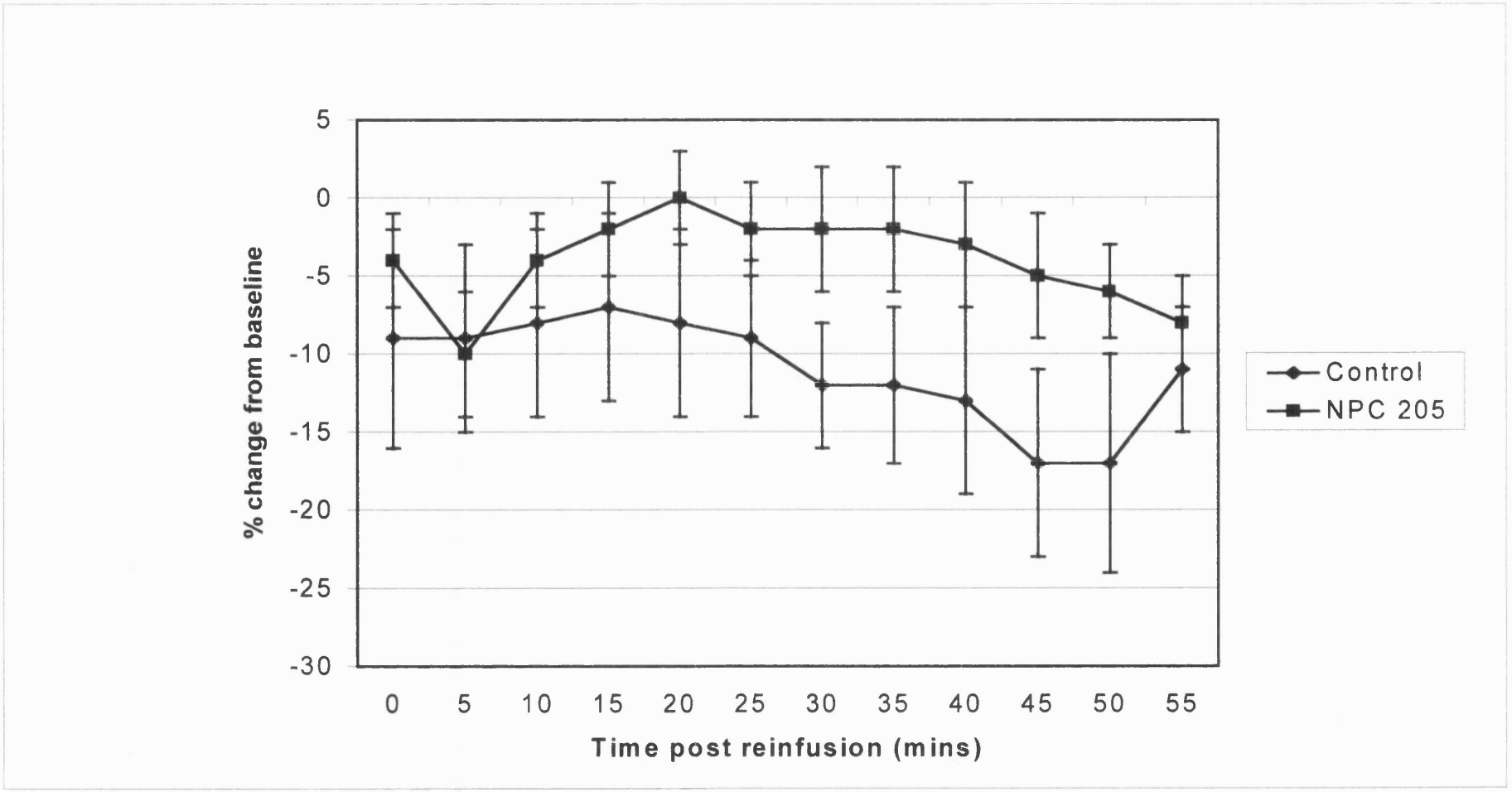

Figure 4: *Systolic blood pressure following reinfusion of shed blood (mean and SEM).*

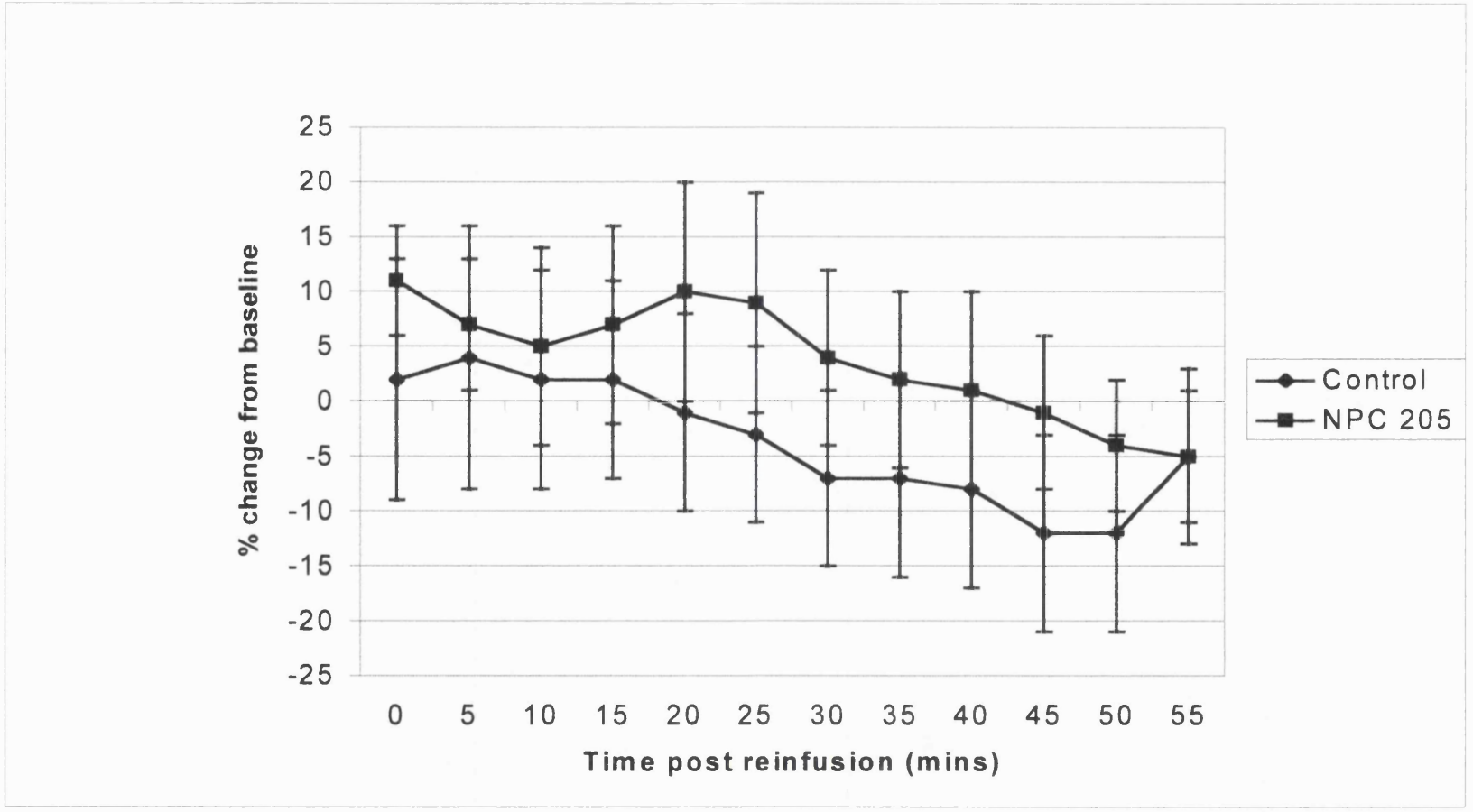

Figure 5: *Diastolic blood pressure following reinfusion of shed blood (mean and SEM).*

Organ blood flows

Results for organ blood flows at 5 and 60 minutes post reinfusion are shown in Table 3 and Figures 6 and 7.

	5 mins	5 mins	60 mins	60 mins
Organ	Control (ml/min/g)	Treated (ml/min/g)	Control (ml/min/g)	Treated (ml/min/g)
Heart	6.9 ± 2.5	6.6 ± 1.2	4.3 ± 0.9	5.4 ± 3.4
Lungs	6.6 ± 4.5	2.9 ± 3.1	8.5 ± 6.2	3.6 ± 5.1
Kidneys	3.3 ± 0.6	2.8 ± 0.6	3.1 ± 0.9	3.1 ± 0.6
Adrenals	6.6 ± 1.4	4.6 ± 1.1	4.5 ± 1.1	6.1 ± 1.8
Forebrain	1.4 ± 0.7	1.0 ± 0.5	1.1 ± 0.4	1.1 ± 0.9
Hindbrain	0.9 ± 0.3	0.8 ± 0.2	0.9 ± 0.3	1.0 ± 0.5
Spleen	1.3 ± 0.6	1.2 ± 0.5	1.1 ± 0.7	1.2 ± 0.6
Liver	0.5 ± 0.2	0.6 ± 0.2	0.3 ± 0.2	0.5 ± 0.2
Duodenum	6.8 ± 2.5	4.9 ± 1.2	2.7 ± 1.2	3.2 ± 2.0
Jejunum	2.6 ± 1.6	2.6 ± 2.2	1.9 ± 1.2	2.2 ± 2.1
Ileum	1.5 ± 1.1	1.5 ± 0.7	1.2 ± 0.7	1.2 ± 0.6
Colon	0.5 ± 0.2	0.5 ± 0.4	0.4 ± 0.2	0.5 ± 0.2
Diaphragm	0.5 ± 0.3	2.0 ± 4.8	0.5 ± 0.2	0.8 ± 1.3

Table 3: *Organ blood flows at 5 and 60 minutes post resuscitation (mean and 95% CI).*

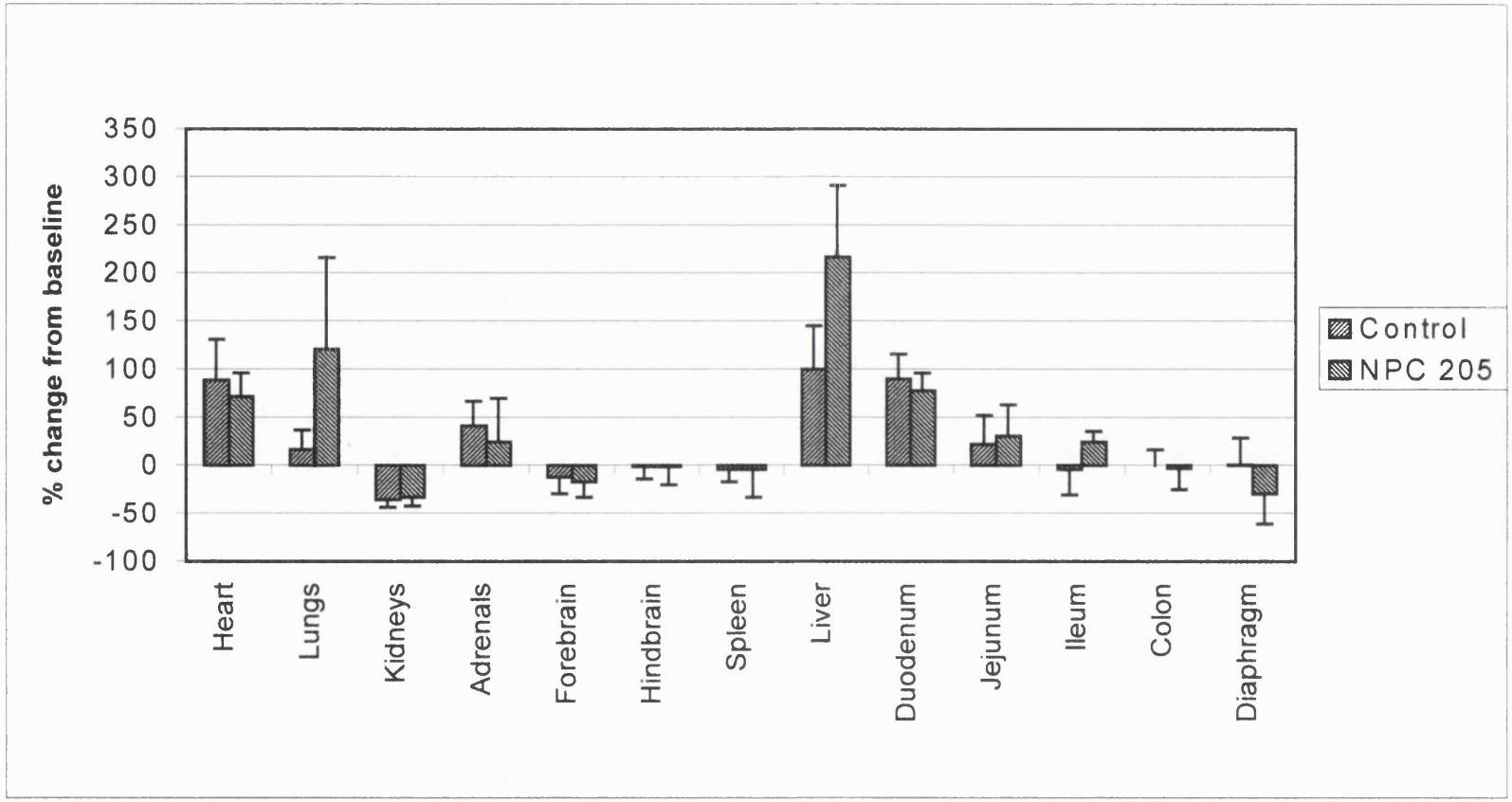

Figure 6: *Percentage changes from baseline in organ blood flows at 5 minutes post reinfusion (mean and SEM).*

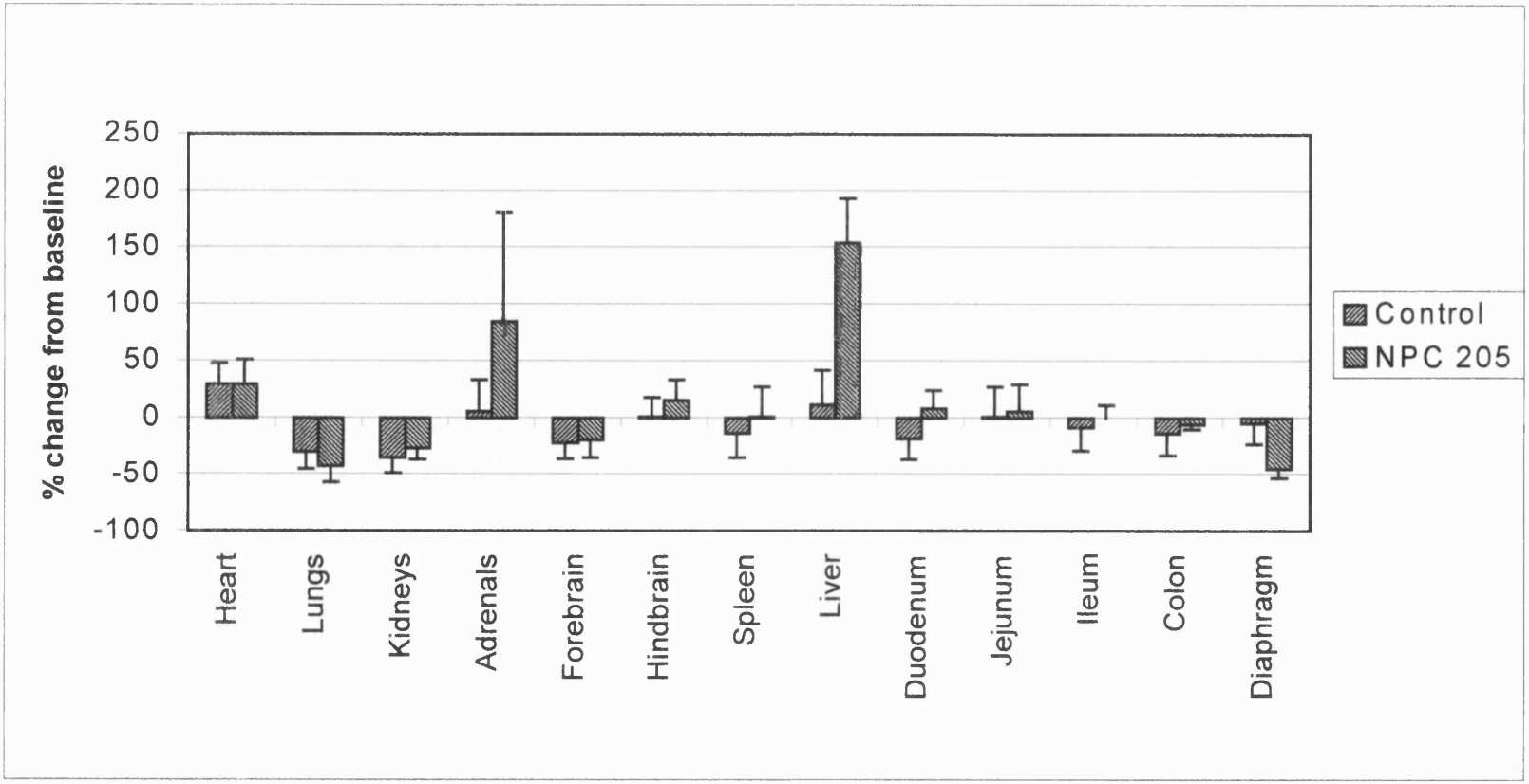

Figure 7: *Percentage changes from baseline in organ blood flows at 60 minutes post reinfusion (mean and SEM).*

Blood flow to the heart showed a significant effect of time (p=0.016) with flows being higher than baseline values at both 5 and 60 minutes for both groups. There were no significant effects for either treatment (p=0.46) or time-treatment interaction (p=0.87) for either group. Renal blood flows also showed a significant effect of time (p=0.004) with values lower than baseline for both groups at both timepoints. There were no significant differences for the effects of treatment (p=0.19) or time-treatment interaction (p=0.72). Blood flows to the cortex and hindbrain showed no significant effects for time (p=0.091 forebrain, p=0.84 hindbrain), treatment (p=0.56 forebrain, p=0.7 hindbrain) or time-treatment interaction (p=0.54 forebrain, p=0.52 hindbrain).

Paired organ samples

For kidney samples, the percentage difference (mean and 95% CI) between right kidney and left kidney was -6.7% ± 15.6% (SD ± 54%), for both groups combined. This indicates that mixing was homogeneous with no evidence of microsphere sedimentation at the level of the kidneys.

Microsphere recovery rates

Microsphere recovery rates for each organ are shown in Figure 8. Recovery exceeded 85% for all the tissues studied.

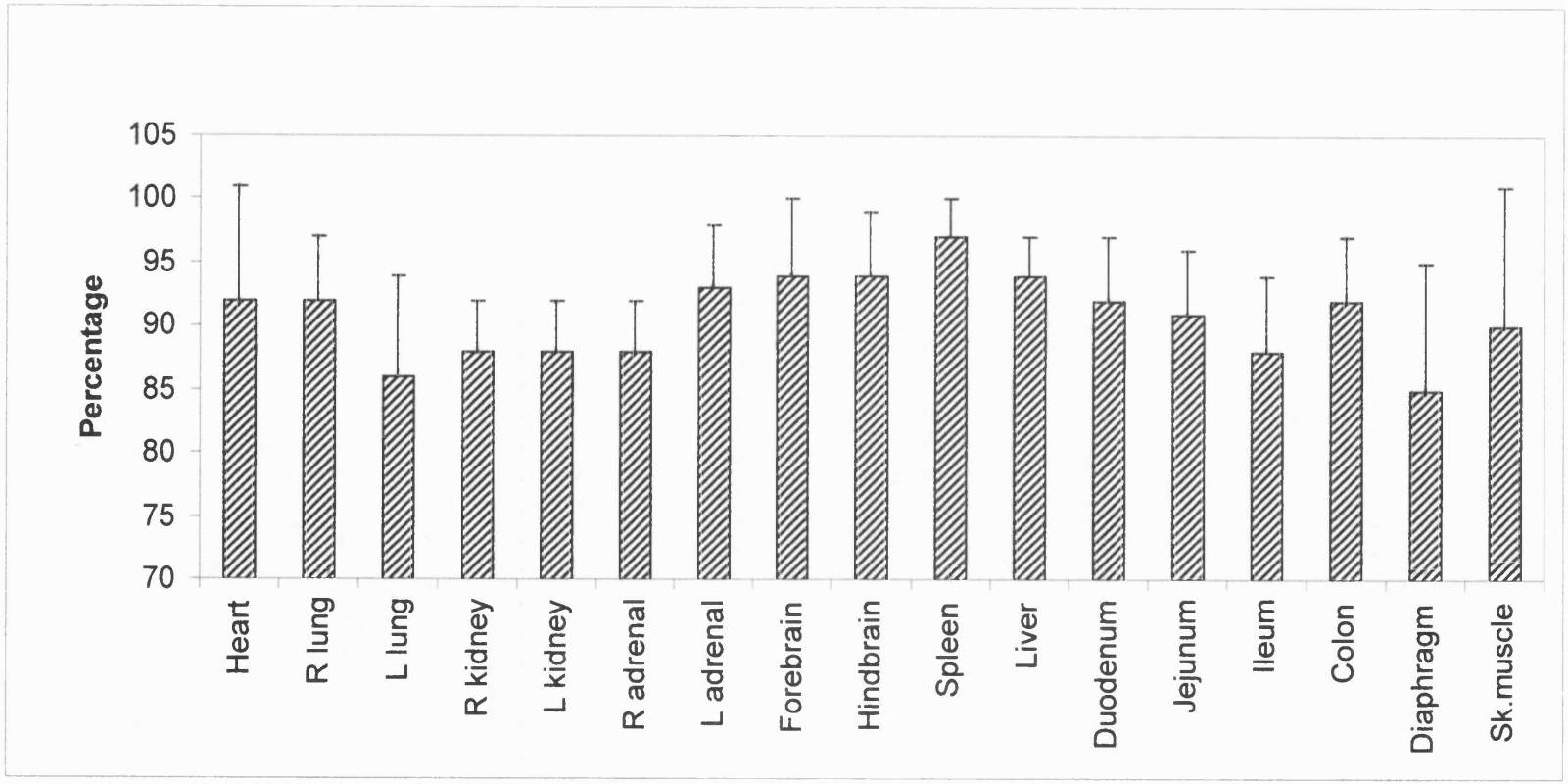

Figure 8: *Microsphere recovery rates (mean and 95%CI).*

Discussion

In prolonged haemorrhagic shock, cardiac depression and peripheral vasodilatation may occur. These lead to declining systemic blood pressure despite aggressive volume resuscitation. This decompensation is associated with increased levels of vasoactive mediators such as cytokines, nitric oxide and adenosine (50). The actions of adenosine are mediated through at least three cell-surface receptors, A1, A2 and A3. Activation of the A1 receptor causes negative chronotropic effects on the sinoatrial node, negative dromotropic effects on the atrioventricular node and inhibits the inotropic, chronotropic, and dromotropic effects of catecholamines (76, 81). A1 receptor stimulation also causes pulmonary and renal vasoconstriction (82, 83) and enhances chemotaxis in activated neutrophils (84). A2 receptors on endothelial and vascular smooth muscle cells mediate vasodilatation (76), inhibit platelet aggregation (78), and inhibit neutrophil adherence to endothelium (84). Activation of the adenosine A3 receptor has been shown to reduce myocardial infarct size following ischaemia (85). Selective A1 adenosine receptor antagonism has been shown to attenuate postdefibrillation cardiovascular depression (77), improve renal function in acute renal failure (78), and to improve short-term survival following splanchnic artery occlusion (78).

Previous studies using the current model have shown that A1 adenosine receptor antagonism is associated with positive inotropic and chronotropic responses during haemorrhagic shock and improved short-term survival following haemorrhagic shock (79, 80). In this study we found that administration of the adenosine A1 antagonist, NPC 205, concurrent with reinfusion of shed blood provided little

haemodynamic advantage compared to shed blood alone. Although inotropic and chronotropic values trended higher with treated animals, there were no significant differences between groups. This lack of significant improvement in haemodynamic variables may result from the lower dosage of NPC 205 used in the current experiment or to the time at which it was administered. Haemodynamic advantage was seen when NPC 205 was administered during but not after the period of shock. Karasawa et al found that the adenosine A1 receptor antagonist KF15372 affected the heart rate of rats subjected to splanchnic artery occlusion but not normal, anaesthetised rats (78). This suggests that the modulatory role of adenosine may differ in ischaemic and non-ischaemic states.

Myocardial blood flow initially increased from baseline values following resuscitation from severe haemorrhagic shock. By sixty minutes post-reinfusion, myocardial blood flow values were close to baseline. Values did not differ between animals treated with NPC 205 and control animals. In both groups of animals there was a rapid return of cerebral blood flow to baseline values with no significant differences between groups suggesting that autoregulatory mechanisms remained intact despite the prolonged ischaemic insult. Renal blood flow was restored more slowly following reperfusion but again there were no differences between groups. In a canine model of haemorrhagic shock, Hirasawa et al also found that cerebral autoregulation was rapidly restored following resuscitation from haemorrhagic shock (59). Renal blood flow returned more slowly compared to the brain, with medullary flow being restored before cortical flow (59).

During haemorrhagic shock, splanchnic blood flow is reduced to divert blood to more vital organs. Although hepatic portal blood flow decreases in response to haemorrhage, flow in the hepatic artery increases to maintain hepatic perfusion (63). In the current experiment, both control and treated animals showed increases in hepatic blood flow at 5 minutes post reinfusion. At 60 minutes, treated animals alone had an increase in liver blood flow compared to baseline. Although these findings need to be confirmed in future studies, similar increases in hepatic blood flow have been reported in dogs following resuscitation from haemorrhagic shock (86). Adenosine mediates the increase in portal venous blood flow seen following alcohol ingestion via its action on A2 receptors (87). Blockade of adenosine A1 receptors in this experiment appears to prolong the hyperaemic response following resuscitation from haemorrhagic shock. It is not possible to determine whether it was hepatic arterial blood flow or portal venous blood flow that increased in the current experiment.

Following resuscitation from haemorrhagic shock, intestinal hypoperfusion may persist and may contribute to multi-organ dysfunction as a result of failure of the barrier function of the gut (50). In this model, duodenal blood flow was increased compared to baseline values in both groups at 5 minutes post reinfusion. Blood flow to other parts of the intestine was not significantly different from baseline values at either time point. Although blood flow was restored promptly, previous studies have shown that both the intestinal barrier function and the absorptive function of the gut may remain abnormal despite restoration of portal blood flow (88).

Conclusions

Although haemodynamic variables showed a rapid return to baseline values during recovery from severe haemorrhage, regional organ blood flows were altered. Myocardial blood flow was significantly increased compared to baseline values, whereas renal blood flow was reduced from baseline values. Cerebral blood flow was restored quickly to baseline values suggesting that autoregulation of the cerebral vasculature remained intact despite long periods of ischaemia. These findings are important as the clinical management of shock is generally guided by haemodynamic considerations, whereas the true aim of therapy should be the restoration of oxygen delivery to the tissues.

Selective adenosine A1 receptor antagonism had only moderate effects on haemodynamic variables when coincident with resuscitation from haemorrhagic shock. Blood flows to the heart, brain and kidneys were not significantly affected compared to control animals, whereas blood flow to the liver did appear to be modulated by the administration of NPC 205. Further studies are required to elucidate the mechanism whereby NPC 205 increases short-term survival following resuscitation from haemorrhagic shock.

Chapter 7: Organ blood flow during anaphylactoid-like circulatory shock following IV administration of a nanoparticulate drug delivery system in dogs: effects of pre-treatment with histamine H1- and H2-receptor antagonists and corticosteroids.

Introduction

Colloidal carriers are now available for therapeutic and diagnostic agents that are difficult to formulate. Carriers may be liquid in the form of emulsions or liposomes, or solid such as microspheres and nanoparticles (89). Nanoparticles range in size from 10 nm to 1000 nm. Drug or antigen may be bound to the surface of the particles or incorporated into the particles as a solid dispersion or solid solution (90). The nature of microparticulate carriers offers a number of potential advantages over standard formulations (91). Particles can be formulated to deliver a relatively high payload of drug, or to release it in a slow, controlled manner. Site-specific drug delivery can be achieved. This has been utilised for delivery of drugs to the eye, joints, respiratory tract and to solid tumours (91).

Following intravenous injection, cells of the reticuloendothelial system rapidly clear nanoparticles from the circulation (90). Within 30 minutes of intravenous injection, 90% of particles can be found in the liver, 5% in the spleen, a few percent in the bone marrow and varying amounts in the lungs (92). Uptake of nanoparticles by the reticuloendothelial system can be reduced, and the blood circulation time increased, by modification of the particle surface to diminish opsonisation and cell adhesion (93, 94). This may be achieved by coating the particles with a hydrophilic

polymer (91). The effectiveness of the coating depends on the features of the polymer itself, the thickness of the coating and the density of coverage (95).

Limited numbers of studies have addressed the potential toxicities associated with injected microparticles (96-98). Phagocytosis of particles by macrophages may be associated with the release of a variety of inflammatory mediators (99). Bolus injection of polystyrene nanospheres has been shown to cause profound cardiovascular depression in dogs (100). During this response, plasma histamine levels increased significantly. Pretreatment of animals with histamine H1 and H2 receptor antagonists blocked the response.

In this study, the effects of bolus injection of polystyrene nanoparticles (200 nm diameter) on regional organ blood flow were evaluated. The particles used were coated with the pluronic stabiliser F108 to prolong circulation time. In addition, the effects of nanoparticulate injection on organ blood flow following corticosteroid and antihistamine pretreatment were also studied, as absence of systemic haemodynamic effects does not preclude regional effects on blood flow. In particular, we examined the blood flows to the brain, heart and kidneys as blood flow is preferentially diverted to these organs during low flow states. Flow to other organs is presented for descriptive purposes.

Methods

The protocol for this study was approved by the Animal Care Committee of Albert Einstein Medical Center, Philadelphia. All work was performed in accordance with the 'Guide for the Care and Use of Laboratory Animals' prepared by the National Research Council of the NIH (NIH publication 86-32, revised 1985).

Preparation of microspheres

Fluorescent microspheres (Molecular Probes, Eugene OR, USA) of 15 μm were vortexed thoroughly for 30 seconds and then placed in an ultrasonic bath for ten minutes. The vial was then vortexed for a second time immediately prior to injection.

Animal preparation

Adult, male, conditioned, colony-bred dogs (14-20 kg, HRP Inc., Denver, PA, USA) that had been fasted overnight were used for the study. Treated animals (n=4) were given corticosteroids (prednisone 2 mg/kg, IM, 12 hourly) for 24 hours prior to the study, and antihistamines (diphenhydramine 10 mg/kg IV, and cimetidine 5 mg/kg IV) twenty minutes prior to the study. Control animals (n=4) received no pre-treatment. Animals were anaesthetised with pentobarbitol 35 mg/kg IV and maintained with a constant infusion of pentobarbitol 4 mg/kg/hr. Animals were laid in dorsal recumbency, intubated, and ventilated with room air using a large animal ventilator (Model 607, Harvard Apparatus, Dover, MA, USA). Minute volume was adjusted to maintain pCO_2 in the physiological range (35-40 mm Hg). Bilateral, cephalic venous cannulae were placed. An 8 French pigtail catheter was placed in the left ventricle via surgical cutdown of the right carotid artery. Position was confirmed

by characteristic waveform analysis. A 16 gauge arterial catheter was placed in each femoral artery via surgical cutdown. Continuous monitoring of left ventricular and systemic arterial haemodynamic variables were performed using Sorenson CC5 Single A-line kit transducers (Abbott Critical Care Systems, Abbott Laboratories, North Chicago, IL, USA) that were calibrated daily. A lead II ECG was recorded. Data were continuously recorded and analysed on a digital data acquisition system (BioWindow®, Modular Instruments, Malvern, PA, USA). Rectal temperature was continuously monitored (Tele-thermometer, Yellow Springs Instruments, Yellow Springs, OH, USA) and temperature maintained at 36-38 ^{0}C by means of heating pads.

Experimental protocol

Following a 10 minute stabilization period, baseline haemodynamic variables were measured. At the end of this period, organ blood flow was measured using fluorescent microspheres. $3x10^{6}$ microspheres were injected via the left ventricular catheter followed by a 5 ml flush of normal saline. Reference blood withdrawal (5 mls/min) into a heparinised syringe was performed via the right femoral artery using a Harvard withdrawal pump (Harvard Apparatus, South Natick, MA, USA). Withdrawal was commenced immediately prior to microsphere injection and was continued for 2 minutes after completion of the flush.

Polystyrene nanospheres (200 nm diameter, Polysciences Inc., Warrington, PA, USA) were prepared in a suspension of sterile water with 5% (v:v) of the pluronic stabilizer F108 (BASF, Parsipanny, NJ, USA). Each dog was given 0.1 ml/kg of a 5% suspension of nanospheres intravenously at a rate of 10 ml/min. Organ blood

flow measurements were repeated at 2.5 min post nanosphere injection and again at 60 min post injection. For the second blood flow measurement, the reference blood withdrawal rate was reduced to 2.5 ml/min and continued for 4 min post microsphere injection in the untreated animals. Preliminary experiments had shown that a rate in excess of this resulted in breaks in the column of blood, presumably due to collapse of the blood vessel.

At the completion of the experimental period, animals were euthanised (Euthanasia-5 solution, Schein Inc., Port Washington, NY, USA) and organs harvested.

Microsphere recovery and organ blood flow determination

These were performed according to the methods recommended by the Fluorescent Microsphere Resource Center (39). Reference blood samples were transferred into labelled vials for further processing. The femoral arterial catheter and the withdrawal syringe were rinsed thoroughly with 2% Tween-80® (Fisher Scientific Co., Pittsburgh, PA, USA) and the rinse added to the blood sample. Ten 1-2 g samples of each organ were individually processed. Samples were taken from similar parts of the organ for each animal. Prior to digestion, 100 µl of a standard solution of green microspheres ($1x10^3$ microspheres) was added to each sample vial using a Pipetman pipette (Rainin Instrument Company, Woburn, MA, USA). This colour acted as the internal standard to ensure that there was no loss of microspheres during recovery.

Blood samples were digested by adding 10 ml of 16N KOH to each 30 ml of diluted blood. Organ samples were digested by adding 5-10 ml of 4N KOH per 1-2 g of solid tissue. Samples were kept in the dark for 24 hours to allow complete digestion. Following digestion, the blood and tissue pieces were individually filtered through 10 μm pore polycarbonate filters (Poretics, Livermore, CA, USA) under negative pressure. The digestion vials and the burette were then washed with 2.0% Tween 80® and the washings filtered through the same filter to recover any residual material. The filter was then removed carefully using forceps and placed into an individual polypropylene test-tube. 1.25 ml of Cellusolve® acetate (Aldrich Chemical, Milwaukee, WI, USA) was then added to each tube using a calibrated pipette (Eppendorf Repeater Pipet, Brinkmann Instruments Ltd., Mississauga, ON, USA, precision <0.05-0.1%). After 4-8 hours, the tubes were vortexed vigorously and a sample of the solution was pipetted into a glass cuvette (0.7 ml volume, 10 mm path length, Starna Cells, INC., Atascadreo CA, USA). Sample fluorescence was measured using a Perkin-Elmer LS-50B luminescence spectrophotometer (Beaconsfield, Bucks) with excitation and emission slit widths of 4nm.

Tissue blood flows were calculated using the following formula:

$$\text{Blood flow (ml/min/g)} = \frac{\text{Fluorescence signal of sample x Reference flow rate (ml/min)}}{\text{Fluorescence signal of reference x Weight of sample (g)}}$$

Microsphere recovery rates were assessed for each organ. Sample loss during extraction was corrected by comparing the value of the fourth colour in the sample to the true value for the internal standard.

Microsphere distribution

Paired kidney samples for both control and treated animals were analysed to ensure evenness of mixing of microspheres.

Statistics

Statistical analyses were performed using Excel software (Microsoft Corporation, Roselle, Il, USA) and SPSS statistical software (version 9.0, Chicago, IL, USA). Baseline values for the two groups are expressed as mean ± standard deviation. Comparisons were made using Student's t-test. A p value <0.05 was considered significant. Paired organ samples were compared using the 95% confidence intervals of the differences between the samples (expressed as the percentage differences). Haemodynamic and blood flow data following injection of nanospheres are expressed as mean ± standard error of the mean. Between groups comparisons were performed using repeated measures analysis of variance (RM-ANOVA). For haemodynamic data, baseline values were used as covariates and all time points subsequent to T=0 were used. For organ blood flows, no covariates were used. Values were compared at baseline, 2.5 minutes and 60 minutes for the heart, kidneys, cortex and hindbrain.

Results

1. Baseline values

Baseline haemodynamic parameters (Table 1), body weights and arterial blood gases were similar for control and pre-treated animals. Organ blood flows at baseline are shown in Table 2.

	Control (n=4)	Pre-treated (n=4)
Mean arterial pressure (mm Hg)	156 ± 10	167 ± 6
Systolic blood pressure (mm Hg)	215 ± 15	227 ± 12
Diastolic blood pressure (mm Hg)	126 ± 13	137 ± 4
Heart rate (bpm)	153 ± 7	171 ± 17

Table 1: *Baseline systemic haemodynamics (mean ± SD)*

	Control	Pre-treated	p value
Heart	1.8 ± 0.1	2.3 ± 0.2	ns
Lungs	4.4 ± 2.0	1.2 ± 0.5	$p<0.05$
Kidneys	5.9 ± 0.6	11.0 ± 2.2	$p<0.05$
Adrenals	3.1 ± 1.2	5.3 ± 1.9	$p<0.05$
Cortex	0.4 ± 0.1	0.7 ± 0.3	ns
Hindbrain	0.4 ± 0.1	0.6 ± 0.1	ns
Spleen	1.5 ± 0.6	1.8 ± 1.0	ns
Liver	0.5 ± 0.6	0.2 ± 0.1	ns
Duodenum	1.2 ± 0.2	2.5 ± 0.6	$p<0.05$
Jejunum	1.0 ± 0.2	1.8 ± 0.8	ns
Ileum	0.6 ± 0.3	1.1 ± 0.4	ns
Colon	0.5 ± 0.2	1.4 ± 0.5	ns
Diaphragm	0.2 ± 0.1	0.6 ± 0.7	ns

Table 2: *Organ blood flow (ml/min/g) (mean ± SD).*

2. Following nanosphere injection

Systemic haemodynamics

Rapid intravenous administration of a 5% dispersion of F108-coated nanospheres caused an immediate decrease in arterial pressures and heart rate in untreated animals (Figures 1 and 2). The maximum effect was observed at approximately 3 minutes post-injection with gradual recovery over the next 60 minutes. The haemodynamic changes seen in animals pretreated with corticosteroids and antihistamines are also shown in Figures 1 and 2.

For mean arterial pressure there was no significant difference for time overall between groups but differences were significant for both the effects of treatment ($p<0.001$) and time-treatment interaction ($p<0.001$). There was no significant effect of time overall on heart rate. There was a significant effect of treatment between the groups ($p=0.02$). The effect of time-treatment interaction was not significant after adjustment for the degrees of freedom using the Greenhouse Geisser test. Apart from the severe sinus bradycardia, no electrocardiographic changes were noted.

Organ blood flow

Organ blood flows at 2.5 minutes following injection of the nanospheres are shown in Figure 3. Figure 4 shows organ blood flows at 60 minutes following nanosphere injection.

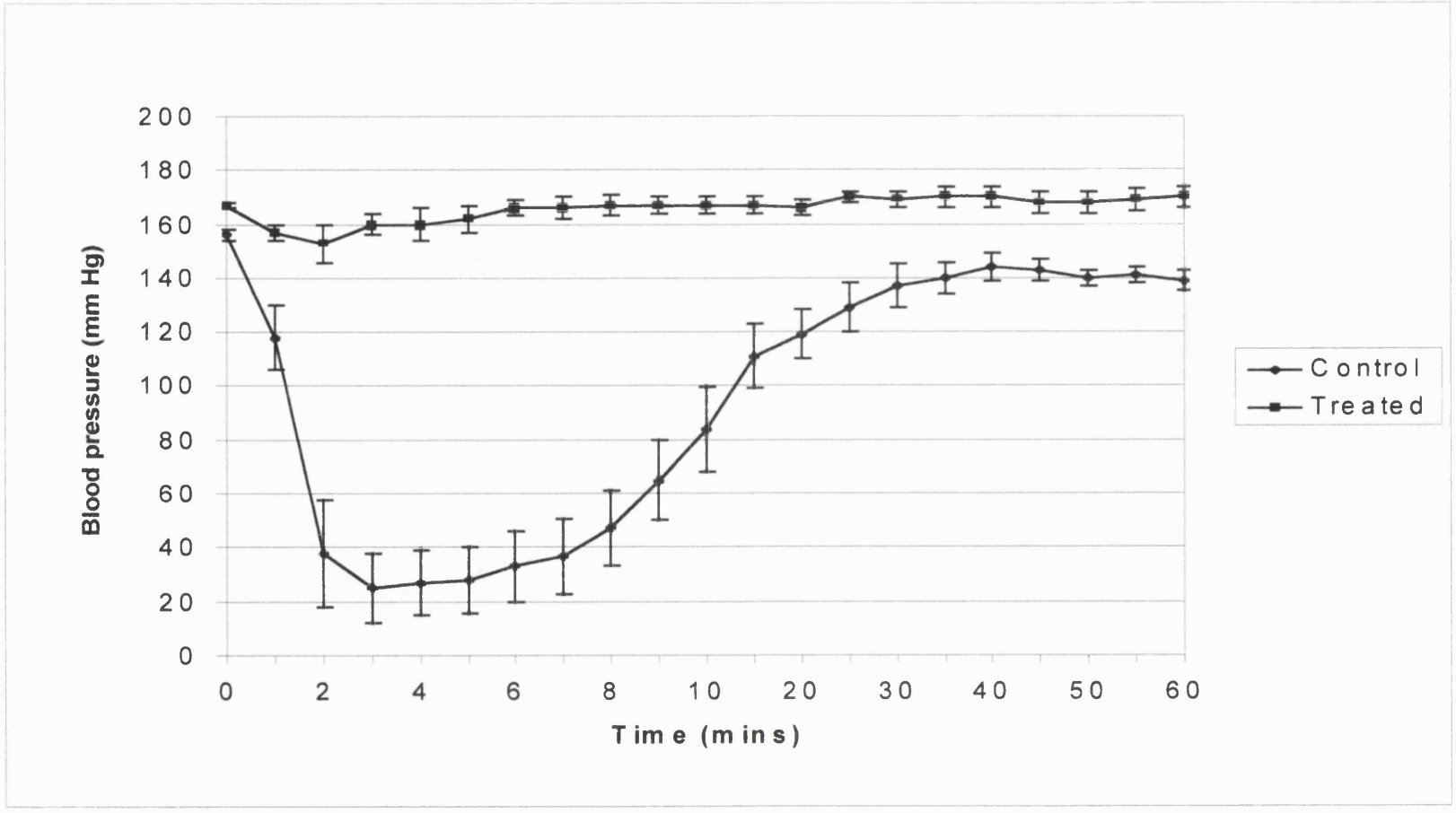

Figure 1: *Mean arterial pressure following injection of nanospheres (mean and SEM)*

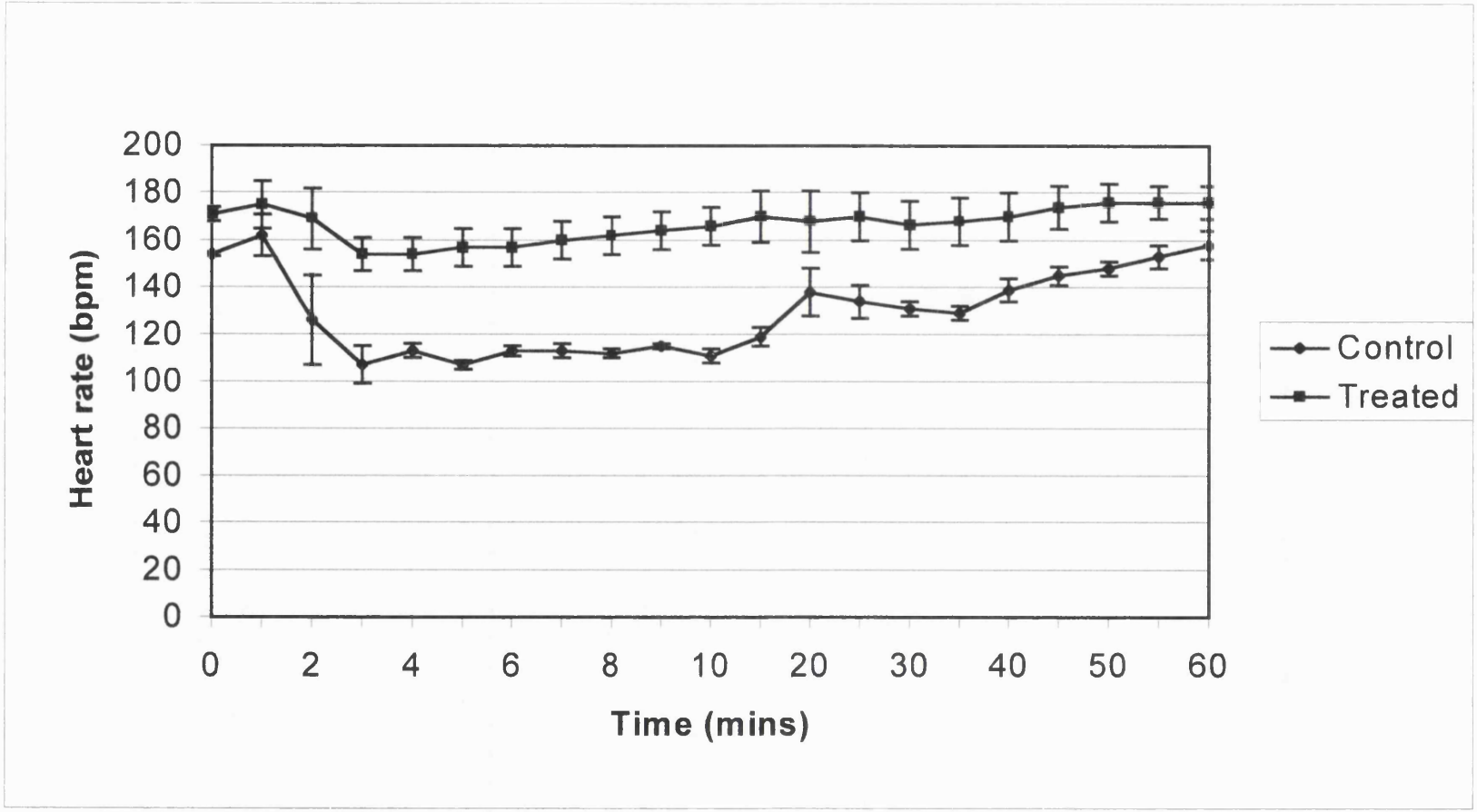

Figure 2: *Heart rate following injection of nanospheres (mean and SEM)*

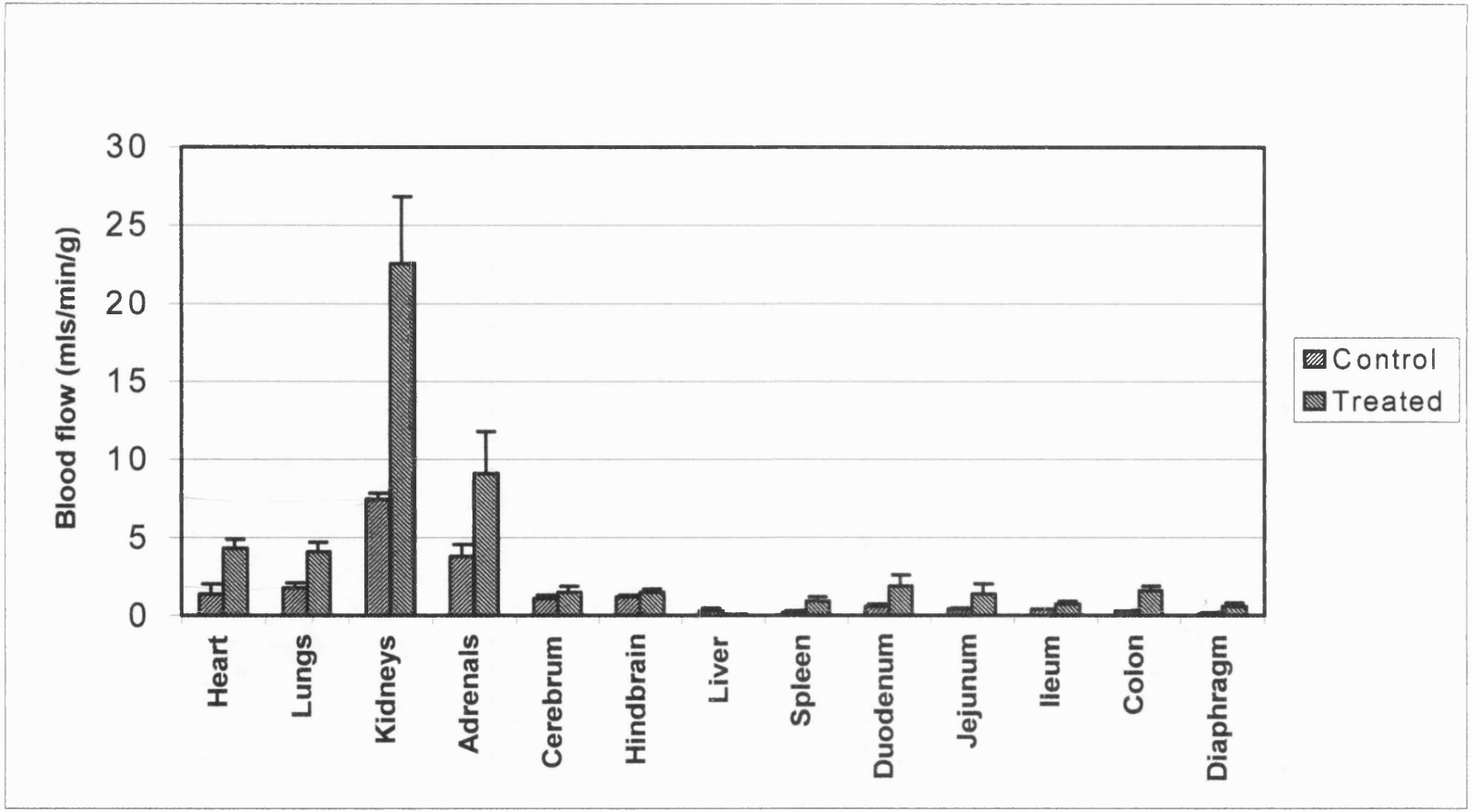

Figure 3: *Organ blood flow at 2.5 minutes following nanosphere injection (mean and SEM).*

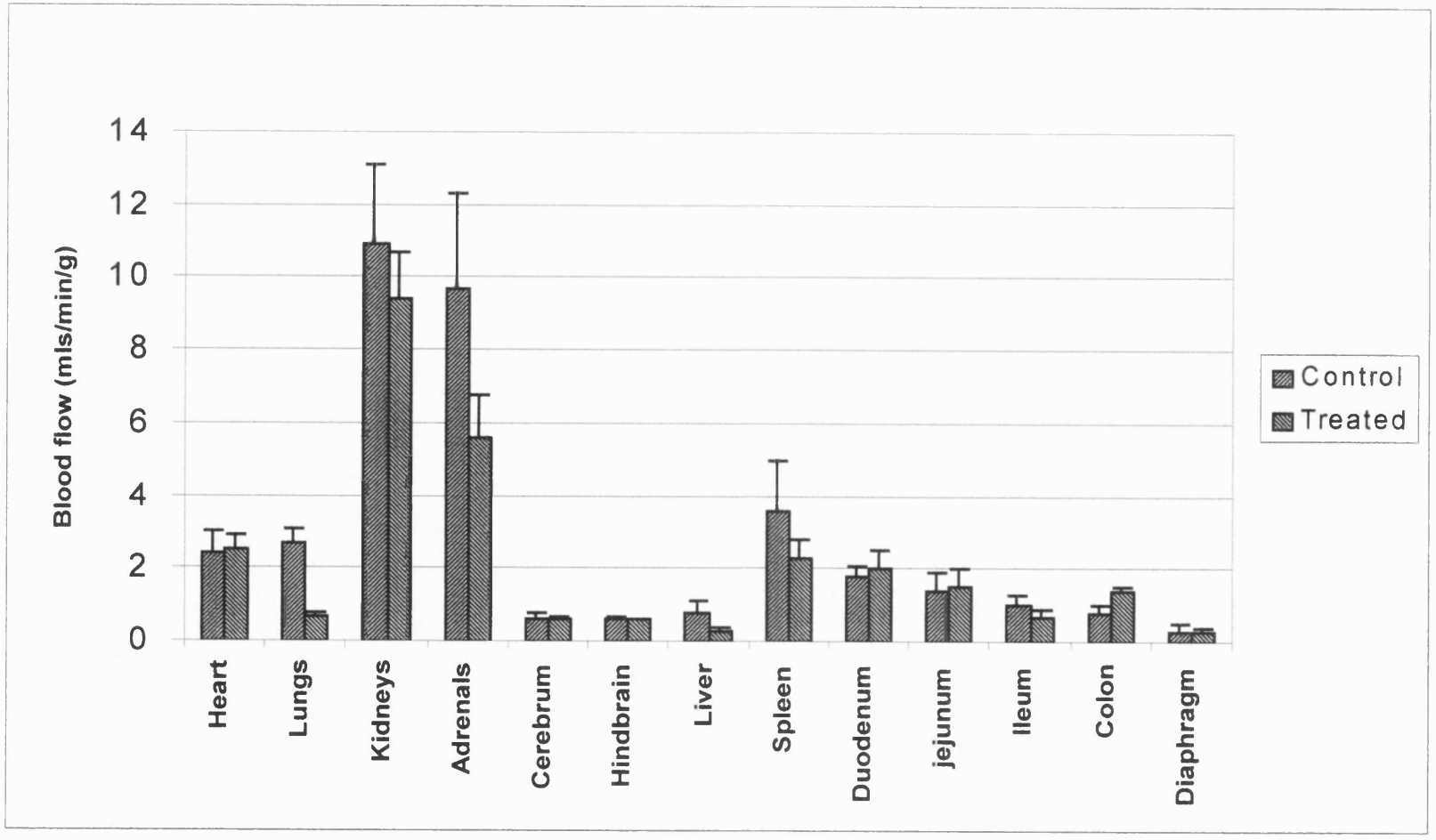

Figure 4: *Organ blood flow at 60 minutes following nanosphere injection (mean and SEM).*

Blood flows to the heart and cortex showed significant effects of time ($p=0.006$ for both heart and cortex) but not treatment ($p=0.34$ for both organs) or time-treatment interaction ($p>0.45$ for both organs). Kidney blood flows showed no significant effects of either time ($p=0.07$) or treatment ($p=0.09$) overall. Time-treatment interaction was significantly different ($p=0.031$) suggesting that the pattern of change over time differed between treated and untreated groups. At 2.5 minutes, kidney blood flow in treated animals was significantly higher than in untreated animals. Blood flows to the hindbrain showed significant effects of time ($p<0.001$) but not treatment ($p=0.16$) or time-treatment interaction ($p=0.38$). Hindbrain blood flow increased significantly in both groups at the 2.5 minute timepoint.

In untreated animals at 2.5 minutes, blood flow to the adrenals, liver and skeletal muscle appeared to be relatively preserved, whereas flows to the lungs, spleen and foregut were reduced. Treated animals showed reductions in splenic, hepatic and foregut blood flows compared to baseline values. At 60 minutes following nanosphere injection, organ blood flows in treated animals were not significantly different from baseline values in any organ. In untreated animals, blood flow to the lungs remained low, while flow to the heart and brain were similar to baseline values. Kidney, adrenal, spleen and foregut blood flows were all increased compared to baseline values.

Paired organ samples

For both groups of animals combined, the mean percentage difference and 95% confidence intervals, between right and left kidney samples was 2.5% ± 9.5% (standard deviation ± 22%). For untreated animals at the nadir of organ blood flow,

the mean percentage difference and 95% confidence intervals was 3% ± 27% (standard deviation ± 17%). These figures suggest that mixing was homogeneous and that there was no microsphere sedimentation at the level of the kidneys.

Microsphere recovery rates

Microsphere recovery rates for each organ are shown in Figure 5 (mean and 95%CI). Recovery rates exceeded 75% for all tissues studied.

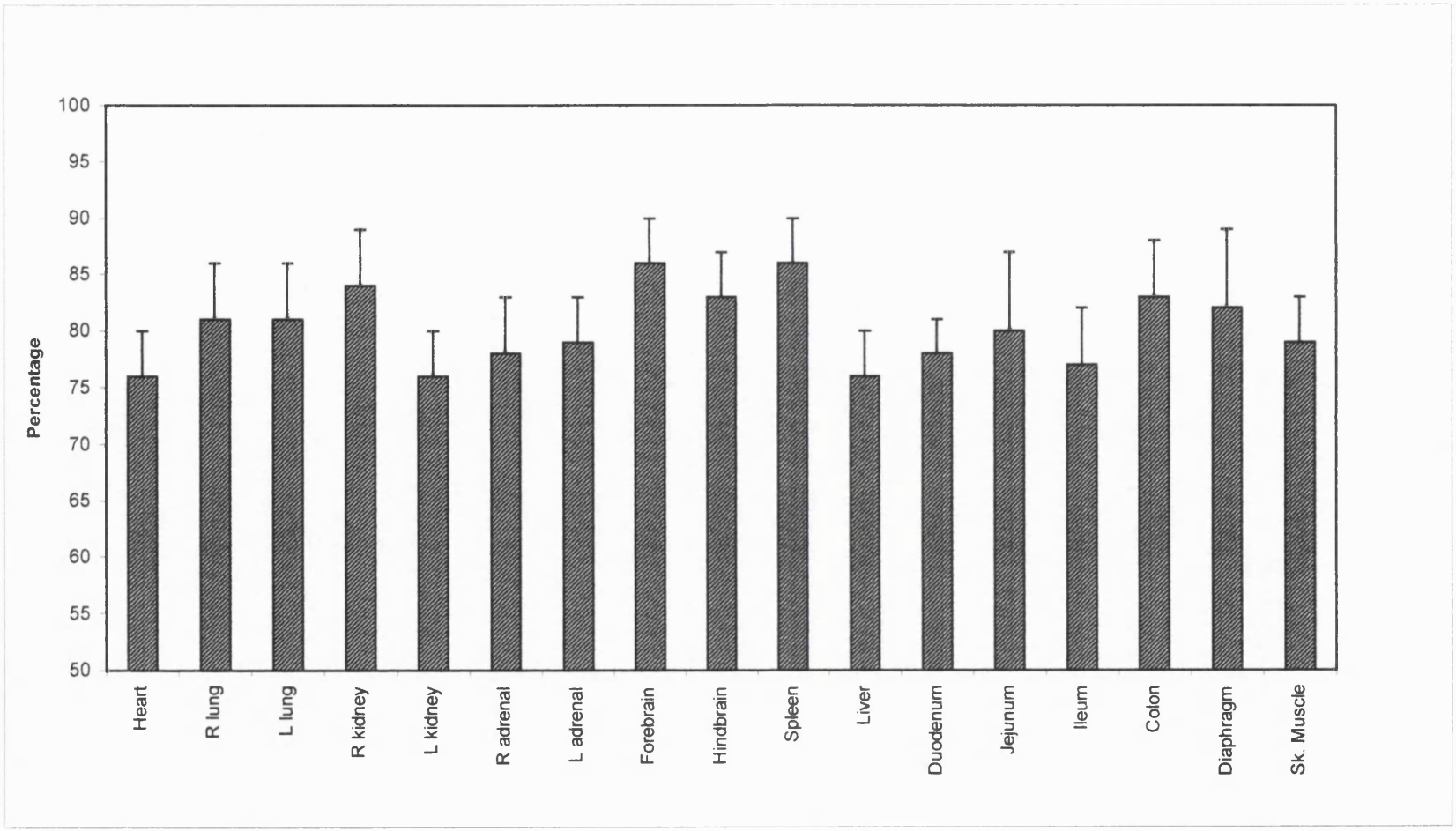

Figure 5: *Microsphere recovery rates (mean and 95% CI).*

Discussion

Nanoparticles represent promising delivery systems for a number of drugs that are difficult to formulate. Particulate systems may serve to protect the drug and the body from one another, allow placement of drug into discrete anatomical compartments that lead to drug retention, and lead to increased levels of drug carried (91). Only a limited number of studies have addressed the safety issues associated with injection of particulate formulations. Toxicity of the carrier substance to macrophages has been demonstrated even when the same material has been previously shown to be safe as a bioimplant (91). Particle-laden macrophages are likely to have impaired phagocytic function, reduced ability to catabolise serum amyloid A, and in the liver, impaired cytochrome P450 mediated metabolism of drugs (89, 97, 98, 101).

Intravenous injection of particles smaller than 7 μm has been shown to cause dose-dependent systemic hypotension in dogs (96). de Garavilla et al showed that rapid infusion of 200nm diameter particles caused a dramatic, short-lived haemodynamic response in dogs, whereas 50 nm particles elicited no response (100). These effects could be avoided by controlling dosing conditions, and were only seen with a nanoparticle-surfactant combination as neither the nanospheres nor the surfactant alone had any haemodynamic effects. In addition, administration of two doses separated by 30-60 minutes resulted in complete attenuation of the haemodynamic response to the second dose (personal communication, de Garavilla). Histamine levels were significantly elevated during the response. Pretreatment of animals with antihistamines abrogated the haemodynamic effects. Splenectomy

substantially reduced the effects suggesting that the spleen was the primary site of histamine release during this reaction.

Histamine, the first mediator of immediate hypersensitivity reactions to be characterised, is released during human systemic allergic reactions (102) as well as in various animal models of systemic anaphylaxis (103, 104). The various physiological actions of histamine result from the stimulation of two types of histamine receptors, H1 and H2. In dogs, H2 receptors mediate systemic and pulmonary vasodilatation, tachycardia and increased cardiac output, whereas H1 receptors cause systemic and pulmonary vasoconstriction and mild cardiac depression (105). The systemic hypotensive response to histamine can be blocked by a combination of H1 and H2 receptor blockade (105). Silverman et al found that although antihistamines could prevent the systemic haemodynamic effects associated with histamine infusion, they did not alter the physiological changes associated with systemic anaphylaxis (106). In these experiments we found that combination blockade with diphenhydramine (H1) and cimetidine (H2) plus steroids, could abrogate the systemic haemodynamic responses following nanosphere injection. These findings suggest that the pathological processes involved following administration of nanospheres may be similar to those seen following intravenous injection of iodinated contrast media. These reactions have been termed anaphylactoid or pseudoallergic as they are not mediated by IgE antibodies (107). In experiments using canine mastocytoma cells, histamine was released following direct stimulation by contrast media (108). Modification of the chemical and physical properties of these radiographic contrast agents can reduce the severity of reactions (109, 110).

Pretreatment with antihistamines and steroids also altered baseline regional blood flows. Blood flow to the kidneys, adrenals and duodenum were higher at baseline in treated animals compared to untreated, whereas total blood flow to the lungs was reduced. Histamine has vasodilatory effects when infused directly into the renal, adrenal and mesenteric vascular beds in dogs (111-113). These effects can be blocked by the action of antihistamines. In contrast, H1 receptor blockade augments systemic vasodilatation and increases the cardiac output and heart rate responses induced by histamine in whole animal studies (105). In the same study, H2 receptor blockade prevented systemic vasodilatation but potentiated histamine-induced pulmonary vasoconstriction. Further studies are needed using the current model to determine whether the results seen are due to effects on histamine-mediated control of blood flow, direct effects of the antihistamines or steroids, or to the unmasking of other vasoactive mediators.

Following administration of nanoparticles to untreated animals, blood flow was preferentially diverted to the cortex and hindbrain with relative preservation of flow to the heart, kidneys and adrenals. Blood flows to the foregut and to the spleen were diminished. These findings are similar to those found in the early stages of haemorrhagic shock. Vital CNS function tends to be preserved during haemorrhagic shock by maintenance of brain perfusion at the expense of other organs (50).

Chen et al (60), using a canine model of haemorrhagic shock, found that blood flow to the brain was not uniform with certain areas receiving proportionally more of the cardiac output than others. These areas included the diencephalon, the brain stem and the cervical spinal cord, areas that appear to affect cerebral blood flow and

metabolism (114). In the current experiment, we divided the brain only into cerebral cortex and hindbrain, finding that flow to both areas was significantly increased during the hypotensive response.

Coronary and hepatic blood flows in our model were also preserved despite significant hypotension. Similar findings have been reported during moderate haemorrhage (57, 62, 63). Renal and adrenal blood flows were near normal. Resting adrenal blood flow is affected by histamine in the dog, but this is overridden by other factors during hypotension with blood flows remaining near baseline values (112).

The gut is particularly susceptible to the effects of shock with intestinal vasoconstriction serving to divert blood flow to the vital organs (57, 64). The effect of moderate haemorrhage on splenic blood flow in small animals is unclear, with flows reported to be normal (64) or reduced (57). In the dog, the spleen is contractile and acts as a reservoir for red cells (115). In response to shock, it is able to contract and empty red cells into the circulation. Splenic blood flow was significantly reduced in untreated animals following infusion of nanospheres. The high volume of red cells contained within the canine spleen may render it more difficult to digest using 4N potassium hydroxide, thus reducing microsphere recovery. In these experiments, microsphere recovery rates did not differ from other tissues.

In animals pretreated with steroids and antihistamines, there was a different pattern of blood flow following nanosphere injection. Blood flows to the heart, lungs, kidneys and adrenals all showed increases from baseline. Flow to the cortex and hindbrain also increased but to a lesser degree than that seen in untreated animals.

Flows to other organs were little changed from baseline. The reasons for the changes in organ blood flow from baseline are unclear. Whilst the dosages of antihistamines used were sufficient to abolish the effects of histamine on measured systemic haemodynamic variables, they may have been insufficient to block the effects of histamine on local blood vessels. Alternatively, blockade of the histamine-mediated systemic vasodilatation may unmask the effects of other vasoactive mediators. Alterations in the kinin system, complement cascade, and coagulation system have all been reported in association with idiosyncratic reactions to contrast media (107). The increase in microspheres in lung tissue is likely to represent non-entrapment in other tissues rather than changes in lung blood flow.

At sixty minutes following nanosphere injection, organ blood flows in treated animals were similar to baseline values for all organs except the liver where flow was moderately increased. In untreated animals, blood flows to the kidneys, adrenals, brain, spleen and gut were increased compared to baseline, suggesting a reactive hyperaemia following a period of low flow.

Conclusions

This study further defines the physiological effects seen following intravenous nanosphere injection in the dog. During anaphylactoid shock in untreated animals, organ blood flow mirrors that seen during haemorrhagic shock, with blood flow diverted away from the splanchnic bed to maintain cerebral and coronary perfusion. Pretreatment with antihistamines and steroids abolishes the haemodynamic effects of nanosphere injection, however, blood flow to the heart, lungs, kidneys and brain is

significantly affected. Further studies are needed to document the mechanisms involved in the redistribution of organ blood flow and the pathophysiological significance of this phenomenon.

Chapter 8: Conclusions regarding the use of fluorescent microspheres to measure organ blood flows.

The use of microspheres as a method of measuring blood flow in experimental animals has gained widespread acceptance. This can be attributed to the advantages of being able to perform multiple consecutive blood flow measurements in different organs, to quantify blood flow in absolute units, to provide accurate and reproducible estimates of flow, and to achieve the above with relative ease (43). Despite a number of limitations, the use of radioactive microspheres is regarded as a "gold standard" for regional blood flow measurement. Radioactivity poses health risks and the tissues require special precautions for use and disposal. Radioactive microspheres also have limited shelf-lives and are consequently relatively expensive.

Early studies using fluorescent-labelled microspheres used light microscopy and manual counting techniques to identify regions of ischaemia or to estimate regional perfusion (15,16). In 1993, Glenny et al reported excellent correlations between radioactive and fluorescent microspheres in the measurement of blood flows to the dog lung, pig heart and pig kidney (17). They reported methods of extracting the fluorescent dye from microspheres, enabling the concentration of fluorescence to be read by an automated fluorescence spectrophotometer.

This current work was prompted by the need to replace the existing radioactive microsphere technique in our laboratory with a non-radioactive method. The practical issues in using a fluorescent spectrophotometric technique proved relatively simple to master. Fluorescence excitation and emission curves for each

coloured microsphere concurred closely with those supplied by the manufacturers. The correlations between the amount of fluorescence and the number of microspheres per ml were >0.99 for the concentrations used in these experiments, thus allowing a wide range of organ blood flows to be measured. The spectrophotometer has the ability to perform up to 15 intensity measurements on a single sample. Lack of a red-sensitive photomultiplier severely limited the number of fluorescent labels that we were able to separate. Use of spectral spillover correction allows measurement of up to ten labels (18). In the absence of a red-sensitive photomultiplier, we could not use dyes with emission wavelengths above that of orange and this limited us to four labels. Machine and operator variability were extremely good in our hands with a coefficient of variability of <2% for all colours. These values compare favourably with those reported by Glenny et al (17).

Factors that may influence the accuracy and reproducibility of blood flow measurement by the microsphere technique have been previously discussed (2, 21, 116). The numbers of microspheres per sample must exceed 400 to give a coefficient of variation of <5%. With between 100-400 microspheres the coefficient of variation increases to between 6-9%, and increases considerably if the number of microspheres per sample is <100. If, after the experiment, the umber of microspheres in small samples is too low, data can be pooled among small samples. The number of microspheres used for each injection for both rat and dog experiments were similar to those reported by other groups (16, 17, 23, 24, 116, 117). The greatest variability seen in the current experiments were in lung and adrenal samples. In all protocols, the lung blood flow measured included both pulmonary and bronchial flow. Non-entrapment of microspheres in the systemic circulation is reported to be low but must

be considered if lung flow is the primary interest in experimental studies (2, 26). Variation in lung blood flow measurements may be improved by air-drying of tissues prior to estimation of blood flow. In this technique, blood flow is based on flow per gram of tissue. Post-mortem alterations in lung water may account for some of the variability (Glenny RW, personal communication). Rat adrenal samples were at the limit of accurate weighing in the current experiments and this may have accounted for some of the increased variability.

Injection of microspheres may have effects on the vascular resistance of tissue samples and this may affect other cardiovascular parameters. We found no significant changes in systemic haemodynamic variables following injection of a total of 0.6 x 10^6 microspheres in rats. After control for haemodynamic variations, we found a maximum mean temporal variation in blood flow in the heart of 26% (95% CI, -8% to 60%), and 21% in the kidney (95% CI, -9 to 45%). These figures are larger than those reported by Prinzen and Glenny (20) but are similar to those reported by Marcus et al (46). It should be noted that Prinzen and Glenny used only two injections of microspheres separated by five minutes as opposed to three injections each separated by ten minutes in the experiments reported above.

Use of fluorescent microspheres to measure blood flow is only valid if the fluorescence signal does not decay with time and the microspheres behave like blood cells in the circulation. In long-term experiments, fluorescent microspheres have been reported to be stable in tissue for periods up to two months (10). Once the microspheres have been dissolved to release the fluorescence, the colour has been reported to be stable for $\leq$7 days (17). In the current experiments, tissue samples were

kept for a maximum of 48 hours prior to digestion and all measurements of fluorescence were made within 24 hours of tissue processing. Aggregation of microspheres is prevented by the use of small amounts of detergent in the injectate and vigorous sonicating and vortexing prior to use. The choice of detergent is important as some have been reported to cause haemodynamic effects in animals (24). Tween 80, the detergent used in the above experiments, is also reported to cause fluorescence in the same spectra as the blue fluorescent microspheres supplied by Molecular Probes (36). The blue-labelled microspheres were not used in the above experiments. Measurement of paired organ blood flows (cerebral hemispheres or kidney samples) provides an internal control to ensure that microspheres are homogeneously mixed and that there is no sedimentation (3, 43). In the above experiments, paired kidney samples were chosen as the right carotid artery was routinely cannulated to allow injection of microspheres (21). The maximum mean variation in paired samples in the rat was 5% (95% CI, -18% to 28%), and in the dog 3% (95% CI, -24% to 30%). DeBehnke has recently reported variations of 13% in paired kidney blood flows in pigs at baseline using the fluorescent microsphere method (118). Variation in conditions of low flow was 10%. The values obtained in our experiments suggest that, at least at the level of the renal arteries, microspheres were homogeneously distributed.

Despite concerns expressed by other authors concerning the digestion of tissues with high fat content (20), we experienced little difficulty. Microsphere recovery in the above experiments exceeded 75% for all tissues in all experiments and generally was >85%. Tissue digestion has been reported to be facilitated by mincing the tissue with a tissue homogeniser (Mullers-Bouman M-L, Prinzen FW, unpublished

observations). Fluorescent as well as radioactive microspheres remain intact during this procedure. Although 16M KOH is used for digestion of reference blood samples, we found that microsphere recovery from vascular tissues such as the canine spleen were not altered from those obtained using 4M KOH. Loss of microspheres during processing is common to all non-radioactive microsphere techniques. We adopted the internal standard test of Chien et al to ensure that microsphere loss during extraction could be corrected (29). Although Chien et al assessed the error associated with this method as being <2%, other groups have not been able to obtain such good results (Prinzen FW, personal communication). In our hands, the error introduced by the internal standard test was at least 6% (Appendix 1). The introduction of automated processing, that allows all the steps after tissue sampling to be performed in a single tube, may obviate the need for sample correction.

Baseline blood flows for both rats and dogs were of similar magnitude to those reported by other investigators. Tuma et al have noted that as a result of the great diversity of organ blood flows, no single protocol will suit every tissue of interest (21). While relatively low numbers of microspheres may be adequate to measure blood flow to high flow organs such as the heart and kidneys, much larger numbers of microspheres would be needed to measure flow to resting skeletal muscle. The choice of anaesthetic agent also has considerable effect on absolute organ blood flow. In the normal physiological state, ketamine increases cerebral metabolism and cerebral blood flow, and is usually associated with stimulant effects on the cardiovascular system with increases in heart rate, blood pressure and cardiac output (119, 120). The survival rate of rats subjected to severe haemorrhage is higher when anaesthetised with ketamine compared to other anaesthetic agents (69). This may result from

improvement in splanchnic perfusion. The effects of pentobarbitol anaesthesia in dogs were studied by Kaihara et al using the microsphere technique (121). They found no differences between anaesthetised and unanaesthetised dogs in the fractional distribution of cardiac output to the heart, liver, spleen, kidneys, and pancreas. The brain and intestines were not studied. Redistribution of cardiac output after pentobarbitol anaesthesia has been reported in rats and primates (122, 123).

The effects of gender on regional blood flow are not known. In the experiments above we used male animals exclusively. Gender-specific differences in tolerance of ischaemia have been noted in a number of studies. Adult female mice had a significantly reduced mortality compared to males following repeated exposure to extreme hypoxia (124). Young gerbils and sexually mature females were more tolerant to carotid artery ligation (73). In contrast, female dogs subjected to normothermic cardiac arrest and resuscitation showed significantly higher levels of hepatic and renal ischaemic injury (74). Results from our studies should not, therefore, be extrapolated to female animals.

The use of fluorescent microspheres for measurement of organ blood flows is relatively new. Compared to the radioactive technique, the principal problems are microsphere isolation and automation. The standard method of isolating fluorescent microspheres is by negative–pressure filtration. This method has been rigorously evaluated and is cheap to perform. However, it is labour intensive and there is the risk of microsphere loss during the transfer of samples from one container to the next. A simplified processing technique has been reported that uses sedimentation to isolate microspheres (36). Tissue or blood samples are digested with 2N KOH for 48 hours

at 60^0C. The sample tubes are then centrifuged and the supernatant carefully removed to leave <1ml. The difference in specific gravity between digestion medium and the microspheres allows formation of a pellet containing microspheres and some debris. The pellet is washed once with detergent (0.5% Tween-80) and the centrifugation step repeated. The pellet is then washed once or twice with distilled water, each time repeating the centrifugation step. After mixing the pellet with dye solvent and sedimentation of debris with a final centrifugation step, the supernatant can be used for spectrophotometry. Using this method, large numbers of sample tubes can be processed simultaneously using a standard laboratory centrifuge. This contrasts with the negative-pressure filtration technique where isolation of microspheres is performed for each sample individually. The sedimentation method also has the advantage that all processing is performed in a single tube reducing the risk of microsphere loss during transfer. In their experiments, Van Oosterhout et al reported <1% loss of total fluorescence (36). Organ blood flows using this technique were compared with those obtained using radioactive microspheres and were found to correlate well.

Automation of fluorescent spectrophotometry has been reported. Glenny et al reported the use of a 96-well microplate reader (17). Compared with the cuvette reader, the fluorescent signal from the microplate reader was linear over a shorter range of microspheres with an earlier plateau due to quenching. This was thought to result from the use of a surface reading instrument with a short path length. Restriction in the number of microspheres used (<2000) resulted in a more linear relationship between fluorescence intensity and microsphere number. When compared with radio-labelled estimates of perfusion, microplate estimates were less

well correlated, had slopes further from unity and intercepts further from the origin than did the same samples read in cuvettes. A new well plate reader has been reported to perform better (R Glenny, personal communication). Spectrometry may also be automated by interfacing an autosampler with a flow cell in the spectrophotometer (20). This approach uses transmission fluorimetry rather than surface fluorescence in the case of well plate readers.

The fluorescent microsphere technique appears to hold most promise in replacing radioactive microspheres. The high sensitivity and good spectral separation mean that the number of microspheres injected can be as low as for radioactive microspheres, and up to ten labels can currently be resolved. Validation studies suggest the accuracy of the fluorescent microsphere method is superior to other non-radioactive microsphere methods. Further automation of the processes of microsphere extraction and quantification of the fluorescent signal are likely to make the use of the fluorescent microsphere technique more attractive to a larger group of investigators.

Appendix 1: Assessment of the variability introduced by the use of the internal standard test for complete microsphere recovery.

Introduction

The problem of loss of microspheres during processing is common to all of the non-radioactive microsphere techniques (20). In 1995, Chien et al introduced a method to determine the amount of microspheres lost during the extraction process and to allow correction for this loss (29). A known aliquot of microspheres of a colour not used in the experiment is added to the tissue and blood samples prior to the extraction process. This colour microsphere acts as the internal standard. After the extraction process is completed, all samples should have comparable signals for this colour.

At least three aliquots of the internal standard are allowed to air dry overnight and then read. The average of these values is taken as the value for 100% recovery. If there is a discrepancy between the signal obtained from the tissue sample and the value for 100% recovery, correction can be made according to the formula

$$I_{true} = I_{obs} (I_{st.true} / I_{st.obs})$$

Where I_{true} is the true fluorescence signal, I_{obs} is the observed (measured) fluorescence signal, $I_{st.true}$ is the true fluorescence standard signal and $I_{st.obs}$ is the measured fluorescence standard signal. Chien et al assessed the error associated with the addition of the internal standard and found it to be <2% (29). Other groups have

independently assessed the error associated with this method and have been unable to obtain such good results. As a result the internal standard has been abandoned (F. Prinzen, personal communication). We sought to study the error inherent in our own use of the internal standard.

Methods

Internal standard solution was prepared by vortexing fluorescent microspheres (15.0 μm, Molecular Probes, Eugene, OR, USA) vigorously for 10-15 seconds. Microspheres were then placed in an ultrasonic water bath for 10 minutes to ensure disaggregation. The microspheres were then vortexed for a second time. 0.1 ml of the concentrated microsphere solution (1×10^6 microsphere per ml) was added to 10 ml of 2% Tween-80® (Fisher Scientific co., Pittsburgh, PA, USA). The resulting solution was vortexed further. 20 standardised aliquots (100 μl) of this internal standard solution were pipetted directly onto 25mm membrane filters (pore size 10 μm, Poretics Corporation, Livermore, CA, USA) using a calibrated pipette (Eppendorf Repeater Pipet, Brinkmann Instruments Ltd., Mississauga, ON, USA, precision 0.05-0.1%). Filters were placed in the dark and allowed to air dry overnight. 20 additional aliquots were individually vacuum filtered through similar membrane filters. All filters were then placed into cryovials and 1.25mls of Cellusolve® acetate (Aldrich Chemicals, Milwaukee, WI, USA) added using a calibrated pipette. Samples were placed in a glass cuvette (0.7 ml volume, path length 10mm, Starna Cells Inc., Atascadreo, CA, USA) and read in a luminescence spectrophotometer (LS-50B, Perkin Elmer Corporation, Beaconsfield, Bucks).

Statistics

Data summarisation and statistical analyses were performed using Excel software (Microsoft Corporation, Roselle, Il, USA).

Results

Results are shown in Figure 1. The coefficient of variation for samples that were air-dried was 6.7% and for vacuum filtered 10.9%.

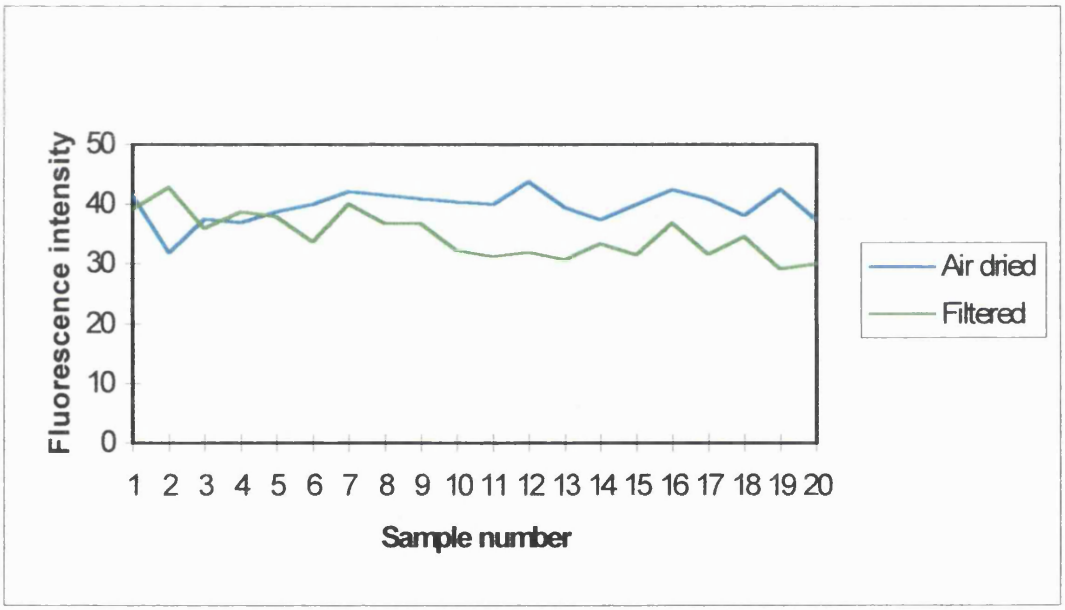

Figure 1: *Fluorescence intensity of air-dried and vacuum filtered internal standards.*

Discussion

Isolation of fluorescent microspheres from blood or tissue samples may be performed by vacuum filtration (17) or by centrifugal sedimentation (36, 125). Austin

et al reported that the recovery of fluorescent microspheres from myocardial tissue was 72.1% ± 1.4% (mean ± SEM) (125). Recovery was assessed by loss of radioactivity from simultaneously injected radioactive microspheres. Van Oosterhout et al assessed microsphere recovery by the use of the internal standard method and by analysis of the supernatant resulting from all rinsing steps from the samples (36). They found that values from tissue samples were 4% lower than those obtained from the directly extracted aliquots of standard solution. This difference was not statistically significant. Less than 1% of the total fluorescence was found in the supernatant. The average loss of microspheres during extraction by vacuum filtration has been reported to be 2.4% (29). The potential variability introduced by the use of an internal standard in these experiments was considerably higher than that obtained by Chien et al (29).

Automation of both microsphere isolation and fluorescence quantification is being developed (R. Glenny and F. Prinzen, personal communication). This may obviate the need for sample correction by the internal standard as all manipulations can be done in the same tube.

If the internal standard is to be used routinely to correct for loss, it should add little if any additional variation into the results. It may be more appropriate to use this technique solely to identify samples where a significant fraction of the signal has been lost during processing, such that these samples can be excluded from further analysis.

Appendix 2: Effects of tissue digestion in different concentrations of KOH on recovery rates of fluorescent microspheres from canine spleen.

Introduction

The canine spleen is contractile and acts as a reservoir of red cells that can empty in response to shock, epinephrine, hypoxia, acidosis, and other stimuli. (115). The volume of splenic autotransfusion is between 4-6 ml/kg of red cells (115, 126). Tissue and blood samples containing fluorescent microspheres must be digested to recover the microspheres. Current guidelines suggest using 4M KOH for the digestion of solid tissue and 16M KOH for the digestion of reference blood samples (17). The large red cell mass contained within the canine spleen led to concern that tissue digestion and, therefore, microsphere recovery would be incomplete following digestion in 4M KOH. To investigate this we varied the concentration of KOH used for tissue digestion and assessed microsphere recovery rates using the internal standard method of Chien et al (29). Anecdotal experience suggested that digestion might be improved by freezing of the tissue and this was also tested.

Methods

Canine spleen samples (0.5-1.5 g) were removed following completion of animal experimentation. Samples were weighed and placed into individual vials. Prior to digestion, 100 µl of a standard solution of green microspheres ($1x10^3$ microspheres) was added to each sample vial using a Pipetman pipette (Rainin Instrument Company, Woburn, MA, USA). Organ samples were digested by adding

5-10 ml of a) 4N KOH, b) 8N KOH, c) 16N KOH, or d) freezing at -10^{0}C for 24 hours followed by the addition of 4N KOH, per 1-2 g of solid tissue (n=10 for each group). Samples were kept in the dark for 24 hours to allow complete digestion. Following digestion, the blood and tissue pieces were individually filtered through 10 μm pore polycarbonate filters (Poretics, Livermore, CA, USA) under negative pressure. The digestion vials and the burette were then washed with 2.0% Tween 80® (Fisher Scientific Co., Pittsburgh, PA, USA) and the washings filtered through the same filter to recover any residual material. The filter was then removed carefully using forceps and placed into an individual polypropylene test-tube. 1.25 ml of Cellusolve® acetate (Aldrich Chemical, Milwaukee, WI, USA) was then added to each tube using a calibrated pipette (Eppendorf Repeater Pipet, Brinkmann Instruments Ltd., Mississauga, ON, USA, precision <0.05-0.1%). After 4-8 hours, a sample of the solution was pipetted into a glass cuvette (0.7 ml volume, 10 mm path length, Starna Cells Inc., Atascadreo, CA, USA) and the fluorescence of the sample determined using a luminescence spectrophotometer (LS-50B, Perkin Elmer Corporation, Beaconsfield, Bucks).

Sample loss during extraction was assessed by comparing the value of the fourth colour in the sample to the true value for the internal standard.

Statistics

Data summarisation and statistical analyses were performed using Excel software (Microsoft Corporation, Roselle, Il, USA). Microsphere recovery rates are shown (mean ± 95%, CI). Groups were compared using Student's t test. A p value <0.05 was considered significant.

Results

Microsphere recovery rates with each technique are shown in Table 1. Values did not differ significantly between techniques.

Digestion technique	% recovery
4N	111 ± 9
8N	108 ± 8
16N	103 ± 9
Frozen / 4N	106 ± 5

Table 1: *Percentage recovery (mean, ± 95% CI) of fluorescent microspheres with varying tissue digestion methods.*

Discussion

Fluorescent microspheres must be physically separated from the tissue or blood sample in order to quantify the amount of fluorescence in each sample. The method used to separate the spheres depends upon the tissue. 4N KOH solution is recommended to digest tissues such as kidney and heart but may not completely digest brain, fascia or cartilage. 2N ethanolic KOH has been suggested for brain and fascia (127). 16N KOH is used for blood samples. The present study suggests that digestion of canine splenic tissue is complete following digestion with 4N KOH for 24 hours, and that no additional benefit is derived from digestion in more concentrated solutions of KOH or by freezing the tissue prior to digestion.

References

1. Rudolph AM, Heymann MA. The circulation of the fetus in utero: method of studying distribution of blood flow, cardiac output and organ blood flow. Circ Res 1967; 21: 163-184
2. Buckberg GD, Luck JC, Payne B, et al. Some sources of error in measuring regional blood flow with radioactive microspheres. J Appl Physiol 1971; 31: 598-604
3. Heymann MA, Payne BD, Hoffman JIE, Rudolph AM. Blood flow measurements with radionuclide-labeled particles. Prog Cardiovasc Dis 1977; 20: 55-79
4. Berman W Jr., Goodlin RC, Heymann MA, et al. The measurement of umbilical blood flow in fetal lambs in utero. J Appl Physiol 1975; 39: 1056-1059
5. Domenech RJ, Hoffman JIE, Noble MIM, et al. Total and regional coronary blood flow measured by radioactive microspheres in conscious and anesthetized dogs. Circ Res 1969; 25: 581-596
6. Edmunds LH Jr., Gold WM, Heymann MA. Lobar distribution of pulmonary arterial blood flow in awake standing dogs. Am J Physiol 1970; 219: 1779-1783
7. Makowski EL, Meschia G, Droegemueller W, Battaglia FC. Measurement of umbilical arterial blood flow to the sheep placenta and fetus in utero. Circ Res 1968; 23: 623-631
8. Hales JRS. Radioactive microsphere techniques for studies of the circulation. Clin Exp Pharmacol Physiol Suppl 1974; 1: 31-46
9. Delaney JP, Grimm E. Canine gastric blood flow and its distribution. Am J Physiol 1964; 207: 1195-1202

10. van Oosterhout MFM, Hales JRS, Glenny RW, et al. Fluorescent microspheres are superior to radioactive microspheres in chronic experiments. Proceedings of the 2nd International Conference on Fluorescent Microsphere Methods, Munich 1995 (abstract).
11. Hale SL, Alker KJ, Kloner RA. Evaluation of nonradioactive, colored microspheres for the measurement of regional myocardial blood flow in dogs. Circulation 1988; 78: 428-434
12. Kowallik P, Schulz R, Guth BD, et al. Measurement of regional myocardial blood flow with multiple colored microspheres. Circulation 1991; 83: 974-982
13. Morita Y, Payne BD, Aldea GS, et al. Local blood flow measured by fluorescence excitation of nonradioactive microspheres. Am J Physiol 1990; 258: H1573-1584
14. Mori H, Haruyama S, Shinozaki Y, et al. New nonradioactive microspheres and more sensitive X-ray fluorescence to measure regional blood flow. Am J Physiol 1992; 263: H1946-H1957
15. Hale SL, Vivaldi MT, Kloner RA. Fluorescent microspheres: a new tool for visualization of ischemic myocardium in rats. Am J Physiol 1986; 251: H863-H868
16. Jasper MS, McDermott P, Gann DS, Engeland WC. Measurement of blood flow to the adrenal capsule, cortex and medulla in dogs after hemorrhage by fluorescent microspheres. J Auton Nerv Syst 1990; 30: 159-168
17. Glenny RW, Bernard S, Brinkley M. Validation of fluorescent-labeled microspheres for measurement of regional organ perfusion. J Appl Physiol 1993; 74: 2587-2597
18. Abel FL, Cooper RH, Beck RR. Use of fluorescent latex microspheres to measure coronary blood flow distribution. Circ Shock 1993; 41: 156-161

19. Schimmel C, Frazer D, Glenny R. Validation of spillover correction for 10 fluorescent labeled microspheres. Proceedings of the Third International Conference on Fluorescent Microsphere Methods, Seattle 1996 (abstract)
20. Prinzen FW, Glenny RW. Developments in non-radioactive microsphere techniques for blood flow measurement. Cardiovasc Res 1994; 28: 1467-1475
21. Tuma RF, Vasthare US, Irion GL, Wiedeman MP. Considerations for the use of microspheres for flow measurements in anesthetized rat. Am J Physiol 1986; 250: H137-H143
22. Millard RW, Baig H, Vatner SF. Cardiovascular effects of radioactive microsphere suspensions and Tween 80 solutions. Am J Physiol 1977; 232: H331-H334
23. Hoffman JIE, Payne BD, Heymann MA, Rudolph AM. The use of microspheres to measure blood flow. In: *Techniques in Life Sciences: Physiology. Techniques in Cardiovascular Physiology*, ed. RJ Linden. 1983, vol 3, part1, pp 1-36. Ireland, Elsevier Scientific.
24. Flaim SF, Morris ZQ, Kennedy TJ. Dextran as a radioactive microsphere suspending agent: severe hypotensive effect in rat. Am J Physiol 1978; 235: H587-H591
25. Bassingthwaite JB, Malone MA, Moffett TC, et al. Validity of microsphere depositions for regional myocardial flows. Am J Physiol 1987; 253: H184-H193
26. Fan F-C, Schuessler GB, Chen RYZ, Chien S. Determinations of blood flow and shunting of 9- and 15-μm spheres in regional beds. Am J Physiol 1979; 237: H25-H33

27. Capurro NL, Goldstein RE, Aamodt R, et al. Loss of microspheres from ischemic canine cardiac tissue: an important technical limitation. Circ Res 1979; 44: 223-227

28. Jugdutt BI, Hutchins GM, Bulkley BH, Becker LC. The loss of radioactive microspheres from canine necrotic myocardium. Circ Res 1979; 45: 746-756

29. Chien GL, Anselone CG, Davis RF, Van Winkle DM. Fluorescent vs. radioactive microsphere measurement of regional myocardial blood flow. Cardiovasc Res 1995; 30: 405-412

30. Matsui H, Yamagata S Jr., Hirano K, et al. Autofluorescence in onset of gastric mucosal injury induced by hemorrhagic shock in rats. Dig Dis Sci 1994; 39: 116-123

31. Lansing Taylor D, Salmon ED. Basic fluorescence microscopy. Methods Cell Biol 1989; 29: 207-237

32. Johnson ID. Introduction to fluorescence techniques. In: *Handbook of fluorescent probes and research chemicals 6th edition*, ed RP Haughland. 1996, pp1-6. Eugene, Molecular Probes.

33. Guilbault GG. Practical fluorescence. In: *Modern Monographs in Analytical Chemistry*, ed GG Guilbault. 1990, vol. 3. New York, Dekker.

34. Anonymous. Fluorescent microsphere physical characteristics. In: *Manual for using fluorescent microspheres to measure regional organ perfusion.* 1996. Seattle, Fluorescent Microsphere Resource Center.

35. Schosser R, Arfors KE, Messmer K. MIC-II – a program for the determination of cardiac output, arterio-venous shunt and regional blood flow using the radioactive microsphere method. Comput Programs Biomed 1979; 9: 19-38

36. van Oosterhout MFM, Willigers MM, Reneman RS, Prinzen FW. Fluorescent microspheres to measure organ perfusion: validation of a simplified sample processing technique. Am J Physiol 1995; 38: H725-H733

37. Anonymous. Standard curves, fluorescent controls, background fluorescence and sources of error. In: *Manual for using fluorescent microspheres to measure regional organ perfusion.* 1996. Seattle, Fluorescent Microsphere Resource Center.

38. Sestier FJ, Mildenberger RR, Klassen GA. Role of autoregulation in spatial and temporal perfusion heterogeneity of canine myocardium. Am J Physiol 1978; 235: H64-H71

39. Anonymous. Microsphere measurement of regional organ perfusion. In: *Manual for using fluorescent microspheres to measure regional organ perfusion.* 1996. Seattle, Fluorescent Microsphere Resource Center.

40. Wicker P, Tarazi RC. Importance of injection site for coronary blood flow determinations by microspheres in rats. Am J Physiol 1982; 242: H94-H97

41. Tsuchiya M, Walsh GM, Frohlich ED. Systemic hemodynamic effects of microspheres in conscious rats. Am J Physiol 1977; 233: H617-H621

42. Hoffman WE, Miletich DJ, Albrecht RF. Repeated microsphere injections in rats. Life Sci 1981; 28: 2167-2172

43. von Ritter C, Hinder RA, Womack W, et al. Microsphere estimates of blood flow: methodological considerations. Am J Physiol 1988; 254: G275-G279

44. Glenny RW, Robertson HT. Fractal properties of pulmonary blood flow: characterization of spatial heterogeneity. J Appl Physiol 1990; 69: 532-545.

45. Sasaki Y, Wagner HN Jr. Measurement of the distribution of cardiac output in unanesthetized rats. J Appl Physiol 1971; 30: 879-884

46. Marcus ML, Kerber RE, Erhardt JC, et al. Spatial and temporal heterogeneity of left ventricular perfusion in awake dogs. Am Heart J 1977; 94: 748-754

47. Waxman K: Physiologic response to injury. In: *Textbook of Critical Care*. 3rd edition, eds Ayres SM, Grenvik A, Holbrook PR and Shoemaker WC. 1995, pp 1395-1402. Philadelphia, WB Saunders.

48. Foëx B. Systemic responses to trauma. Br Med Bull 1999; 55: 726-743

49. Griffiths RD, Hinds CJ, Little RA. Manipulating the metabolic response to injury. Br Med Bull 1999; 55: 181-195

50. Peitzman AB, Harbrecht BG, Udekwu AO, et al. Hemorrhagic shock. Curr Probl Surg 1995; 32: 927-1002

51. Blahitka J, Rakusan K. Blood flow in rats during hemorrhagic shock: differences between surviving and dying animals. Circ Shock 1977; 4: 79-93

52. Bereiter DA, Zaid AM, Gann DS. Effect of rate of hemorrhage on release of ACTH in cats. Am J Physiol 1986; 250: E76-E81

53. Jones MT, Gillham B. Factors involved in the regulation of adrenocorticotropic hormone/beta-lipotropic hormone. Physiol Rev 1988; 68: 743-750

54. Wiggers CJ. Experimental hemorrhagic shock. In: *Physiology of shock.* 1950, pp 121-146. New York, Commonwealth.

55. Bellamy RF, Maningas PA, Wenger BA. Current shock models and clinical correlations. Ann Emerg Med 1986; 15: 1392-1395

56. Capone A, Safar P, Stezoski SW, et al. Uncontrolled hemorrhagic shock outcome model in rats. Resuscitation 1995; 29: 143-152

57. Peitzman AB. Hypovolemic shock. In: *Pathophysiologic foundations of critical care,* eds Pinsky MR, Dhainaut JFA. 1993, pp 161-169. Baltimore, Williams and Wilkins.

58. American College of Surgeons Committee on Trauma. Advanced Trauma Life Support. 1997. Chicago, American College of Surgeons.

59. Hirasawa H, Odaka M, Tabata Y, et al. Tissue blood flow in brain, liver, renal cortex, and renal medulla in experimental hemorrhagic shock. Crit Care Med 1977; 5: 141-145

60. Chen RYZ, Fan F-C, Schuessler GB, et al. Regional cerebral blood flow and oxygen consumption of the canine brain during hemorrhagic hypotension. Stroke 1984; 15: 343-350

61. Bronshvag MM. Cerebral pathophysiology in hemorrhagic shock. Nuclide scan data, fluorescence microscopy, and anatomic correlations. Stroke 1980; 11: 50-59

62. Bellamy RF, Pederson DC, DeGuzman LR. Organ blood flow and the cause of death following massive hemorrhage. Circ Shock 1984; 14: 113-127

63. Lautt WW. Relationship between hepatic blood flow and overall metabolism: the hepatic arterial buffer response. Fed Proc 1983; 42: 1662-1666

64. Carter EA, Tompkins RG, Yarmush ML, et al. Redistribution of blood flow after thermal injury and hemorrhagic shock. J Appl Physiol 1988; 65: 1782-1788

65. Haljamäe H. Microcirculation and hemorrhagic shock. Am J Emerg Med 1984; 2: 100-107

66. Bagge U, Amundsen B, Lauritzen C. White cell deformability and plugging of skeletal muscle capillaries in hemorrhagic shock. Acta Physiol Scand 1980; 180: 159-163

67. Mazzoni MC, Borgström P, Intaglietta M, Arfors K-E. Lumenal narrowing and endothelial cell swelling in skeletal muscle capillaries during hemorrhagic shock. Circ Shock 1989; 29: 27-39

68. Tung C-S, Chu K-M, Tseng C-J, Yin T-H. Adenosine in hemorrhagic shock: possible role in attenuating sympathetic activation. Life Sci 1987; 41: 1375-1382

69. Longnecker DE, Sturgill BC. Influence of anesthetic agent on survival following hemorrhage. Anesthesiology 1976; 45: 516-521

70. Longnecker DE, McCoy S, Drucker WR. Anesthetic influence on response to hemorrhage in rats. Circ Shock 1979; 6: 55-60

71. Farnebo L-O, Hallman H, Hamberger B, Jonsson G. Catecholamines and hemorrhagic shock in awake and anesthetized rats. Circ Shock 1979; 6: 109-118

72. Iyenger N, Laycock JF. The cardiovascular response to hemorrhage in female rats is influenced by the estrous cycle. Ann N Y Acad Sci 1993; 22: 603-605

73. Payan HM, Conard JR. Carotid ligation in gerbils: influence of age, sex, and gonads. Stroke 1977; 8: 194-196

74. Zwemer CF, O'Connor EM, Whitesall SE, D'Alecy LG. Gender differences in 24-hour outcome following resuscitation after 9 minutes of cardiac arrest in dogs. Crit Care Med 1997; 25: 330-338

75. Conlay LA, Evoniuk G, Wurtman RJ. Endogenous adenosine and hemorrhagic shock: effects of caffeine administration or caffeine withdrawal. Proc Natl Acad Sci USA 1988; 85: 4483-4485

76. Belardinelli L, Linden J, Berne RM. The cardiac effects of adenosine. Prog Cardiovasc Dis 1989; 32: 73-97

77. Wesley RC Jr., Porzio D, Sadeghi M. Effect of selective A_1 adenosine antagonism of postdefibrillation cardiovascular depression: evidence for an antiadrenergic role of endogenous adenosine. Cardiovasc Res 1993; 27: 129-133

78. Karasawa A, Rochester JA, Lefer AM. Effects of adenosine, an adenosine-A_1 antagonist, and their combination in splanchnic occlusion shock in rats. Circ Shock 1992; 36: 154-161

79. de Garavilla L, Tocker J, Valentine H, Hanson R. A1-selective adenosine antagonists improve cardiovascular function during hemorrhagic shock in rats. Circulation 1987; 76: supp IV 154 (abstract)

80. de Garavilla L. NPC 205, a potent adenosine antagonist, improves survival following hemorrhagic shock in rats. FASEB J 1989; 3: A1872 (abstract)

81. Romano FD, Naimi TS, Dobson JG Jr. Adenosine attenuation of catecholamine-enhanced contractility of rat heart in vivo. Am J Physiol 1991; 260: H1635-H1639

82. Biaggioni I, King LS, Enayat N, Robertson D, Newman JH. Adenosine produces pulmonary vasoconstriction in sheep. Circ Res 1989; 65: 1516-1525

83. Murray RD, Churchill PC. Effects of adenosine receptor agonists in the isolated, perfused rat kidney. Am J Physiol 1984; 247: H343-H348

84. Forman MB, Velasco CE, Jackson EK. Adenosine attenuates reperfusion injury following regional myocardial ischaemia. Cardiovasc Res 1993; 27: 9-17

85. Tracey WR, Magee W, Masamune H, et al. Selective activation of adenosine A3 receptors with N6-(3-chlorobenzyl)-N-5'-methylcarboxamidoadenosine (BB-MECA) provides cardioprotection via KATP channel activation. Cardiovasc Res 1998; 40: 138-145

86. Hirsch LJ, Rone AS. Hepatic arterial and portal flow in cardiogenic and hemorrhagic shock in awake dogs. Circ Shock 1982; 9: 17-26

87. Carmichael FJ, Saldivia V, Varghese GA, et al. Ethanol-induced increase in portal blood flow: role of acetate and A1- and A2-adenosine receptors. Am J Physiol 1988; 255: G417-G423

88. Granger DN, Valleau JD, Parker RE, et al. Effects of adenosine on intestinal hemodynamics, oxygen delivery, and capillary fluid exchange. Am J Physiol 1978; 235: H707-H719

89. Douglas SJ, Davis SS, Illum L. Nanoparticles in drug delivery. Crit Rev Ther Drug Carrier Syst 1987; 3: 233-261

90. Kreuter J. Nanoparticles and microparticles for drug and vaccine delivery. J Anat 1996; 189: 503-505

91. O'Mullane JE, Artursson P, Tomlinson E. Biopharmaceutics of microparticulate drug carriers. Ann N Y Acad Sci 1987; 507: 120-140

92. Bradfield JWB. A new look at reticuloendothelial blockade. Br J Exp Pathol 1980; 61: 617-623

93. Tröster SD, Müller U, Kreuter J. Modification of body distribution of poly(methyl methacrylate) nanoparticles in rats by coating with surfactants. Int J Pharm 1990; 61: 85-100

94. Gref R, Minamitake Y, Peracchia MT, et al. Biodegradable long-circulating polymeric nanospheres. Science 1994; 263: 1600-1603

95. Napper DH. In: *Polymeric Stabilisation of Colloidal Dispersions.* 1983, pp 197-215. London, Academic Press.

96. Slack D, Motoko K, Simmons GH, DeLuca PP. Acute hemodynamic effects and blood pool kinetics of polystyrene microspheres following intravenous administration. J Pharm Sci 1981; 70: 660-664

97. Nugent KM. Intralipid effects on reticuloendothelial function. J Leukoc Biol 1984; 36: 123-132

98. Peterson TC, Renton KW. Depression of cytochrome P-450-dependent drug biotransformation in hepatocytes after the activation of the reticuloendothelial system by dextran sulfate. J Pharmacol Exp Ther 1984; 229: 299-304

99. Nathan CF. Secretory products of macrophages. J Clin Invest 1987; 79: 319-326

100. de Garavilla L, Peltier N, Merisko-Liversidge E. Controlling the acute hemodynamic effects associated with IV administration of particulate drug dispersions in dogs. Drug Dev Res 1996; 37: 86-96

101. Fuks A, Zucker-Franklin D. Impaired Kupffer cell function precedes development of secondary amyloidosis. J Exp Med 1985; 161: 1013-1028

102. Smith PL, Kagey-Sobotka A, Bleeker ER, et al. Physiologic manifestations of human anaphylaxis. J Clin Invest 1980; 66: 1072-1080

103. Mjörndal TO, Chesrown SE, Frey MJ, et al. Effect of beta-adrenergic stimulation on experimental canine anaphylaxis in vivo. J Allergy Clin Immunol 1983; 71: 62-70

104. Bleeker ER, Walden SM, Wagner E, et al. Immunologic and physiologic changes during canine anaphylaxis and asthma. Chest 1985; 87: suppl 164S-167S

105. Tucker A, Weir EK, Reeves JT, Grover RF. Histamine H_1- and H_2-receptors in pulmonary and systemic vasculature of the dog. Am J Physiol 1975; 229: 1008-1013

106. Silverman HJ, Taylor WR, Smith PL, et al. Effects of antihistamines on the cardiopulmonary changes due to canine anaphylaxis. J Appl Physiol 1988; 64: 210-217

107. Greenberger PA, Patterson R. Adverse reactions to radiocontrast media. Prog Cardiovasc Dis 1988; 31: 239-248

108. Baxter AB, Lazarus SC, Brasch RC. In vitro histamine release induced by magnetic resonance imaging and iodinated contrast media. Invest Radiol 1993; 28: 308-312

109. Ennis M, Amon EU, Lorenz W. Histamine release from canine lung and liver mast cells induced by radiographic contrast media. Agents Actions 1989; 27: 101-103

110. Salem DN, Findlay SR, Isner JM, et al. Comparison of histamine release effects of ionic and non-ionic radiographic contrast media. Am J Med 1986; 80: 382-384

111. Banks RO, Inscho EW, Jacobsen ED. Histamine H1 receptor antagonists inhibit autoregulation of renal blood flow in the dog. Circ Res 1984; 54: 527-535

112. Houck PC, Lutherer LO. Regulation of adrenal blood flow: response to hemorrhagic hypotension. Am J Physiol 1981; 241: H872-877

113. Pawlik W, Tague LL, Tepperman BL, et al. Histamine H1- and H2-receptor vasodilation of canine intestinal circulation. Am J Physiol 1977; 233: E219-E224

114. Meyer JS, Teraura T, Sakamoto K, Kondo A. Central neurogenic control of cerebral blood flow. Neurology 1971; 21: 247-262

115. Hoekstra JW, Droen SC, Hedges JR. Effects of splenectomy on hemodynamic performance in fixed volume canine hemorrhagic shock. Circ Shock 1988; 25: 95-101

116. Dole WP, Jackson DL, Rosenblatt JI, Thompson WL. Relative error and variability in blood flow measurements with radiolabeled microspheres. Am J Physiol 1982; 243: H371-H378

117. Christensen CW, Gross GJ, Hardman HF, et al. Effects of histamine receptor stimulation on regional myocardial blood flow. Am J Physiol 1983; 245: H461-H467

118. DeBehnke D. Effects of graded doses of endothelin-1 on coronary perfusion pressure and vital organ blood flow during cardiac arrest. Acad Emerg Med 2000; 7: 211-221

119. Pavlin EG, Su JY. Cardiopulmonary pharmacology. In: *Anesthesia,* ed. RD Miller. 1994, pp 125-156. New York, Churchill Livingstone.

120. Reves JG, Glass PSA, Lubarsky DA. Nonbarbiturate intravenous anesthetics. In: *Anesthesia,* ed. RD Miller. 1994, pp 247-289. New York, Churchill Livingstone.

121. Kaihara S, Van Heerden PD, Migita T, Wagner HN Jr. Measurement of distribution of cardiac output. J Appl Physiol 1968; 25: 696-700

122. Sasaki Y, Wagner HN Jr. Measurement of the distribution of cardiac output in unanesthetized rats. J Appl Physiol 1971; 30: 879-884

123. Forsyth RP, Hoffbrand BI. Redistribution of cardiac output after sodium pentobarbitol anesthesia in the monkey. Am J Physiol 1970; 218: 214-217

124. Stupfel M, Valleron A-J, Demeestere M, Massé H. Hypoxia survival variations in male and female mice as functions of chronological and environmental factors. Aviat Space Environ Med 1978; 49: 1087-1092

125. Austin GE, Tuvlin MB, Martino-Salzman D, et al. Determination of regional myocardial blood flow using fluorescent microspheres. Am J Cardiovasc Pathol 1993; 4: 352-357

126. Horton JW, Longhurst JC, Colin D, Mitchell JH. Cardiovascular effects of hemorrhagic shock in spleen intact and splenectomized dogs. Clin Physiol 1984; 4: 533-548

127. Van Oosterhout MFM, Prinzen FW, Reneman RS. The fluorescent microsphere method for determination of organ blood flow. FASEB J 1994; 8: A854 (abstract)

Acknowledgments

I would like to thank my supervisors, Dr. Larry de Garavilla and Dr. Mervyn Singer. Thanks to all those at Temple University Hospital and Albert Einstein Medical Center, in particular Justin Kaplan, Dawn Clas and Brian Nester. This work would not have been started without Bob Buckman or Bill Dalsey. It would not have been finished but for my father, thanks Dad.